Light
Everywhere

Molecular Spectroscopy Basics

Erik KERSTEL
University of Grenoble Alps







Interaction of EM radiation with molecules

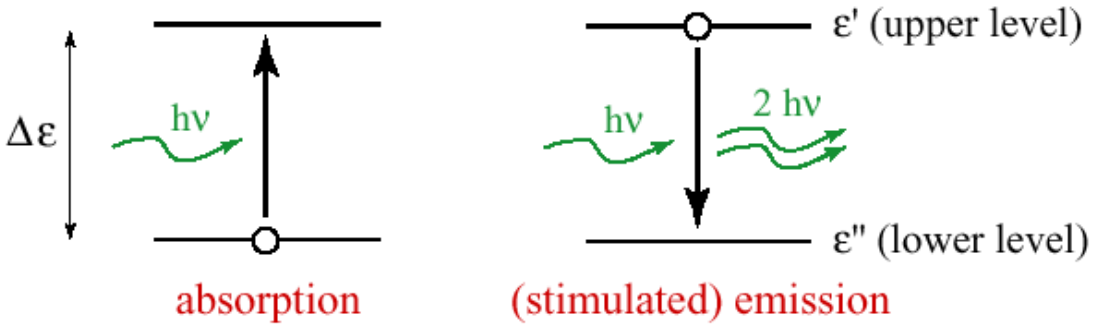

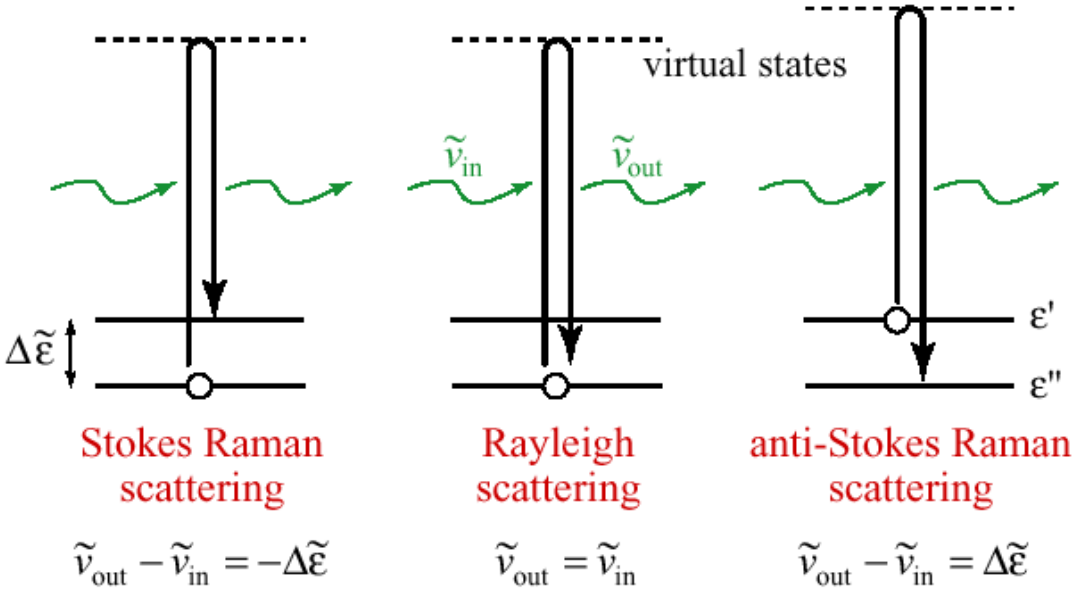

Interaction of EM radiation with molecules

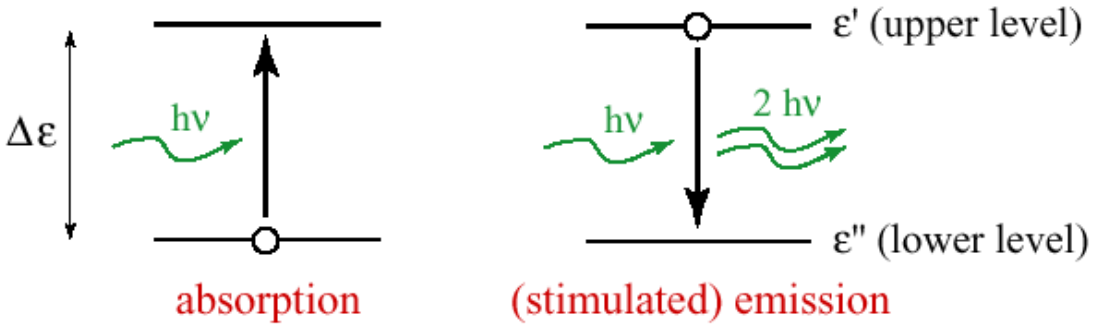

$$\psi' \leftarrow \psi'' + h\nu \qquad \text{(absorption)}$$

$$\psi' \rightarrow \psi'' + h\nu \qquad \text{(spontaneous emission)}$$

$$\psi' + h\nu \rightarrow \psi'' + 2h\nu \qquad \text{(stimulated emission)}$$

Two-level system and Einstein coefficients

spectral energy density $\rho(\nu)$ [J m^{-3} s]

$$\rho(\nu)d\nu = \frac{8\pi h\nu^3}{c^3}\frac{d\nu}{e^{h\nu/kT}-1}$$

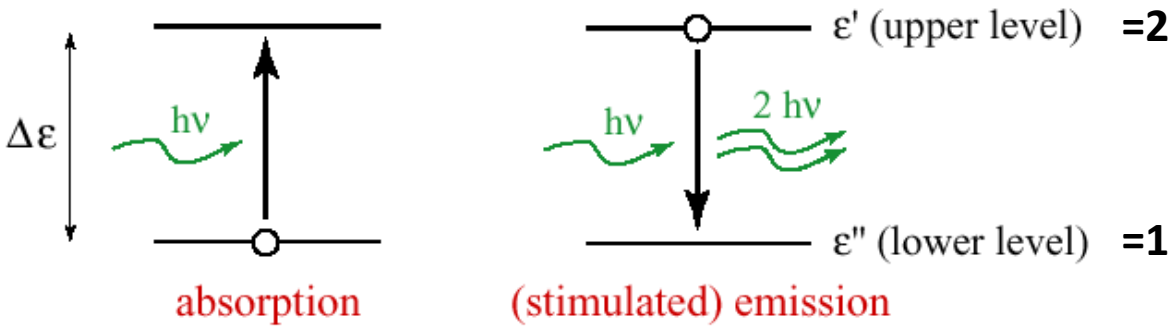

If no other than the indicated two levels are present, the rate equations for population transfer in the isolated system can be written:

$$\left(\frac{dn_1}{dt}\right)_{B_{12}} = -B_{12}n_1\rho(\nu)$$

absorption: Einstein coefficient B_{12} [J^{-1}m^{3}s^{-2}]

$$\left(\frac{dn_1}{dt}\right)_{B_{21}} = B_{21}n_2\rho(\nu)$$

stimulated emission: Einstein coefficient B_{21} [J^{-1}m^{3}s^{-2}]

$$\left(\frac{dn_1}{dt}\right)_{A_{21}} = A_{21}n_2$$

spontaneous emission: Einstein coefficient A_{21} [s^{-1}]

Two-level system and Einstein coefficients

In steady state the population change is zero at any temperature and the population ratio n_1/n_2 determined by the Boltzmann distribution. We then find:

$$\begin{cases} A_{21} = \dfrac{8\pi h\nu^3}{c^3} B_{21} \\ g_2 B_{21} = g_1 B_{12} \end{cases}$$

Note the third-power dependence on the transition frequency of A_{21}:
Spontaneous emission is generally a slow process in the IR region of the spectrum.

Be aware that the ratio of Einstein A_{21} and B_{21} coefficients critically depends on the representation (units!) of the Planck law $\rho(\nu)$.
See, e.g., Hilborn, R. C. (1982). *Einstein coefficients, cross sections, f values, dipole moments, and all that*. American Journal of Physics, *50*(11), 982–986… And its Erratum ibid. (1983) 51(5), 471!!

Einstein coefficients and the transition dipole moment

The interaction between the molecule and the EM radiation is most often through the electric field.
The resulting electric dipole interaction term takes the form $-\boldsymbol{\mu} \cdot \boldsymbol{E}$. Here $\boldsymbol{\mu}$ is the (instantaneous) dipole moment of the molecule:

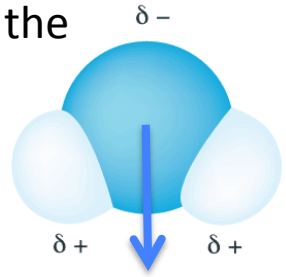

$$\boldsymbol{\mu} \equiv \mathbf{p} = \sum_i q_i \mathbf{r}_i$$

This dipole experience a net force equal to zero, but a non-zero torque equal to $\boldsymbol{\mu} \times \boldsymbol{E}$.
In an oscillating electric field, the molecule will start rotating, just like the rotating dipole will generate an oscillating EM field.

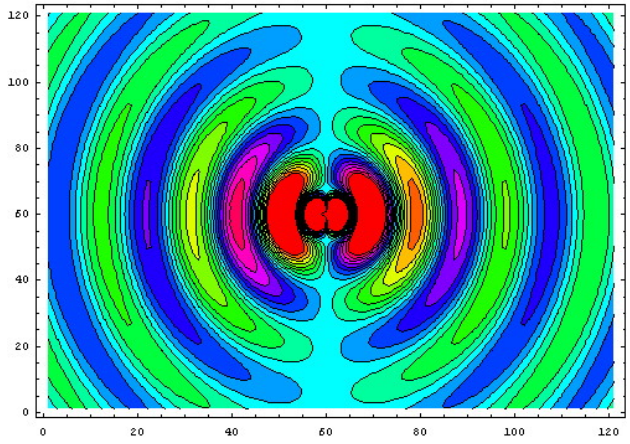

As we will show later, in pure rotational spectroscopy, the electric field of the radiation interacts with the permanent dipole moment of the molecule.

In electronic and vibrational spectroscopies, the electric field interacts with a **changing** dipole moment during the transition from an initial to a final state.

Einstein coefficients and the transition dipole moment

The coupling between the electric field and the transition dipole moment induces the transition from the initial state *1* to the final state *2*:

$$\mathbf{R}^{21} = \int \psi_2^* \mathbf{p} \psi_1 \, d\tau \equiv \langle \psi_2 | \mathbf{p} | \psi_1 \rangle \equiv \langle 2 | \mathbf{p} | 1 \rangle$$

The direction of $\mathbf{R}^{21}$ determines the interaction with polarized radiation

The square of the magnitude of the generally complex vector $\mathbf{R}^{21}$ gives the transition probability and is directly related to the Einstein *A*-coefficient:

$$A_{21} = \frac{16\pi^3 \nu^3}{3\varepsilon_0 h c^3} \left| \mathbf{R}^{21} \right|^2$$

Note again the proportionality of A_{21} on the third power of the transition frequency: Spontaneous emission is generally a slow process in the IR region of the spectrum.

Einstein coefficients and the transition dipole moment

Or, in the case of degenerate energy levels:

$$A_{21} = \frac{16\pi^3\nu^3}{3\varepsilon_0 hc^3}\frac{g_1}{g_2}\left(\mathfrak{R}^{21}\right)^2$$

Where the weighted square of the transition dipole moment is defined as [see, e.g., Simeckova, M.; Jacquemart, D.; Rothman, L. S.; Gamache, R. R.; Goldman, A., Einstein A-coefficients and statistical weights for molecular absorption transitions in the HITRAN database. Journal of Quantitative Spectroscopy and Radiative Transfer 2006, 98 (1), 130-155]:

$$\left(\mathfrak{R}^{21}\right)^2 = \frac{1}{g_1}\sum_{m,m'}\left|\mathbf{R}^{2m'1m}\right|^2$$

Simple case: two-level atom in a classical radiation field

Assumptions:

(1) Transition is "slow", such that the wavefunctions are equal to the corresponding stationary state wavefunctions with **slowly varying coefficients**.

.

$$\psi(t) = \sum_n C_n(t)\psi_n e^{-iE_n t/\hbar}$$

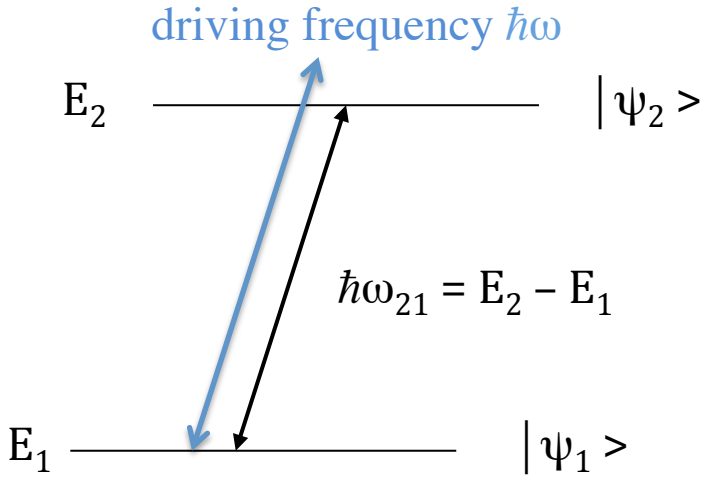

(2) First-order perturbation theory: $H = H_0 + H_1(t)$

(3) Weak field: $H_1(t) = \begin{vmatrix} 0 & W_{12} \\ W_{21} & 0 \end{vmatrix}$ with $\begin{cases} W_{12} = -\langle 1|\mathbf{p}(\mathbf{r})\cdot\mathbf{E}_0\cos(\omega t)|2\rangle = \gamma\hbar\ (e^{i\omega t} + e^{-i\omega t}) \\ W_{21} = -\langle 2|\mathbf{p}(\mathbf{r})\cdot\mathbf{E}_0\cos(\omega t)|1\rangle = \gamma\hbar\ (e^{i\omega t} + e^{-i\omega t}) \end{cases}$

(4) Rotating Wave Approximation: neglect fast oscillating terms, i.e., $\omega+\omega_{21}$

(5) Initial populations are $C_1(0)=1$ and $C_2(0)=0$

Two-level atom in a classical radiation field: Rabi oscillations

The time-dependent Schrödinger equation $i\hbar\frac{\partial\psi(t)}{\partial t} = \left(H_0 + H_1(t)\right)\psi(t)$

then yields the following result for the time-dependent population of the two levels:

$$\begin{cases} \dfrac{dC_1}{dt} = -i\gamma C_2 e^{i(\omega-\omega_{21})t} \\ \dfrac{dC_2}{dt} = -i\gamma C_1 e^{-i(\omega-\omega_{21})t} \end{cases}$$

$$\begin{cases} \Delta\omega = \omega - \omega_{21} \quad \text{detuning} \\ \Omega = \sqrt{\gamma^2 + \left(\dfrac{\Delta\omega}{2}\right)^2} \\ C_2(t) = -i\gamma\dfrac{\sin(\Omega t)}{\Omega} e^{\frac{-i\Delta\omega t}{2}} \\ \left|C_2(t)\right|^2 = \gamma^2\dfrac{\sin^2(\Omega t)}{\Omega^2} \end{cases}$$

Rabi frequency $\omega_R = 2\gamma$: zero-detuning atomic inversion frequency

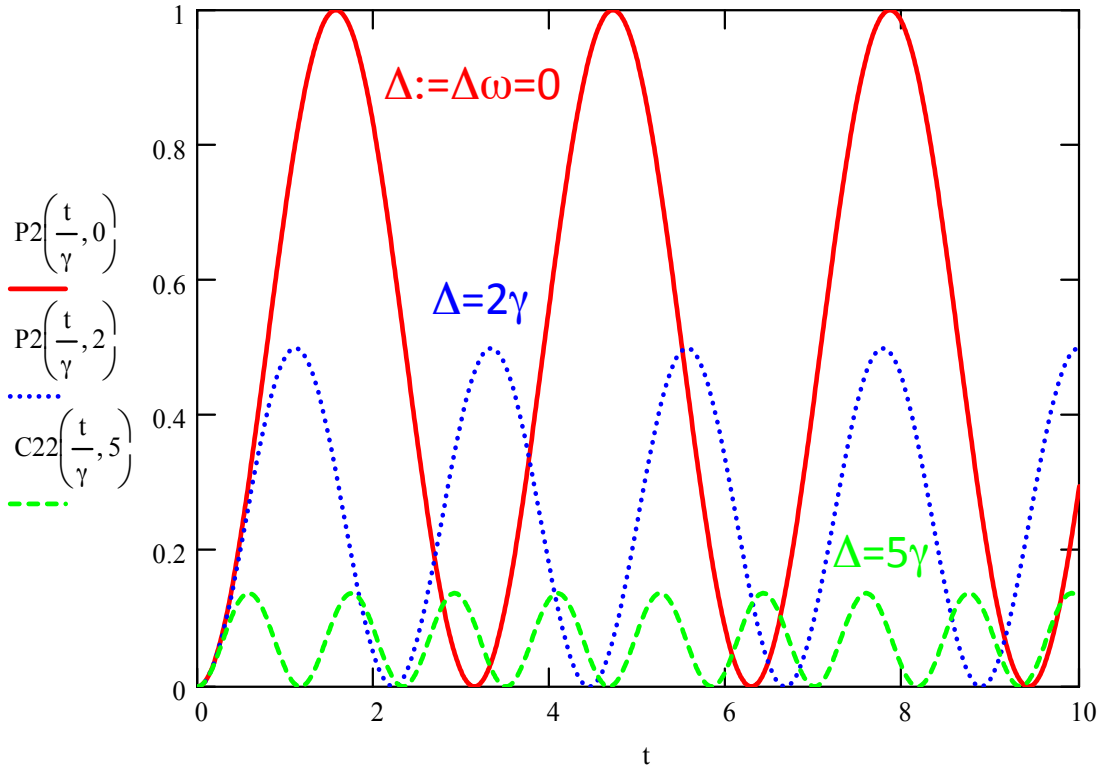

Rabi oscillations: experimental observation in a single molecule

Gerhardt et al. *Coherent State Preparation and Observation of Rabi Oscillations in a Single Molecule*, Phys. Rev. A (2009).

Low doping rates (~10^{-6}) in a cryogenic matrix yield one dye molecule in the tight focus of the laser beam.

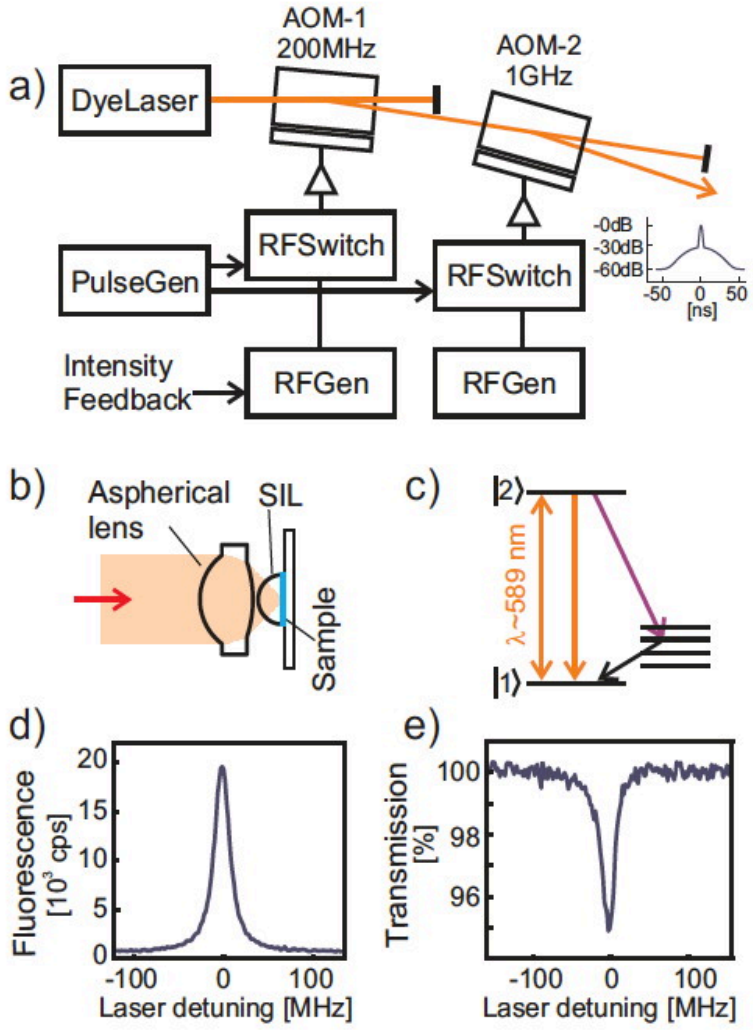

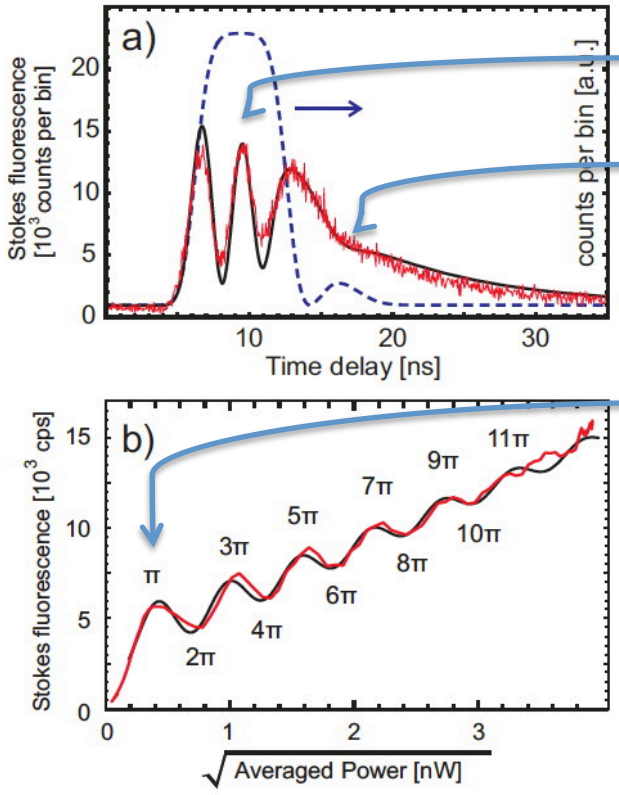

2 Rabi cycles, damped

spontaneous emission

population inversion

$\propto E \propto \omega_R$

FIG. 2: Raw Stokes-shifted fluorescence of a single molecule (red curve) and a theoretical fit (black curve): a) as a function of delay with respect to the optical pulse. The blue dashed line displays the measured excitation pulse intensity. b) as a function of the square root of the excitation pulse power using an optical pulse of 4 ns length. The data correspond to the vertical cut at $\Delta = 70$ MHz in Fig. 3a.

Two-level atom in a classical radiation field: line width

The upper state population as a function of the detuning: towards an absorption profile …

$$\begin{cases} \Delta\omega = \omega - \omega_{21} \\ \Omega = \sqrt{\gamma^2 + \left(\frac{\Delta\omega}{2}\right)^2} \\ C_2(t) = -i\gamma \frac{\sin(\Omega t)}{\Omega} e^{\frac{-i\Delta\omega t}{2}} \\ \left|C_2(t)\right|^2 = \gamma^2 \frac{\sin^2(\Omega t)}{\Omega^2} \end{cases}$$

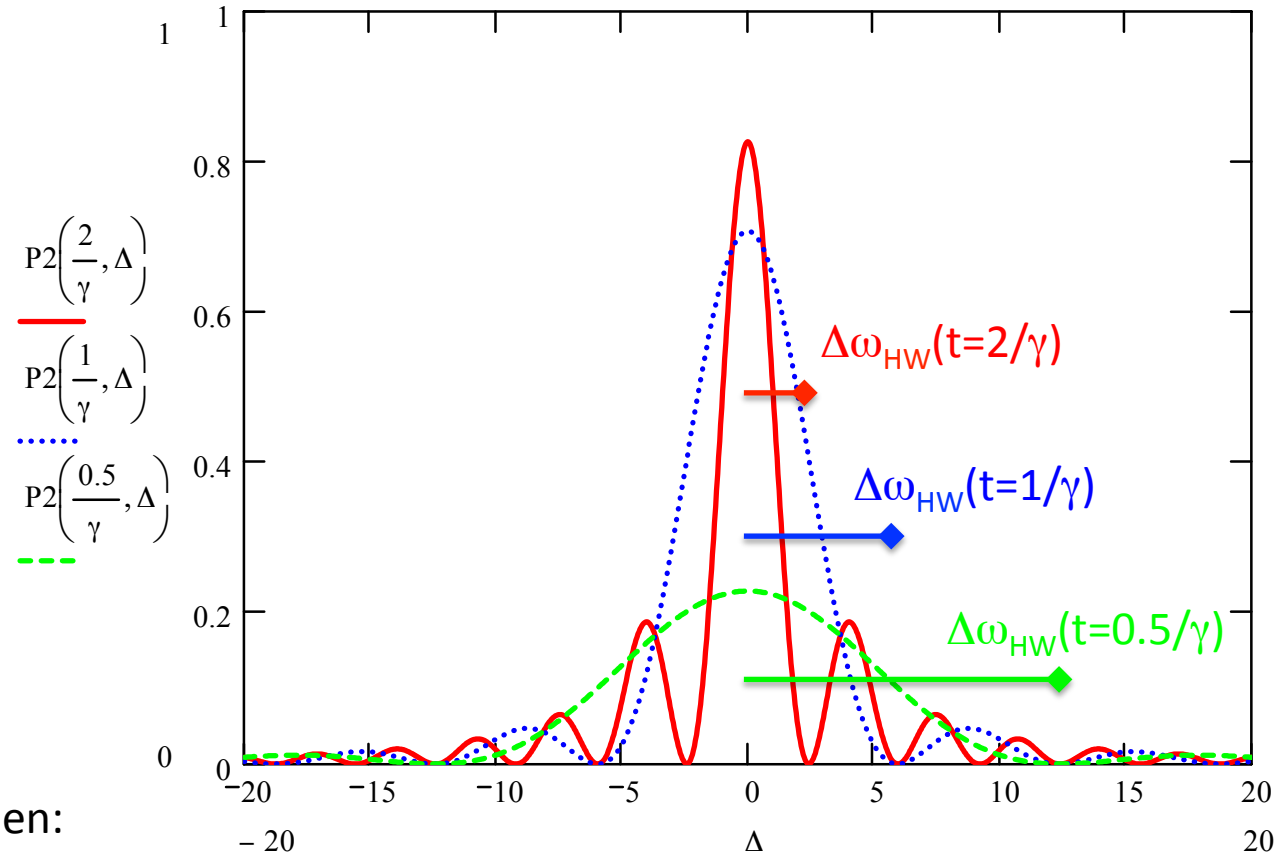

if $\gamma \ll \Delta\omega$ (weak field), then:

$$\left|C_2(\tau)\right|^2 = 0 \Rightarrow \tau = t_\pi = \frac{2\pi}{\Delta\omega_{HW}} \Rightarrow \hbar\Delta\omega_{HW} \cdot \tau = \left(\hbar\frac{2\pi}{\tau}\right) \cdot \tau = h$$

$$\Delta E \cdot \Delta t \geq \hbar$$

Absorption line profiles

In order to uncouple the issue of the line shape from that of the line (absorption) intensity, we generally deal with normalized line shapes:

$$\int g(\omega)d\omega = \int g(\nu)d\nu = \int g(\lambda)d\lambda = 1$$

Furthermore, the line is characterized by its FWHM or HWHM, which can be attributed to different line broadening mechanism that may be operative alone, or in combination.

There are two classes of broadening mechanisms:

homogeneous broadening: the radiation field with frequency inside the profile interacts with all molecules of the same kind

inhomogeneous broadening: the radiation interacts with only a subsample of all molecules

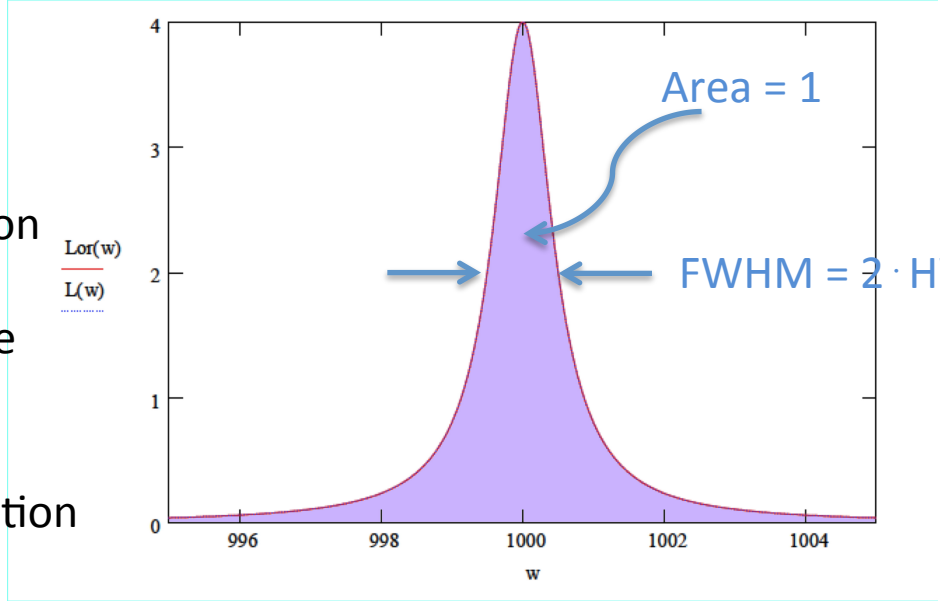

Natural line broadening

The line profile of the transition is determined by the finite life time of the states.
The most common case is that in which the upper state life time τ is limited by spontaneous emission: $\tau = 1/A_{21}$. This case can be described as a damped harmonic oscillator:

$$m\ddot{x} + \lambda\dot{x} + kx = F(t)$$

If we take as initial conditions *x*(0)=0 and an impulse force *F(t)=δ(t)*, we find:

$$x(t) = \frac{\omega_0}{k\sqrt{1-\xi^2}} e^{-\frac{\gamma}{2}t} \sin\left(\omega_0\sqrt{1-\xi^2}\,t\right)$$

$$= \frac{\omega_0}{k\sqrt{1-\xi^2}} e^{-\frac{\gamma}{2}t} \sin\left(\omega_d t\right)$$

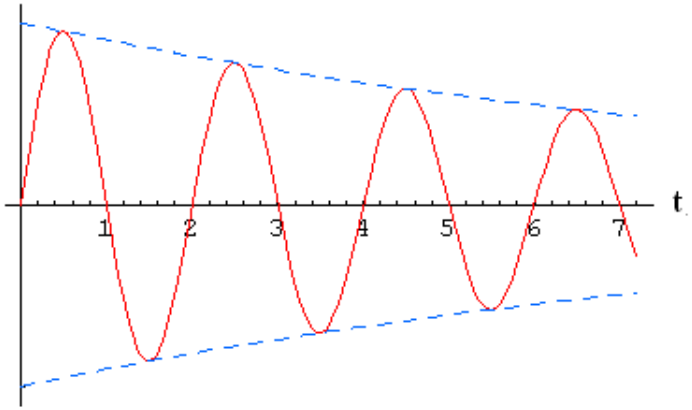

with

$$\omega_0 = \sqrt{\frac{k}{m}}, \quad \omega_d = \omega_0\sqrt{1-\xi^2}, \text{ the undamped and damped radial frequencies}$$

$$\gamma = \frac{\lambda}{m} = 2\xi\omega_0, \quad \xi = \frac{\lambda}{2\sqrt{km}}, \text{ the dacay constant and the damping ratio}$$

Natural line broadening

The radiated power is proportional to the square of the electric field, which in turn is proportional to the frequency spectrum $A(\omega)$ of x(t):

$$A(\omega) = \int_0^\infty x(t) e^{-i\omega t}\, dt$$

The line shape thus becomes:

$$g(\omega) \propto A(\omega)A^*(\omega) = C \frac{4\omega_0^2}{\left(\omega_0^2 - \omega^2\right)^2 + \left(\gamma\omega\right)^2}$$

For optical transitions, $\gamma << \omega_0$ (i.e., $\xi << 1$), and herewith the above reduces to:

$$g(\omega) \propto A(\omega)A^*(\omega) = C \frac{1}{\left(\omega - \omega_0\right)^2 + \left(\frac{\gamma}{2}\right)^2}$$

with γ the FWHM of the Lorentzian

Natural line broadening

The normalized function is know as the Lorentzian line shape

$$g_L(\omega-\omega_0)=\frac{\gamma}{2\pi}\frac{1}{(\omega-\omega_0)^2+\left(\frac{\gamma}{2}\right)^2}$$

with γ the FWHM

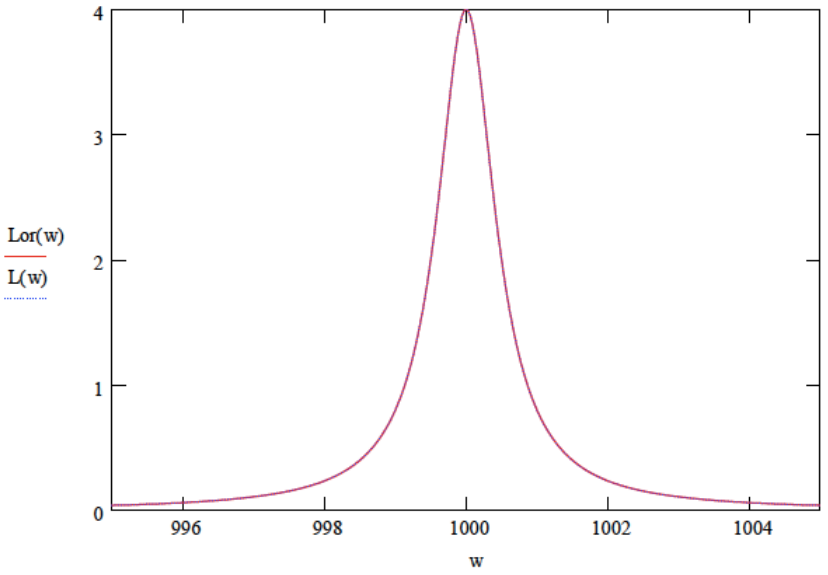

Radiation at a frequency inside the Lorentz profile will interact will all atoms of the same kind: Natural line broadening is a homogeneous broadening mechanism.

Doppler broadening

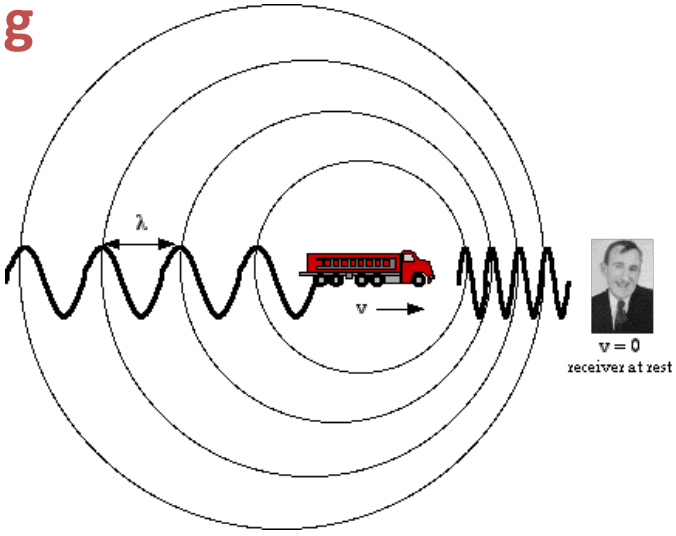

Doppler broadening is caused by the finite width of the distribution of velocities of the atoms or molecules.
For the molecule moving with velocity ***u*** to absorb radiation with wavenumber $|\boldsymbol{k}|=2\pi/\lambda$, the applied radiation should be of frequency:

$$\omega = \omega_0 + \mathbf{k}\cdot\mathbf{u} = \omega_0\left(1+\frac{u}{c}\right)$$

or: $u = c\left(\frac{\nu}{\nu_0}-1\right)$ and: $du = \left(\frac{c}{\nu_0}\right)d\nu$

Substitution in the Maxwell-Boltzmann distribution $f(u)du = \left(\frac{m}{2\pi kT}\right)^{\frac{1}{2}} e^{-\frac{mu^2}{2kT}}du$

and assuming an infinitesimally narrow natural linewidth yields a Gaussian distribution for the Doppler broadened line profile:

$$g_D(\nu)d\nu = \int_{-\infty}^{\infty}\delta\left(\nu-\nu_0\left(1+\frac{u}{c}\right)\right)f(u)du\,d\nu = \frac{c}{\nu_0}\frac{1}{v_{th}\sqrt{\pi}}e^{-\left(\frac{c}{v_{th}}\frac{\nu-\nu_0}{\nu_0}\right)^2}d\nu$$

$$v_{th} = \sqrt{\frac{2kT}{m}}$$

Doppler broadening

The result is the normalized Gaussian distribution for the Doppler broadened line profile:

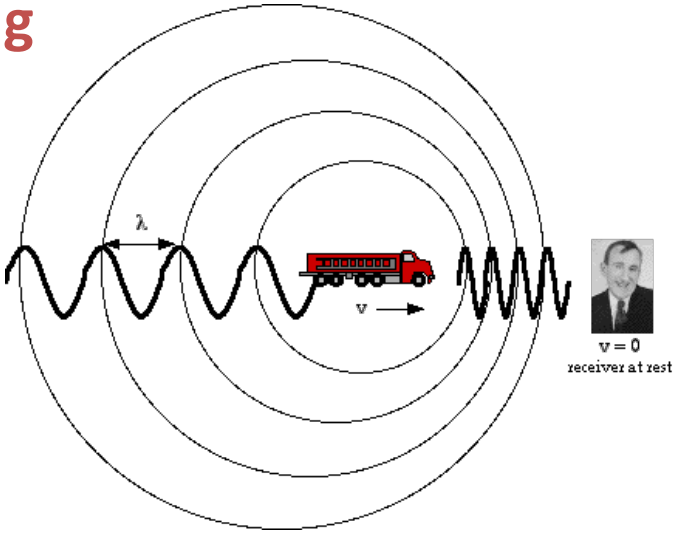

$$g_D(\nu-\nu_0)d\nu = \left(\frac{4\ln 2}{\pi}\right)^{\frac{1}{2}} \frac{1}{\Delta\nu_D} e^{-(4\ln 2)\left(\frac{\nu-\nu_0}{\Delta\nu_D}\right)^2}$$

$$\Delta\nu_D = \frac{\nu_0}{c}\left(8\ln 2\,\frac{kT}{m}\right)^{\frac{1}{2}} \qquad \text{(FWHM)}$$

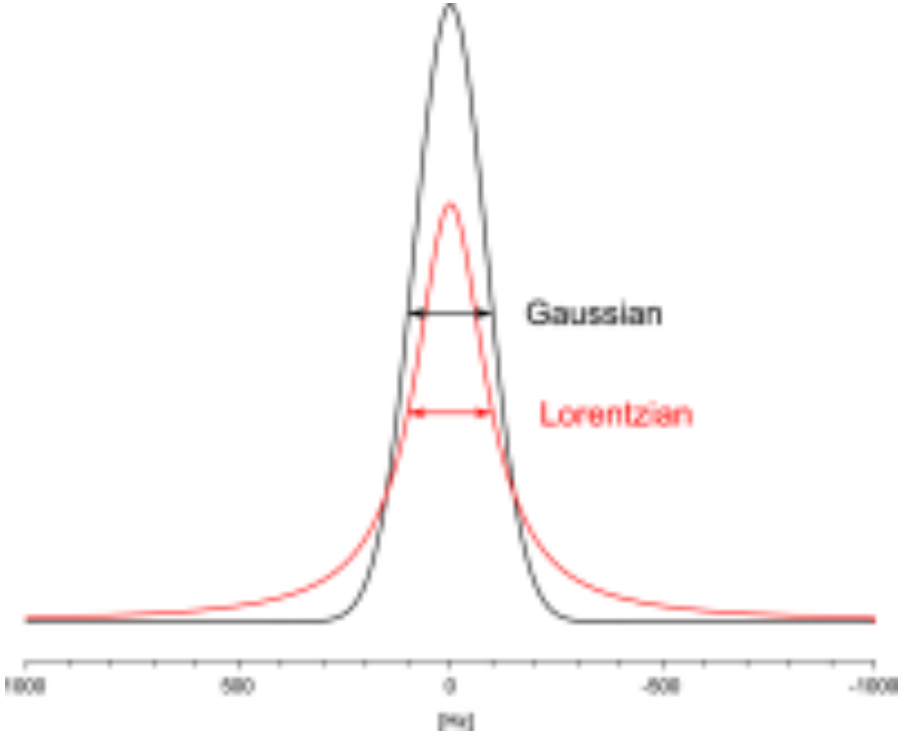

Collisional broadening

We discuss here the model in which 'hard' collisions are assumed to completely dephase the oscillating dipole:

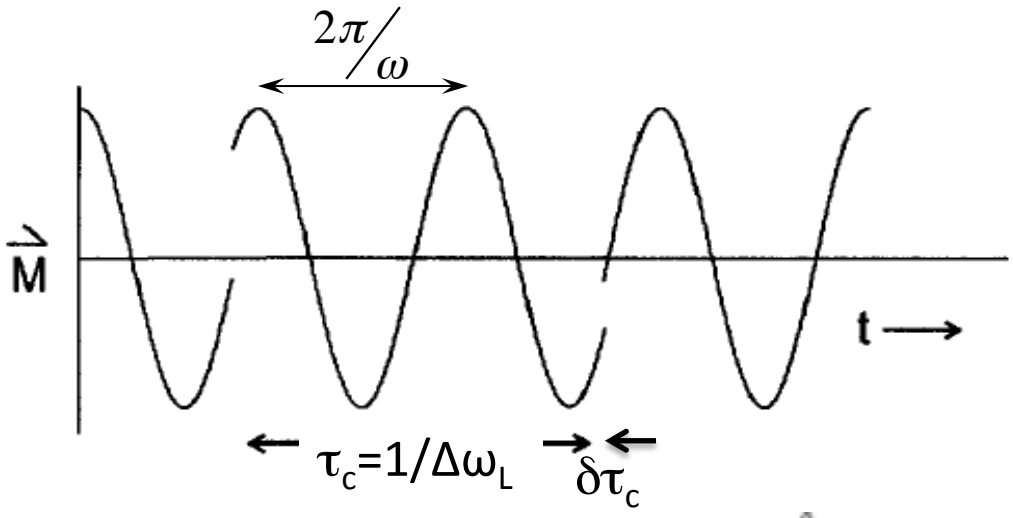

Fourier transform of such a randomly, but periodically restarted sinewave then yields a Lorentzian line profile with HWHM = $\Delta\omega_L = 1/\tau_c$ and thus:

$$\Delta\nu_L = \frac{1}{2\pi\tau_c} = \frac{f_c}{2\pi}$$

$$g_L(\nu)d\nu = \frac{1}{\pi}\frac{\Delta\nu_L}{(\nu-\nu_0-\Delta)^2+(\Delta\nu_L)^2}d\nu$$

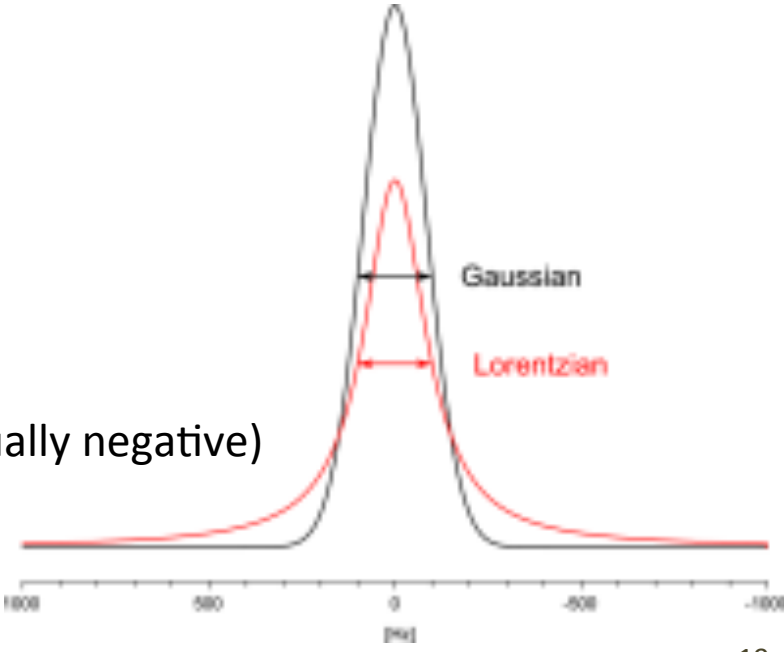

Here Δ represents the pressure-induced line shift (usually negative)

Collisional broadening = pressure broadening

Kinetic theory of an ideal gas gives the following result for the collision frequency (i.e., the number of collisions experienced by one molecule):

$$f_c = \sigma n \sqrt{\frac{8kT}{\pi \mu}} = \sigma p \sqrt{\frac{8}{\pi \mu kT}}$$

where σ represents the collision cross-section (m^2), n the number density of molecules (m^{-3}), p the pressure (Pa), μ the reduced mass (kg), and T the temperature (K). This gives for the full width at half maximum of the pressure broadened Lorentzian line profile:

$$\gamma = 2\Delta\nu_L = \frac{1}{\pi \tau_c} = \frac{f_c}{\pi} = \frac{\sigma}{\pi} \sqrt{\frac{8kT}{\pi \mu}} n = \frac{\sigma}{\pi} \sqrt{\frac{8}{\pi \mu kT}} \; p$$

Collisional broadening = pressure broadening

Determination of the collisional cross-section from intermolecular forces as given by the Van der Waals equation of state:

$$\left(p + \frac{n^2 a}{V^2}\right)(V - nb) = nRT$$

here, b is the molar volume:

$$V = \frac{b}{N_A} = \frac{4\pi r^3}{3} \Rightarrow r = \sqrt[3]{\frac{3b}{4\pi N_A}}$$

$$\sigma = \pi\left(r_A + r_B\right)^2$$

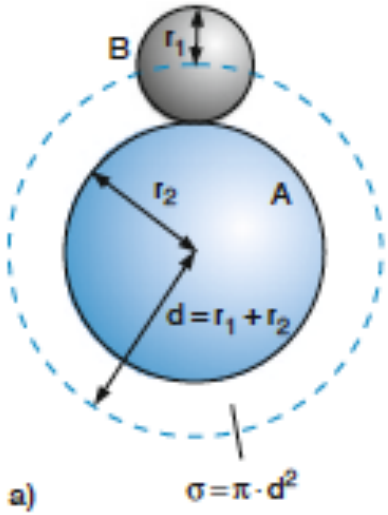

For example:

CO_2: b=42.67 10^{-6} m^3/mol, thus r = 257 pm

N_2: b=39.13 10^{-6} m^3/mol, thus r = 249 pm

→ calculate ~0.065 cm^{-1}/atm pressure broadening by N_2 of a CO_2 line at RT. Surprisingly close to the experimental value!

Mixed Lorentz and Gaussian line shape: The Voigt profile

In practice the line shape is Lorentzian or Gaussian only in the limiting cases of very low or very high pressure (in the IR). Otherwise the line shape is obtained by replacing the Dirac delta-function in our derivation of the Doppler profile by the Lorentzian profile.

$$g_V(\nu)d\nu = \int_{-\infty}^{\infty} g_L\left(\nu - \nu_0\left(1+\frac{u}{c}\right)\right) f(u)du\,d\nu$$

The so-defined Voigt profile *) is thus obtained as the convolution of the Lorentz and Doppler profiles:

$$g_V(\nu-\nu_0) = \int g_L((\nu-\nu_0)-\Delta)\, g_D(\Delta)\, d\Delta$$

*) Woldemar Voigt. *Das Gesetz der Intensitätsverteilung innerhalb der Linien eines Gasspektrums*. Verlag d. K. B. Akad. d. Wiss., 1912.

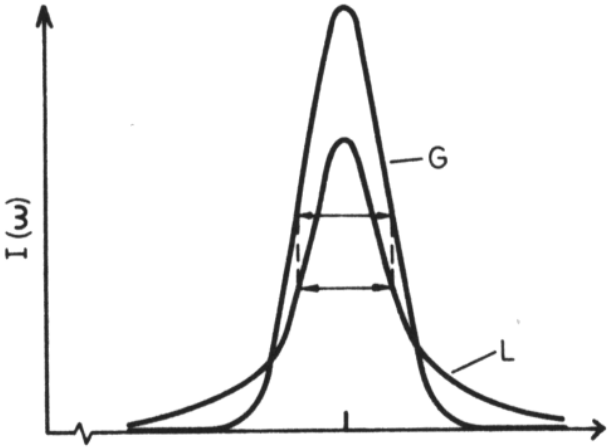

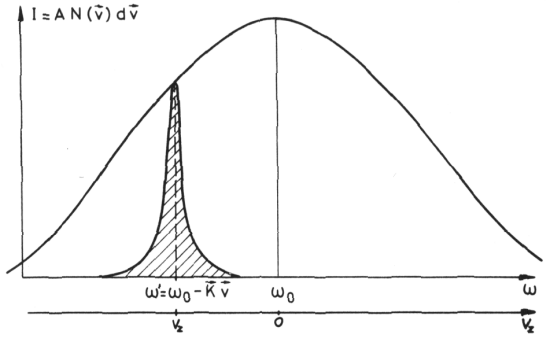

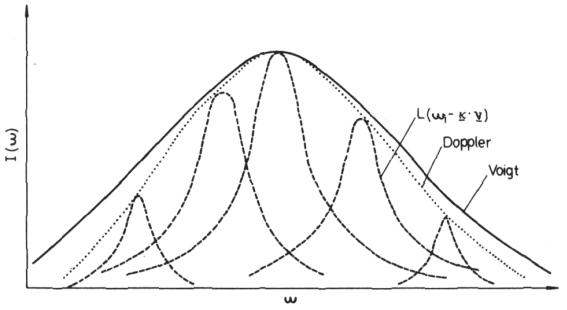

Mixed Lorentz and Gaussian line shape: The Voigt profile

Pressure dependence of the total (Voigt) linewidth

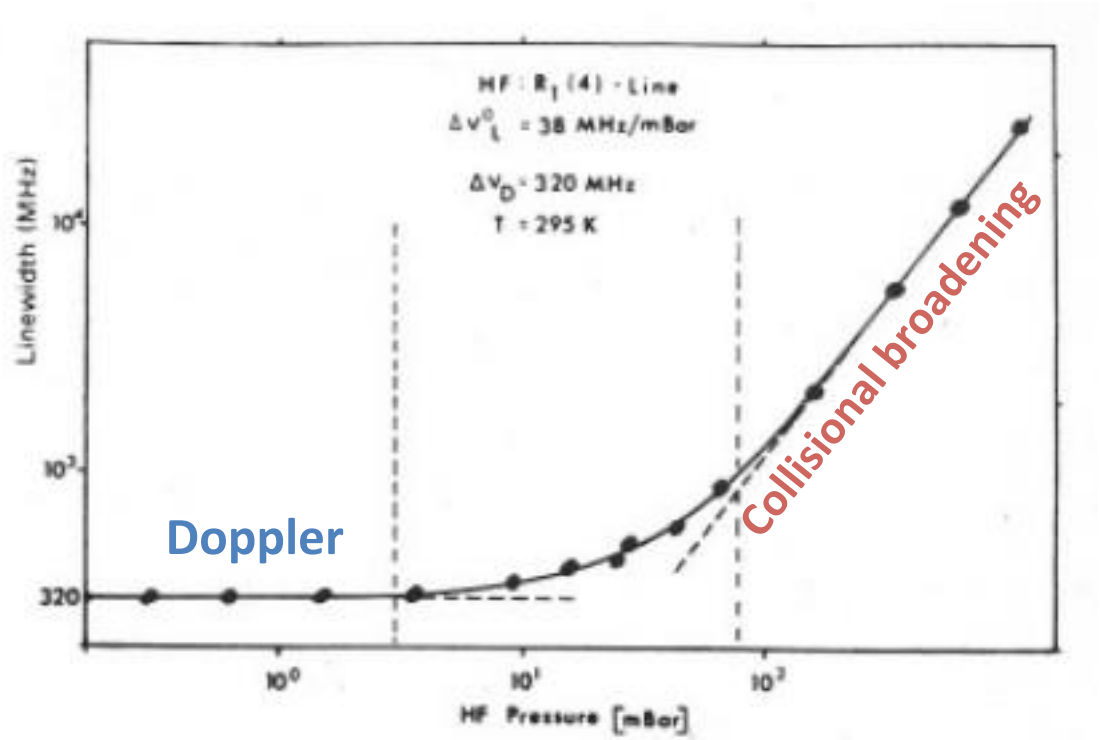

Linewidth dependence of HF absorption line on pressure.

Adapted from Ha Tran, SPEC-ATMOS Fréjus 2015

Beyond the Voigt profile

Dicke narrowing is the effect of a reduction of Doppler broadening due to velocity changing ("averaging") collisions, which may either be "soft" or "hard" (generally determined by the relative mass of the absorber and the matrix molecules).

detailed balance:

$$f\left(\vec{v} \rightarrow \vec{v}'\right) \cdot f_{MB}\left(\vec{v}\right) = f\left(\vec{v}' \rightarrow \vec{v}\right) \cdot f_{MB}\left(\vec{v}'\right)$$

change $\vec{v} \rightarrow \vec{v}' < \vec{v}$ more probable than
change $\vec{v} \rightarrow \vec{v}' > \vec{v}$

→ reduction of Doppler broadening

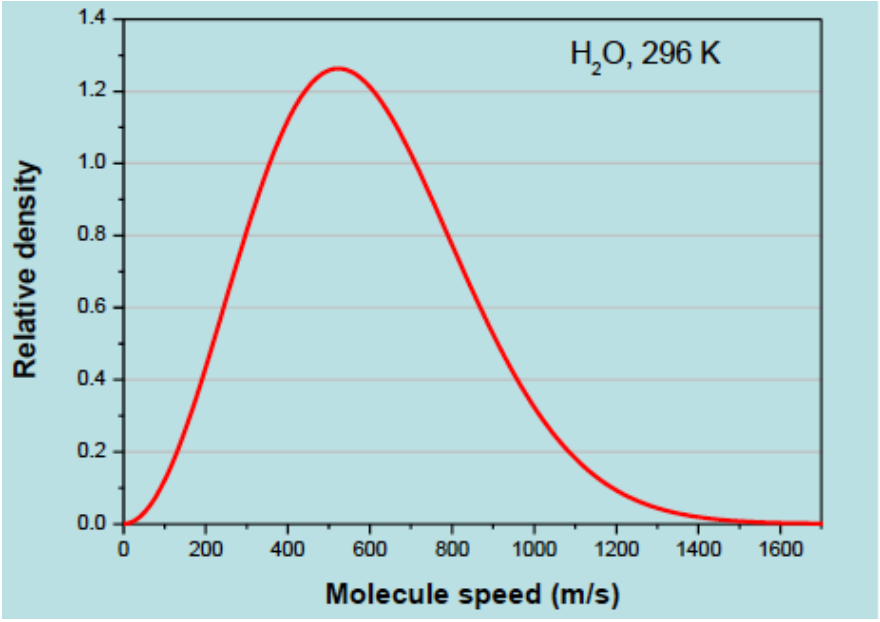

Galatry, soft collision, model: small changes per collision; Dicke narrowing parameter β related to diffusion coefficient

Nelkin-Ghatak or Raution, hard collision, model: velocity changing rate related to diff. coeff.

Adapted from Ha Tran, SPEC-ATMOS Fréjus 2015

Beyond the Voigt profile: Dicke narrowing

Dicke narrowing is the effect of a collisional narrowing due to velocity changing collisions

Here the H_2 J=0←2 quadrupole transition observed by Campargue et al., PCCP (2012):

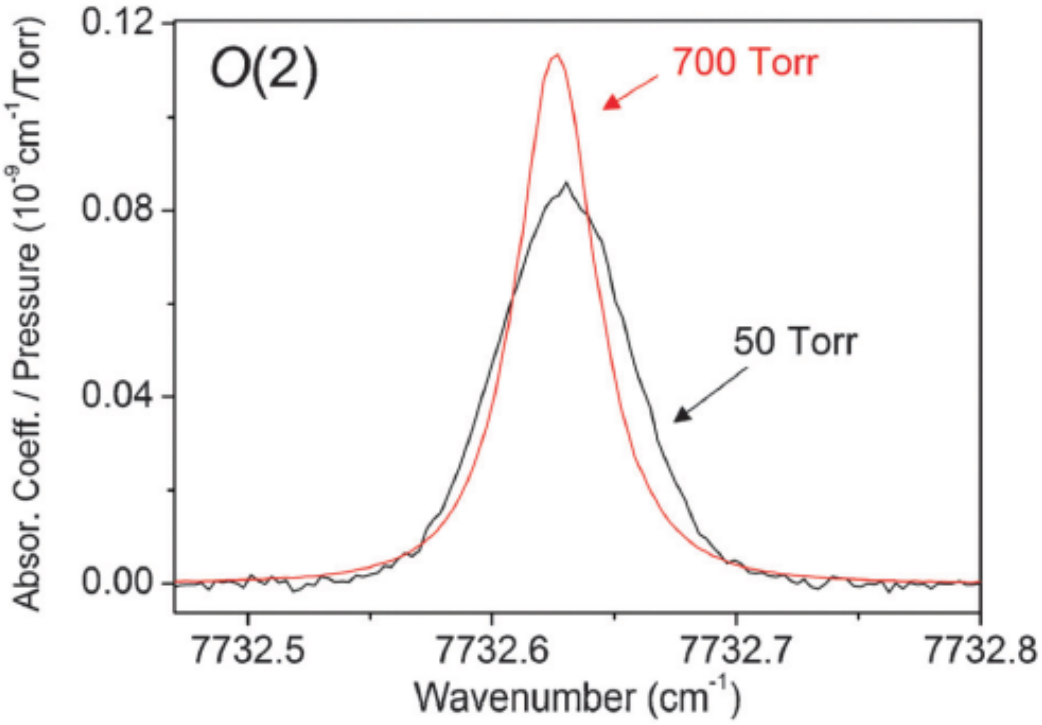

The absorption coefficients have been divided by the pressure. Note the pressure shift of -0.003 cm^{-1}.

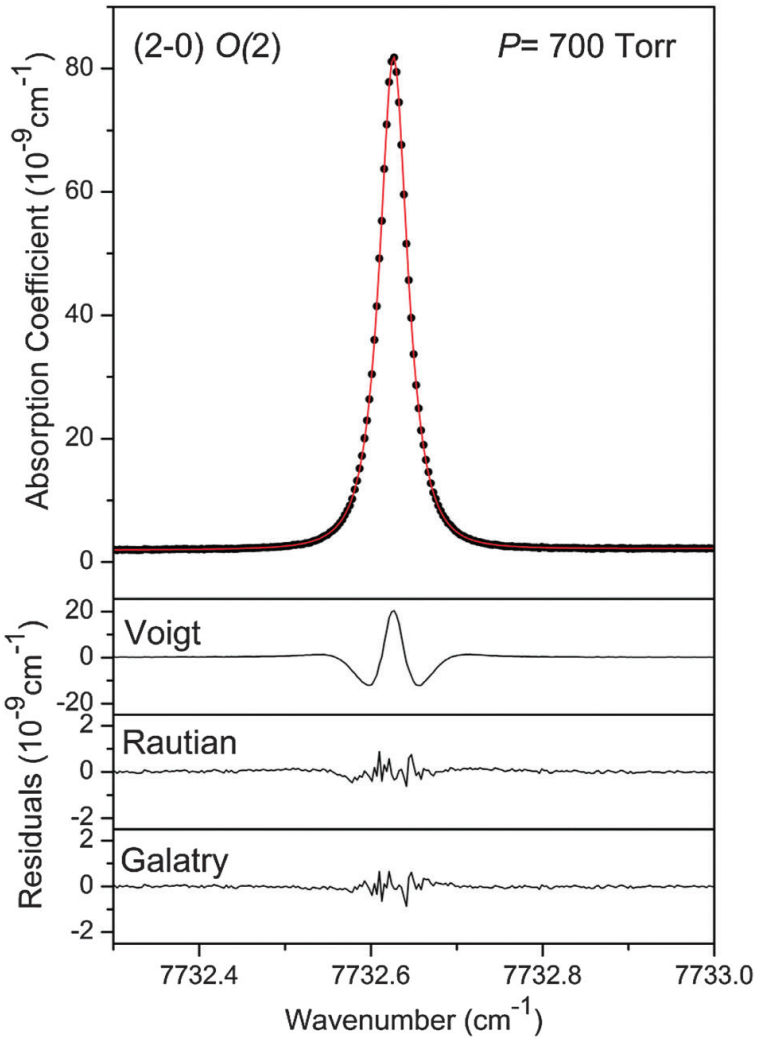

Beyond the Voigt profile

Dicke narrowing is the effect of a reduction of Doppler broadening due to velocity changing ("averaging") collisions, which may either be "soft" or "hard" (generally determined by the relative mass of the absorber and the matrix molecules).

Speed-dependence accounts for the collisional line width (narrowing) and line center shift being dependent upon the speed of the absorber.

Correlations between velocity-changing and dephasing collisions may need to be taken into account.

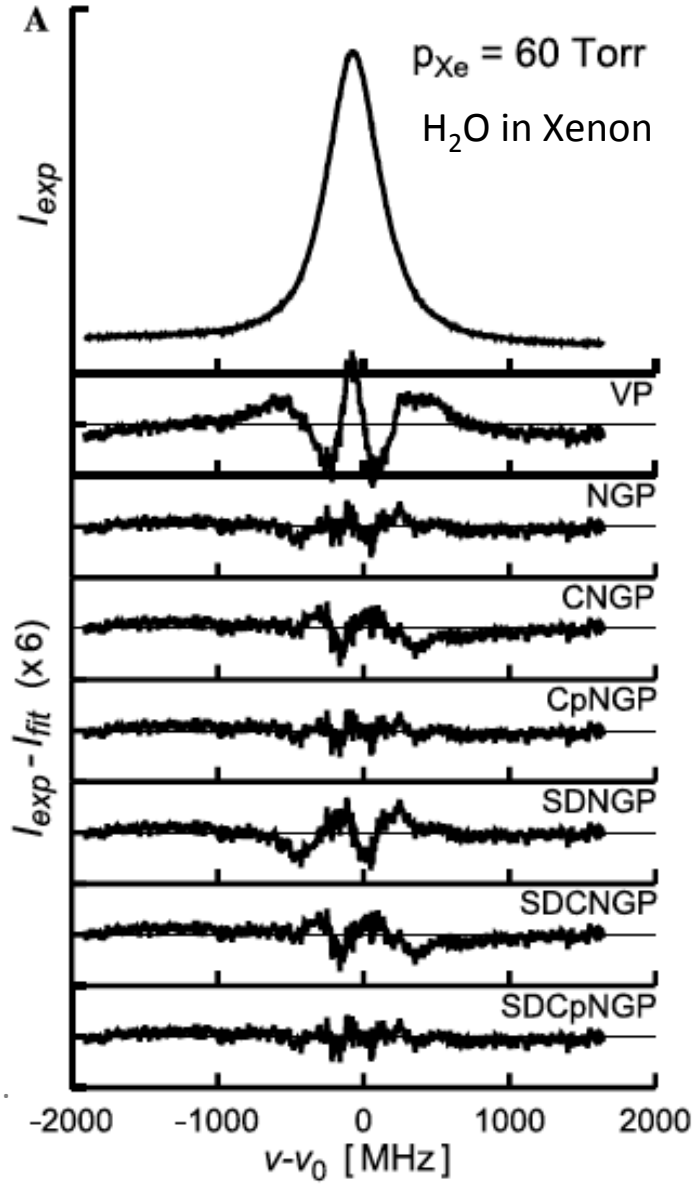

Lisak et al.(2004). An accurate comparison of lineshape models on H_2O lines in the spectral region around 3 μm. *Journal of Molecular Spectroscopy*, *227*(2), 162–171

Beyond the Voigt profile

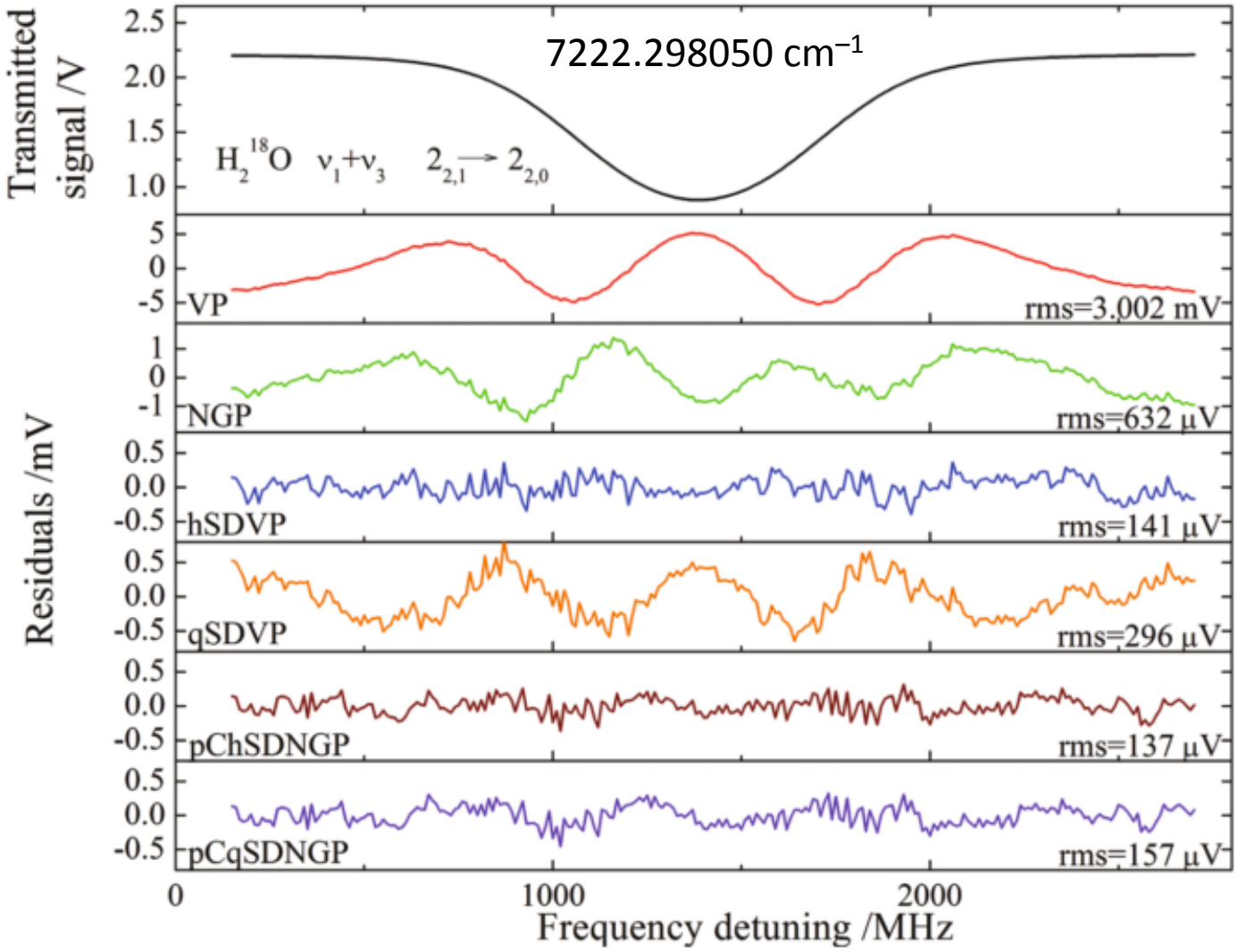

≡ Hartmann-Tran Profile

Tennyson *et al.* (2014). Recommended isolated-line profile for representing high-resolution spectroscopic transitions (IUPAC Technical Report). *Pure and Applied Chemistry*, *86*(12), 1931–1943

Beyond the Voigt profile

Table 1 Summary of line-profile models considered. *N* is the number of parameters required to characterize the line shape for a single isolated transition at a given temperature for a given pair of molecules.

Acronym	Profile name	Parameters		Mechanism		
		N		SD[a]	VC[a]	Correlation
DP	Doppler	1	Γ_D	No	No	No
LP	Lorentz	2	Γ, Δ	No	No	No
VP	Voigt	3	Γ_D, Γ, Δ	No	No	No
GP	Galatry	4	$\Gamma_D, \Gamma, \Delta, \nu_{VC}$	No	Soft	No
RP	Rautian	4	$\Gamma_D, \Gamma, \Delta, \nu_{VC}$	No	Hard	No
HTP	Hartmann–Tran =pCqSDNGP	7	$\Gamma_D, \Gamma_0, \Delta_0, \Gamma_2, \Delta_2, \nu_{VC}, \eta$	Yes	Hard	Yes

Recommended profile by IUPAC Task Group on “Intensities and line shapes in high-resolution spectra of water isotopologues from experiment and theory” for implementation in future databases (read: HITRAN):

“The proposed line shape is based on six temperature-dependent, collisional parameters for each line and perturber plus the Doppler width, Γ_D, fixed to its theoretical value. These parameters give the model the flexibility to include all the major “non-Voigt” effects.”
“Considering the relatively large number of parameters required for the full HTP model and the correlations between them, fitting measured individual spectra is unlikely to yield a well-constrained parameter set. This means that a multi-spectrum procedure must be used. Furthermore, to remove the partial correlations between the various parameters, it is essential to use spectra recorded in a **broad pressure range** and with a **high signal-to-noise ratio**.”

Power broadening: a physically intuitive picture

In case of a strong radiation field, $n_2 \neq 0$ and $\Delta n \neq n_1$. To be precise, $\Delta n = n_1 - n_2 < n = n_1 + n_2$ and the determination of the total number density n is no longer quantitative.

We assume that the molecule is coherently driven back and forth between the lower and the upper level and that other relaxation mechanisms (collisions!) can be neglected. It therefore spends on average only half of one Rabi cycle in the upper state.

Using the time-energy uncertainty relation we obtain:

$$\Delta E \cdot \Delta t \approx \hbar$$

$$\left(h\Delta\nu_P\right)\cdot\left(\frac{\tau_R}{2}\right) \approx \hbar$$

$$\Delta\nu_P \approx \frac{1}{\pi\tau_R} = \frac{\omega_R}{2\pi^2} = \frac{\gamma}{\pi^2}$$

$$\Delta\nu_P \approx \frac{\mu E}{\pi h}$$

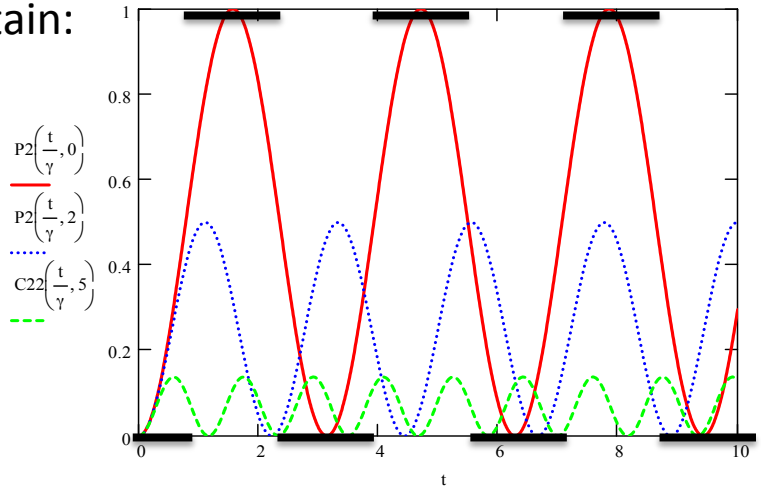

The observed line width increases linearly with the electric field strength ∝ √(laser power)

$$I = \frac{1}{2}\varepsilon_0 E^2 c$$

The Bouguer - Lambert - Beer law of linear absorption

The decrease in intensity *dI* of a light beam of intensity I, due to an infinitesimally small slab of absorber with thickness *dz,* is proportional to the absorption coefficient α:

$$dI = -\alpha\ I\ dx$$

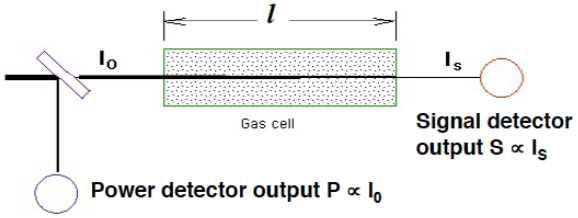

Integration of which yields:

$$\frac{I}{I_0} = e^{-\alpha l} = e^{-\Delta n \sigma l} \quad \text{with} \quad \alpha(\nu) = \left[n_1 - \frac{g_1}{g_2} n_2 \right] \sigma(\nu) = \Delta n\ \sigma(\nu)$$

$n_2, g_2=3$

$$\sigma(\nu) = S \cdot f(\nu)$$

$n_1, g_1=1$

$$S = \frac{h\nu}{c} \frac{1}{Q_{tot}(T)} \left(g_1 B_{12} e^{-\frac{E_1}{kT}} - g_2 B_{21} e^{-\frac{E_2}{kT}} \right)$$

In the weak-field case and relatively low temperature, $n_2 \approx 0$, and we may write:

$$\frac{I}{I_0} = e^{-\alpha l} = e^{-S \cdot f(\nu) \cdot n \cdot l}$$

The Bouguer – Beer law of linear absorption

Spectrum registration by direct absorption of tunable laser radiation

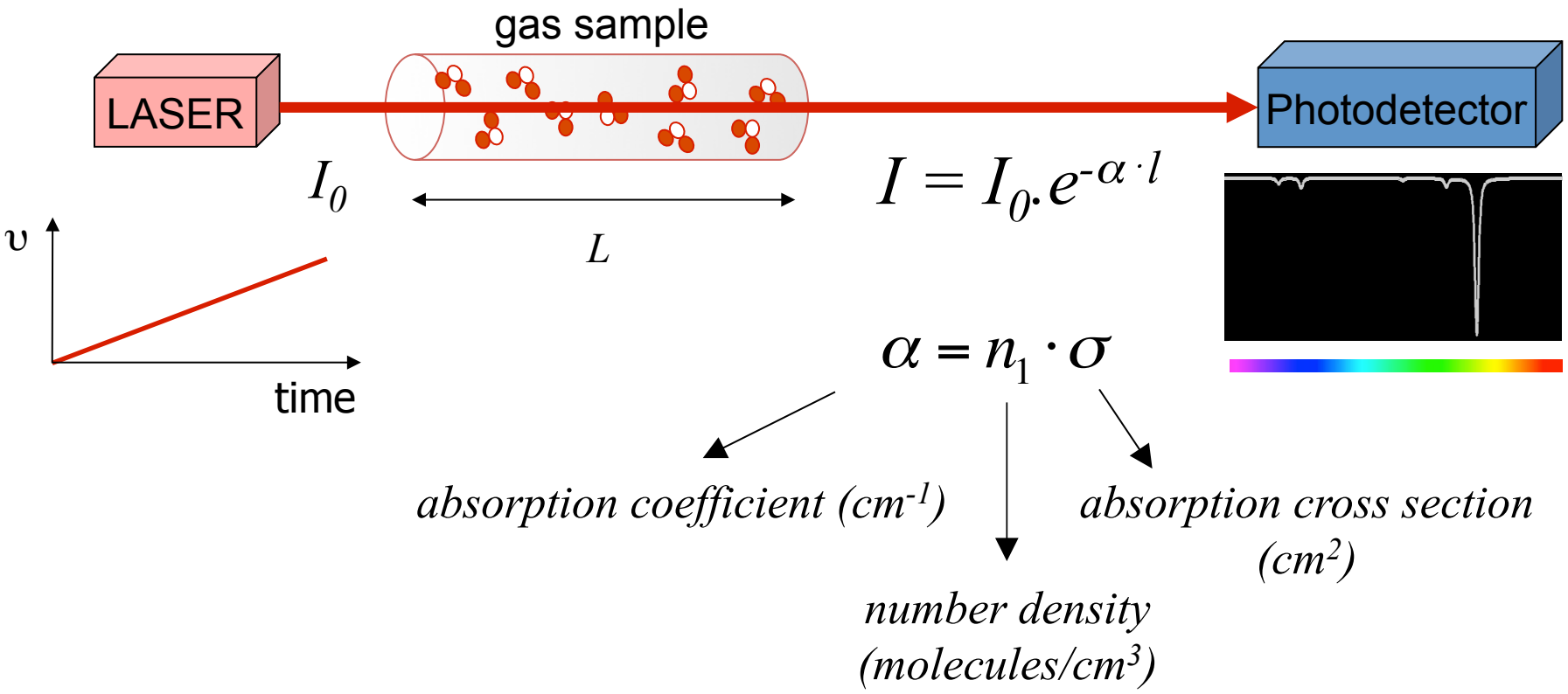

The Bouguer – Beer law of linear absorption

Spectrum registration by direct absorption of tunable laser radiation

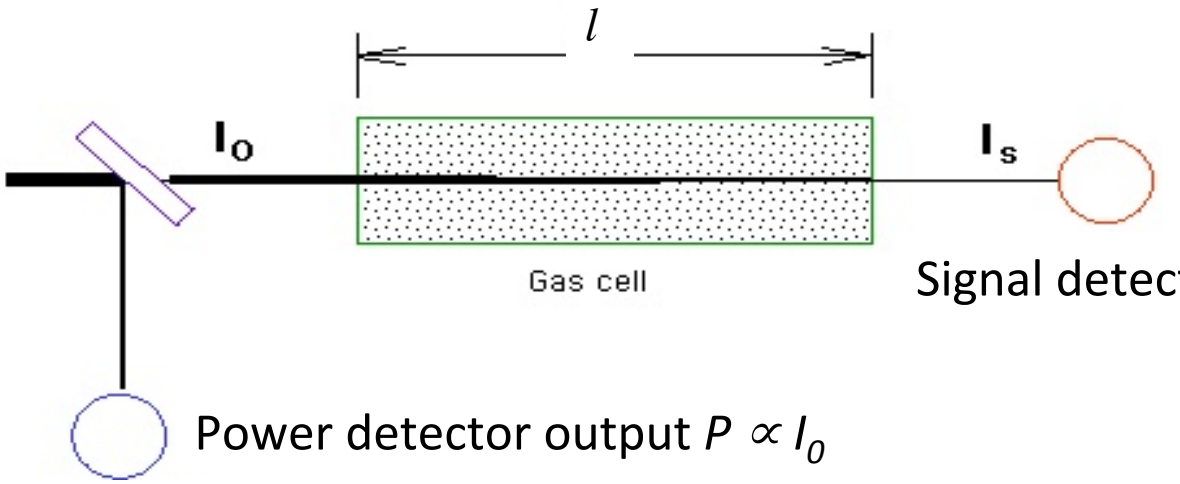

$$\frac{I_S}{I_0} = \alpha(\nu) = \sigma(\nu) \int_{-\infty}^{\infty} d(\nu) \, d\nu = S \, f(\nu) \cdot n \cdot l = -\ln\left(\frac{I_S}{I_0}\right)$$

$\int_{-\infty}^{\infty}$ absorbance $d\nu$ = line strength × 1 × number density × path length

Note: accurate determination of integrated absorption requires a very accurate frequency scale!

The Bouguer – Beer law of linear absorption

absorptance (transmission)

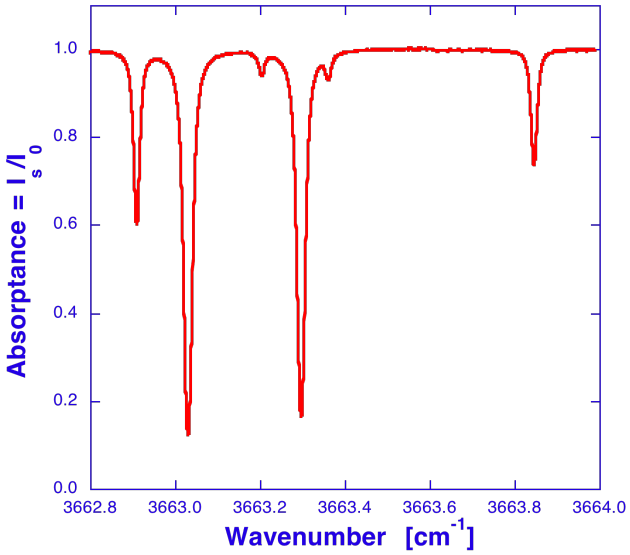

$$a = -Ln\left(\frac{I_s}{I_0}\right)$$

absorbance (a)

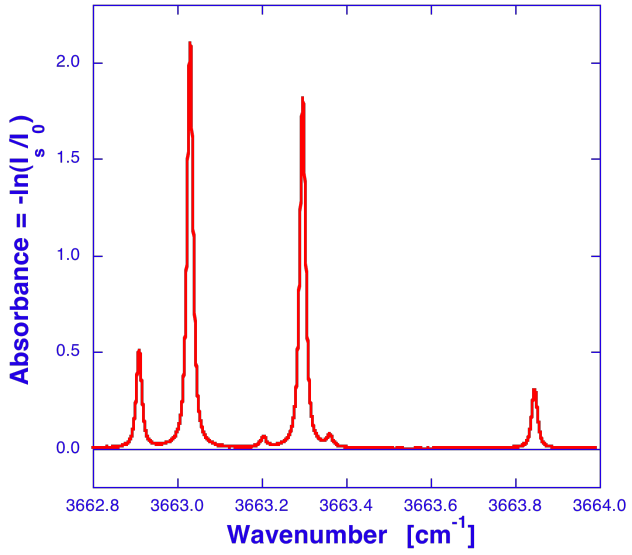

- intensities (area) proportional to molecular concentration
- spectrum is sum of its constituents

The Bouguer – Beer law of linear absorption

Quantitative absorption spectroscopy: using the Bouguer-Lambert-Beer law

The absorbance a, and in this way the molecular density n, is derived through Bouguer's law

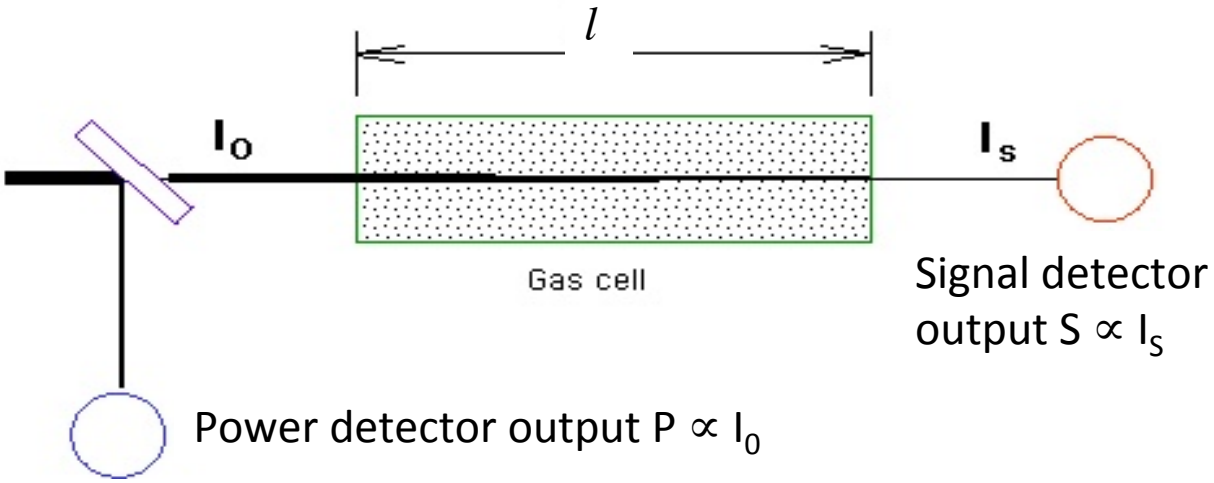

$$\frac{I_S}{I_0} = e^{-\alpha \cdot l} \quad \Rightarrow \quad a = S \cdot f(\nu) \cdot n \cdot l = -\ln\left(\frac{I_S}{I_0}\right)$$

$$-\ln\left(\frac{S}{P}\right) = -\ln\left(\frac{k_s \cdot I_S}{k_p \cdot I_0}\right) = -\ln\left(\frac{I_S}{I_0}\right) - \ln\left(\frac{k_s}{k_p}\right)$$

measured — absorbance — constant off-set

A note on units

Wavelength λ [L] μm (10^{-6} m), nm (10^{-9} m), Å (10^{-10} m)

Wavenumber $\tilde{\nu}$ [L^{-1}] cm^{-1}

Frequency ν [T^{-1}] Hz (s^{-1}), MHz (10^6 Hz), GHz (10^9 Hz), THz (10^{12} Hz)

Angular frequency ω [T^{-1}] radians/second

Energy E [ML^2T^{-2}] J, or derived units such as cm^{-1}, eV

Conversion based on the following relations:

$$\nu = \omega/(2\pi) = c/\lambda = c\ \tilde{\nu}$$

$$E = h\nu = h\omega = hc/\lambda = q_e V$$

symbol	quantity	value / unit
c	speed of light in vacuum	2.997 924 58 10^{10} cm s^{-1}
e	electron / proton charge	1.602 177 10^{-19} C
h	Planck constant	6.626 075 10^{-34} J s
R	molar gas constant	8.314 510 J mol^{-1} K^{-1}
N_A	Avogadro constant	6.022 137 10^{23} mol^{-1}
k	Boltzmann constant	1.380 658 10^{-23} J K^{-1}
u	atomic mass unit	1.660 540 10^{-27} kg
m_p	proton rest mass	1.672 623 10^{-27} kg
m_e	electron rest mass	9.109 389 10^{-31} kg
a_0	Bohr radius	0.529 177 25 10^{-10} m

USEFUL CONVERSION FACTORS (Hollas)

Unit	cm^{-1}	MHz	kJ	eV	kJ mol^{-1}
1 cm^{-1}	1	29 979.25	$1.986\,45 \times 10^{-26}$	$1.239\,84 \times 10^{-4}$	$1.196\,27 \times 10^{-2}$
1 MHz	$3.335\,64 \times 10^{-5}$	1	$6.626\,08 \times 10^{-31}$	$4.135\,67 \times 10^{-9}$	$3.990\,31 \times 10^{-7}$
1 kJ	$5.034\,11 \times 10^{25}$	$1.509\,19 \times 10^{30}$	1	$6.241\,51 \times 10^{21}$	$6.022\,14 \times 10^{23}$
1 eV	8065.54	$2.417\,99 \times 10^{8}$	$1.602\,18 \times 10^{-22}$	1	96.485
1 kJ mol^{-1}	83.593 5	$2.506\,07 \times 10^{6}$	$1.660\,54 \times 10^{-24}$	$1.036\,43 \times 10^{-2}$	1

A note on units

Dimensional arguments considering $a(\nu) = \alpha(\nu) \cdot l = S \cdot f(\nu - \nu_0) \cdot n \cdot l$

a is dimensionless

α has dimension of inverse length [L^{-1}]
l has dimension of length [L]
n has dimension of molecules per volume [L^{-3}]
f has dimension of inverse line width [T], or inverse wavenumber [L]

S has dimension of [$L^{-1}L^3T^{-1}$]=[L^2T^{-1}], or [$L^{-1}L^3L^{-1}$]=[L]

Thus, a convenient unit for S is cm/molecule, if we express l in cm, n in molecules per cubic cm, and f in inverse reciprocal centimeter (= cm).

Example: a weak, water isotopologue line near λ=2.7 µm has S=6 10^{-23} $^{cm}/_{molec}$.
Given an absorption path length of 20 meters, and a pressure of 13 mbar at 300K, what is the fractional absorption if the line width is 300 MHz? (assume 100% Lorentz).

$n=N/V=p/(kT)=3.2\ 10^{17}$ molec/cm^3; $\Delta\nu$=300 MHz=0.01 cm^{-1}
$a = 6\ 10^{-23}$ cm·molec^{-1} $(1/\pi)$ $(0.01\ \text{cm}^{-1})^{-1}$ $3.2\ 10^{17}$ molec·cm^{-3} 2000 cm = 1.2
$I/I_0 = \exp(-a) = 0.3$, thus 70% absorption!

A note on units

Line strength units

$$a(\nu) = \alpha(\nu) \cdot l = S \cdot f(\nu - \nu_0) \cdot n \cdot l$$

Unfortunately, in practice there is a plethora of units in use for *S*, e.g., giving the number density by its corresponding pressure at a given temperature.

	$cm^{-2}\,atm^{-1}$ at 300°K	$cm^{-1}\,sec^{-1}\,atm^{-1}$ at 300°K	$cm^{-2}\,atm^{-1}$ at T	$cm^{-1}\,sec^{-1}\,atm^{-1}$ at T	$cm^{-2}\,atm^{-1}$ at STP	$cm^{-1}\,sec^{-1}\,atm^{-1}$ at STP
$cm^{-2}\,atm^{-1}$ at 300°K	1.0	3.3356×10^{-11}	$3.3333T \times 10^{-3}$	$1.1119T \times 10^{-13}$	9.1053×10^{-1}	3.0372×10^{-11}
$cm^{-1}\,sec^{-1}\,atm^{-1}$ at 300°K	2.997925×10^{10}	1.0	$9.9931T \times 10^{7}$	$3.3333T \times 10^{-3}$	2.7297×10^{10}	9.1053×10^{-1}
$cm^{-2}\,atm^{-1}$ at T	$\frac{300}{T}$	$\frac{1.0007}{T} \times 10^{-8}$	1.0	3.3356×10^{-11}	$\frac{273.16}{T}$	$\frac{9.1116}{T} \times 10^{-9}$
$cm^{-1}\,sec^{-1}\,atm^{-1}$ at T	$\frac{8.9938}{T} \times 10^{12}$	$\frac{300}{T}$	2.997925×10^{10}	1.0	$\frac{8.1891}{T} \times 10^{12}$	$\frac{273.16}{T}$
$cm^{-2}\,atm^{-1}$ at STP	1.0983	3.6634×10^{-11}	$3.6609T \times 10^{-3}$	$1.2211T \times 10^{-13}$	1.0	3.3356×10^{-11}
$cm^{-1}\,sec^{-1}\,atm^{-1}$ at STP	3.2925×10^{10}	1.0983	$1.0975T \times 10^{8}$	$3.6609T \times 10^{-3}$	2.997925×10^{10}	1.0
$cm\ mole^{-1}$	2.4617×10^{4}	8.2113×10^{-7}	$8.2056T \times 10^{1}$	$2.7371T \times 10^{-9}$	2.2414×10^{4}	7.4766×10^{-7}
$cm^{2}\,sec^{-1}\,mole^{-1}$	7.3799×10^{14}	2.4617×10^{4}	$2.4600T \times 10^{12}$	$8.2056T \times 10^{1}$	6.7197×10^{14}	2.2414×10^{4}
cm millimole^{-1} (also called dark)	2.4617×10^{1}	8.2113×10^{-10}	$8.2056T \times 10^{-2}$	$2.7371T \times 10^{-12}$	2.2414×10^{1}	7.4766×10^{-10}
$cm^{2}\,sec^{-1}\,millimole^{-1}$	7.3799×10^{11}	2.4617×10^{1}	$2.4600T \times 10^{9}$	$8.2056T \times 10^{-2}$	6.7197×10^{11}	2.2414×10^{1}
$cm^{-2}\,liter\,mole^{-1}$	2.4617×10^{1}	8.2113×10^{-10}	$8.2056T \times 10^{-2}$	$2.7371T \times 10^{-12}$	2.2414×10^{1}	7.4766×10^{-10}
$cm^{-1}\,sec^{-1}\,liter\,mole^{-1}$	7.3799×10^{11}	2.4617×10^{1}	$2.4600T \times 10^{9}$	$8.2056T \times 10^{-2}$	6.7197×10^{11}	2.2414×10^{1}
$cm\ molecule^{-1}$	4.0877×10^{-20}	1.3635×10^{-30}	$1.3626T \times 10^{-22}$	$4.5450T \times 10^{-33}$	3.7220×10^{-20}	1.2415×10^{-30}
$cm^{2}\,sec^{-1}\,molecule^{-1}$	1.2255×10^{-9}	4.0877×10^{-20}	$4.0849T \times 10^{-12}$	$1.3626T \times 10^{-22}$	1.1158×10^{-9}	3.7220×10^{-20}

[a] In converting from the units labeled in the top horizontal row to the units labeled in the left vertical column, move along the top row to the appropriate unit and down the column to the number which appears against the unit to be converted to. This numerical factor is the multiplicative factor. For example, S in units of cm $mole^{-1}$ can be converted to S in $cm^{-2}\,atm^{-1}$ at 300 K by using $S(cm^{-2}\,atm^{-1}\ \text{at}\ 300\ K) = (4.0623 \times 10^{-5}) \cdot S(cm\ mole^{-1})$. Also S in units of cm $mole^{-1}$ can be converted to S in cm $molecule^{-1}$ using $S(cm\ molecule^{-1}) = (1.6605 \times 10^{-24}) \cdot S(cm\ mole^{-1})$

	cm $mole^{-1}$	$cm^{2}\,sec^{-1}\,mole^{-1}$	cm millimole^{-1} (also called dark)	$cm^{2}\,sec^{-1}\,millimole^{-1}$	$cm^{-2}\,liter\,mole^{-1}$	$cm^{-1}\,sec^{-1}\,liter\,mole^{-1}$	cm $molecule^{-1}$	$cm^{2}\,sec^{-1}\,molecule^{-1}$
$cm^{-2}\,atm^{-1}$ at 300°K	4.0623×10^{-5}	1.3550×10^{-15}	4.0623×10^{-2}	1.3550×10^{-12}	4.0623×10^{-2}	1.3550×10^{-12}	2.4464×10^{19}	8.16(× 1
$cm^{-1}\,sec^{-1}\,atm^{-1}$ at 300°K	1.2178×10^{6}	4.0623×10^{-5}	1.2178×10^{9}	4.0623×10^{-2}	1.2178×10^{9}	4.0623×10^{-2}	7.3340×10^{29}	2.44 × 1
$cm^{-2}\,atm^{-1}$ at T	$\frac{1.2187}{T} \times 10^{-2}$	$\frac{4.0651}{T} \times 10^{-13}$	$\frac{1.2187}{T} \times 10^{1}$	$\frac{4.0651}{T} \times 10^{-10}$	$\frac{1.2178}{T} \times 10^{1}$	$\frac{4.0651}{T} \times 10^{-10}$	$\frac{7.3391}{T} \times 10^{21}$	2.44 × 1
$cm^{-1}\,sec^{-1}\,atm^{-1}$ at T	$\frac{3.6535}{T} \times 10^{8}$	$\frac{1.2187}{T} \times 10^{-2}$	$\frac{3.6535}{T} \times 10^{11}$	$\frac{1.2187}{T} \times 10^{1}$	$\frac{3.6535}{T} \times 10^{11}$	$\frac{1.2187}{T} \times 10^{1}$	$\frac{2.2002}{T} \times 10^{32}$	7.33 × 1
$cm^{-2}\,atm^{-1}$ at STP	4.4614×10^{-5}	1.4882×10^{-15}	4.4614×10^{-2}	1.4882×10^{-12}	4.4614×10^{-2}	1.4882×10^{-12}	2.6867×10^{19}	8.96 × 1
$cm^{-1}\,sec^{-1}\,atm^{-1}$ at STP	1.3375×10^{6}	4.4614×10^{-5}	1.3375×10^{9}	4.4614×10^{-2}	1.3375×10^{9}	4.4614×10^{-2}	8.0546×10^{29}	2.68 × 1
$cm\ mole^{-1}$	1.0	3.3356×10^{-11}	1.0 × 10^{3}	3.3356×10^{-8}	1.0 × 10^{3}	3.3356×10^{-8}	6.0221×10^{23}	2.00 × 1
$cm^{2}\,sec^{-1}\,mole^{-1}$	2.997925×10^{10}	1.0	2.997925×10^{13}	1.0 × 10^{3}	2.997925×10^{13}	1.0 × 10^{3}	1.8054×10^{34}	6.02 × 1
cm millimole^{-1} (also called dark)	1.0×10^{-3}	3.3356×10^{-14}	1.0	3.3356×10^{-11}	1.0	3.3356×10^{-11}	6.0221×10^{20}	2.00 × 1
$cm^{2}\,sec^{-1}\,millimole^{-1}$	2.997925×10^{7}	1.0 × 10^{-3}	2.997925×10^{10}	1.0	2.997925×10^{10}	1.0	1.8054 × 10^{31}	6.02 × 1
$cm^{-2}\,liter\,mole^{-1}$	1.0 × 10^{-3}	3.3356×10^{-14}	1.0	3.3356×10^{-11}	1.0	3.3356×10^{-11}	6.0221×10^{20}	2.00 × 1
$cm^{-1}\,sec^{-1}\,liter\,mole^{-1}$	2.997925×10^{7}	1.0 × 10^{-3}	2.997925×10^{10}	1.0	2.997925×10^{10}	1.0	1.8054 × 10^{31}	6.02 × 1
$cm\ molecule^{-1}$	1.6605×10^{-24}	5.5390×10^{-35}	1.6605×10^{-21}	5.5390×10^{-32}	1.6605×10^{-21}	5.5390×10^{-32}	1.0	3.33 × 1
$cm^{2}\,sec^{-1}\,molecule^{-1}$	4.9782×10^{-14}	1.6605×10^{-24}	4.9782×10^{-11}	1.6605×10^{-21}	4.9782×10^{-11}	1.6605×10^{-21}	2.997925×10^{10}	1.0

Smith et al., Intensities and collision broadening parameters from infrared spectra. In *Molecular spectroscopy: Modern research*, Rao, K. N., Ed. Academic Press: 1985; Vol. III.

Molecular spectroscopy: The Born-Oppenheimer approximation

Full QM treatment, including all particles (nuclear and electronic) is a formidable task, even for many small molecules. The B-O approximation:

Since nuclei move much slower than electrons the electronic Schrödinger equation is solved for stationary nuclei at a given internuclear distance R

$\Rightarrow$

Concept of potential energy surfaces

The electronic potential energy becomes part of the potential in which the nuclei move

Separation of energies

$$E = E_{el} + E_{vib} + E_{rot} + E_{trans}$$

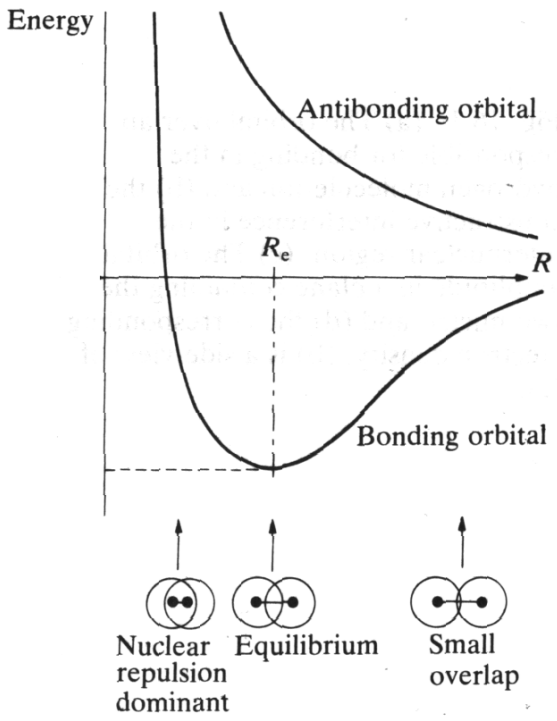

Molecular spectroscopy: The Born-Oppenheimer approximation

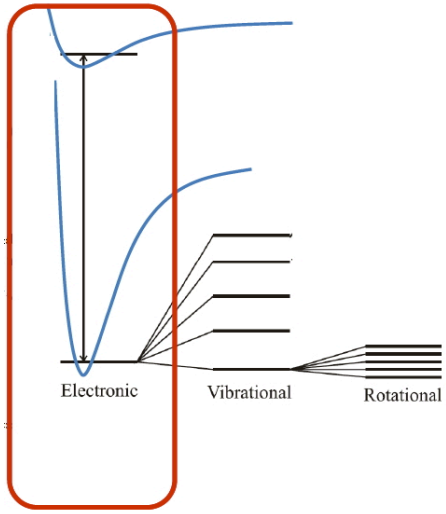

Hamiltonian $H = T + V$ = KE + PE

$$H = T_e + T_n + V_{ee} + V_{nn} + V_{en}$$

Stationary nuclei: $T_n = 0,\ V_{nn} = constant$, such that:

$$H_e \psi_e = E_e \psi_e \text{ , with: } H_e = T_e + V_{ee} + V_{en}$$

This gives the PE as a function of the nuclear coordinates, the PES

B-O approx.: E_e is part of the potential energy field in which the nuclei move:

$$H_n \psi_n = E_n \psi_n \text{ , with: } H_n = T_n + V_{nn} + E_e$$

$$\psi = \psi_e(q,\sigma;Q) \cdot \psi_n(Q), \text{ and: } E = E_e + E_n$$

Since the energy differences are large: $\psi_n = \psi_v \psi_r$, and: $E_n = E_v + E_r$

Thus: $\psi = \psi_e(q,\sigma;Q)\ \psi_v(Q)\ \psi_r(Q)$, and: $E = E_e + E_v + E_r$

Molecular spectroscopy: Potential Energy Surfaces

We can solve the electronic Schrödinger equation for each nuclear configuration:

$$\left\{-\sum_{i=1}^{n}\frac{\hbar^2}{2m_e}\nabla_i^2 + V(q,Q)\right\}\psi_e(q,\sigma;Q) = E_e(Q)\psi_e(q,\sigma;Q)$$

The nuclei now move on the effective potential energy surface $E_e(Q)$ that is obtained by solving the above equation for all values of the nuclear coordinates Q:

$$\left\{-\sum_{i=1}^{N}\frac{\hbar^2}{2M_i}\nabla_i^2 + E_e(Q)\right\}\psi_n(Q) = E_n\psi_n(Q)$$

As an example we show the H_3 PES representation of the prototype exchange reaction $H+H_2 \rightarrow H_2+H$ in the linear configuration (bending angle of 180°) as a prototype of the general bimolecular exchange reaction $A+BC \rightarrow AB+C$:

Molecular spectroscopy: Potential Energy Surfaces

As an example we show the H_3 PES representation of the prototype exchange reaction $H+H_2 \rightarrow H_2+H$ in the linear configuration (bending angle of 180°) as a prototype of the general bimolecular exchange reaction $A+BC \rightarrow AB+C$:

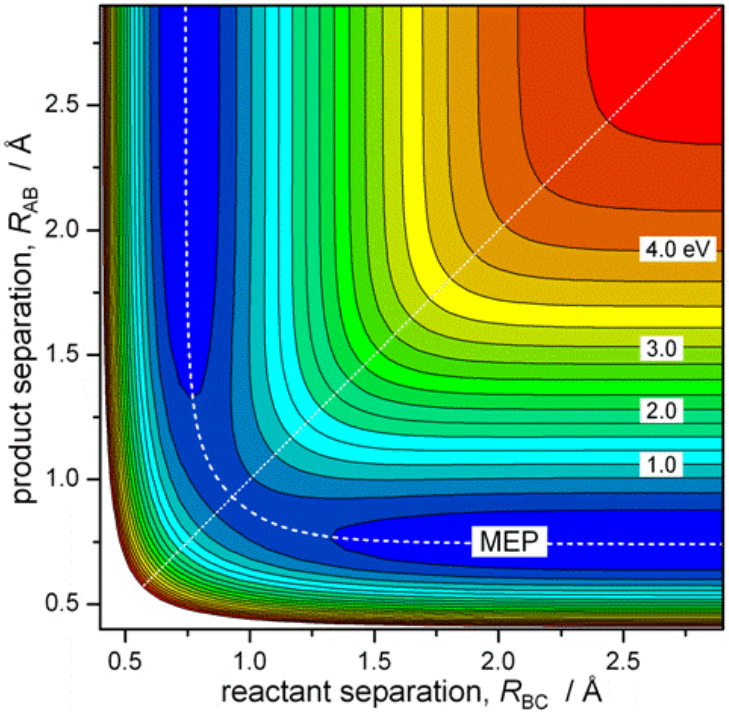

Figure 1: Contour plot of the H_3 potential energy surface in linear geometry (*A-B-C* bending angle α = 180°). The minimum energy path (MEP) from the reactant (R_{AB} large) to the product valley (R_{BC} large) is indicated. The diagonal line separates the reactant and product regions of the potential. Both lines cross at the transition state (saddle point on the potential).

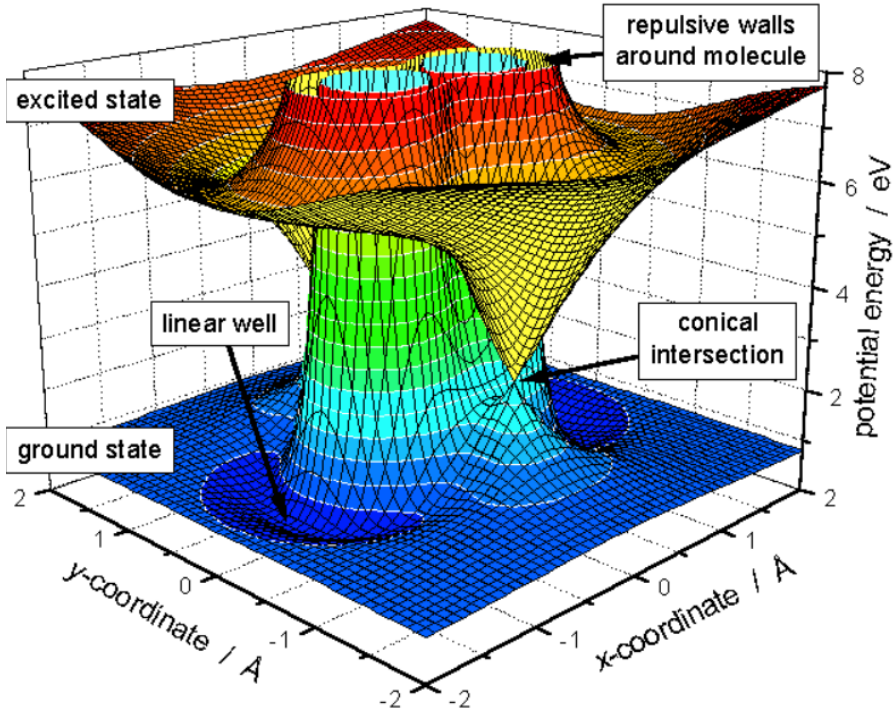

Figure 3: 3D surface plot of the ground and first excited state of the H_3 potential energy surface. At equilateral triangular geometry (D_{3h} symmetry), the ground state energy surface touches the surface of the first excited state and forms a conical intersection (cf. Fig. 1).

Molecular spectroscopy: Potential Energy Surfaces

Another example is given by the He-Cl_2 Van der Waals dimer, which has potential minima in both the linear (180°) and T-shaped (90°-bending angle) configurations. Spectroscopic data confirmed early on that the ground state is T-shaped, but it took about another decade before a reasonable consensus was reached about the equilibrium ground state geometry

The frequencies of intermolecular normal modes of both configurations are similar but the vibrational ZPE of the linear configuration is larger because of its greater number of vibrational degrees of freedom. The difference in vibrational ZPE exceeds the difference in electronic energies, which makes the T-shaped configuration the ground vibrational state.

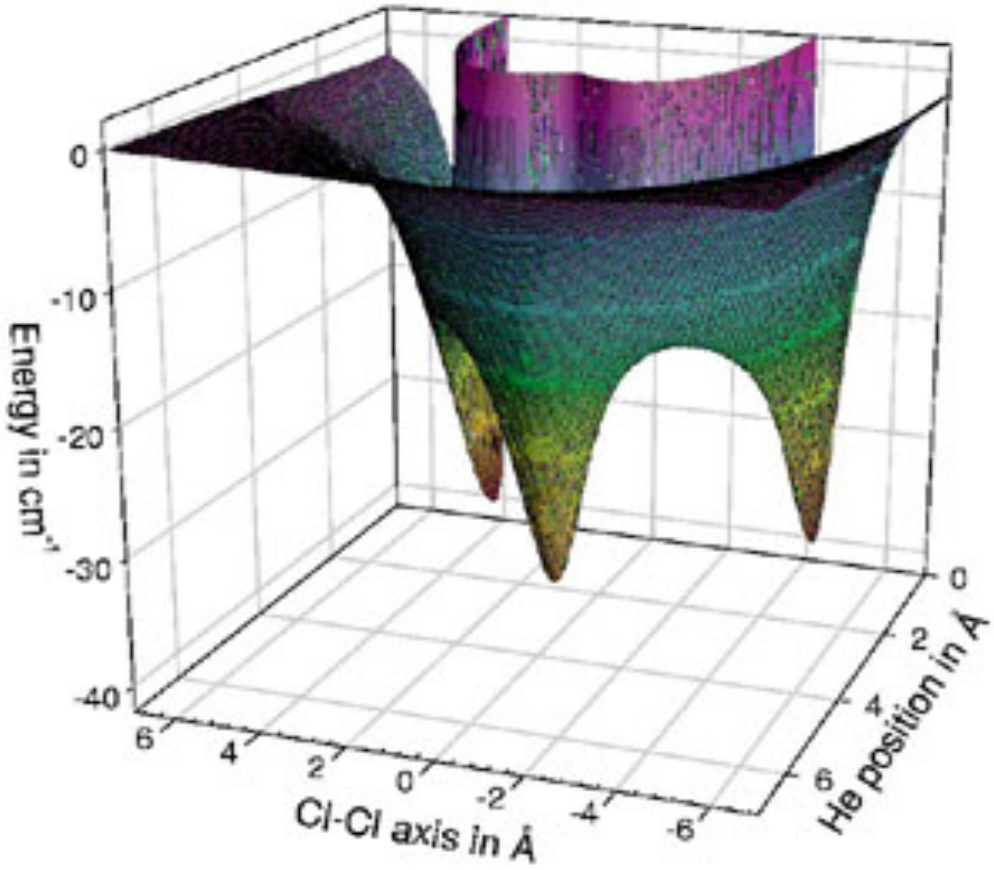

Figure from Kenneth Janda, University of California, Irvine.

See: Cybulski & Holt, *Ab initio potential energy surfaces for He–Cl2, Ne–Cl2, and Ar–Cl2*, J. Chem. Phys. 110, 7745 (1999), and references therein.

Molecular spectroscopy: Potential Energy Surfaces and energy levels

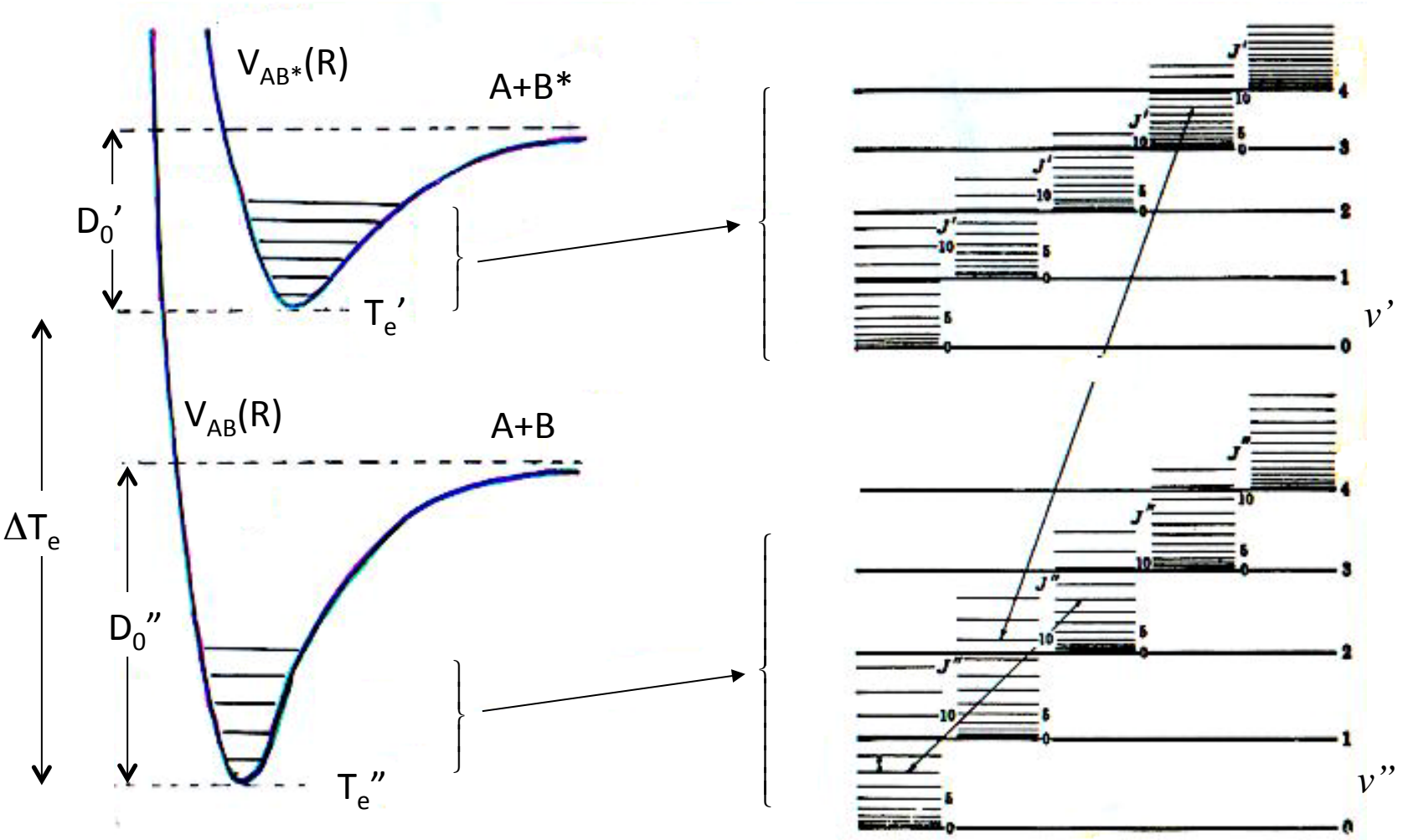

Molecular spectroscopy: rotation

What are the associated frequencies?

consider rotating molecule, e.g. $H^{35}Cl$ (permanent dipole on which the EM field can act)

Classically: orbital angular momentum $L = I\omega = I\,2\pi\nu$, thus: $\nu = L/(2\pi I)$

Quantum:
$$\nu_J = \frac{\hbar\sqrt{J(J+1)}}{2\pi I} \approx \frac{\hbar J}{2\pi I}$$

(all data from: Herzberg, *Spectra of diatomic molecules*)

$$I = \mu r_e^2 = \frac{m_1 m_2}{m_1 + m_2} r_e^2 = \frac{35 \cdot 1.66054 \cdot 10^{-27} kg}{36} (1.2746 \ \ \text{Å})^2 = 2.623 \cdot 10^{-47} \ \ kg \cdot m^2$$

$$\nu_1 = \frac{h}{4\pi^2 I} = \frac{6.62610^{-34} Js}{4\pi^2 \cdot 2.6210^{-47} kgm^2} = 6.4110^{11} s^{-1} \cong 21.3 cm^{-1}$$

(true: 21.18 cm^{-1}; MW-FIR)

Molecular spectroscopy: electronic motion

What are the associated transition frequencies?

consider electron orbiting around H-atom:

$$I = \mu r_e^2 \approx m_{elec} a_0^2 = 9.109 \cdot 10^{-31} kg \ (0.529 \ \ \text{Å})^2 = 2.549 \cdot 10^{-51} \ \ kg \cdot m^2$$

$$\nu_1 = \frac{h}{4\pi^2 I} = \frac{6.62610^{-34} Js}{4\pi^2 \cdot 2.54910^{-51} kg m^2} = 6.59 \ 10^{15} \ \ s^{-1} \cong 21{,}910 \ \ cm^{-1} \cong 27.3 \ \ eV$$

(true 1s → 2p: 10.2 *eV; VUV*)

Estimated frequencies are of the right order of magnitude!

Molecular spectroscopy: Rotation

Classical angular momentum of a rigid body is related to the moment of inertia tensor and the angular frequency vector in the following way:

$$\mathbf{L} = \mathbf{I} \cdot \vec{\omega} = \begin{vmatrix} I_{xx} & I_{xy} & I_{xz} \\ I_{yx} & I_{yy} & I_{yz} \\ I_{zx} & I_{zy} & I_{zz} \end{vmatrix} \cdot \begin{pmatrix} \omega_x \\ \omega_y \\ \omega_z \end{pmatrix} = \begin{pmatrix} I_{xx}\omega_x + I_{xy}\omega_y + I_{xz}\omega_z \\ I_{yx}\omega_x + I_{yy}\omega_y + I_{yz}\omega_z \\ I_{zx}\omega_x + I_{zy}\omega_y + I_{zz}\omega_z \end{pmatrix}$$

with $r^2=x^2+y^2+z^2$:

$$I_{xx} = \sum_{i=1}^{n} m_i \left(r_i^2 - x_i^2\right) \qquad I_{xy} = I_{yx} = -\sum_{i=1}^{n} m_i x_i y_i$$

$$I_{yy} = \sum_{i=1}^{n} m_i \left(r_i^2 - y_i^2\right) \qquad I_{xz} = I_{zx} = -\sum_{i=1}^{n} m_i x_i z_i$$

$$I_{zz} = \sum_{i=1}^{n} m_i \left(r_i^2 - z_i^2\right) \qquad I_{yz} = I_{zy} = -\sum_{i=1}^{n} m_i y_i z_i$$

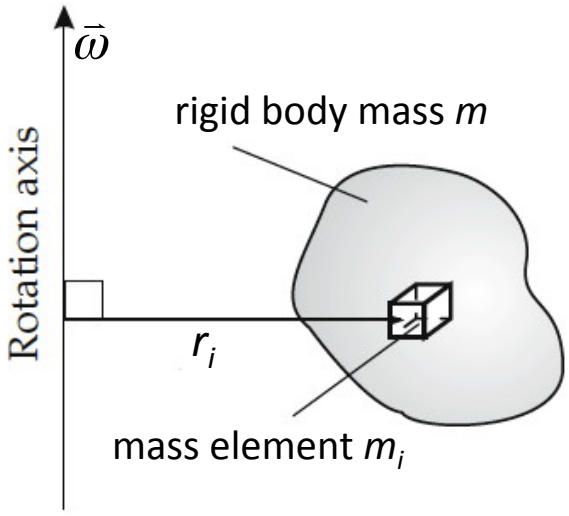

Molecular spectroscopy: Rotation

In the principal axis coordinate system the moment of inertia tensor $\mathbf{I}$ is diagonal:

$$\mathbf{L} = \mathbf{I}\cdot\vec{\omega} = \begin{vmatrix} I_a & 0 & 0 \\ 0 & I_b & 0 \\ 0 & 0 & I_c \end{vmatrix} \cdot \begin{pmatrix} \omega_a \\ \omega_b \\ \omega_c \end{pmatrix} = \begin{pmatrix} I_a\omega_a \\ I_b\omega_b \\ I_c\omega_c \end{pmatrix}$$

$$I_a \le I_b \le I_c$$

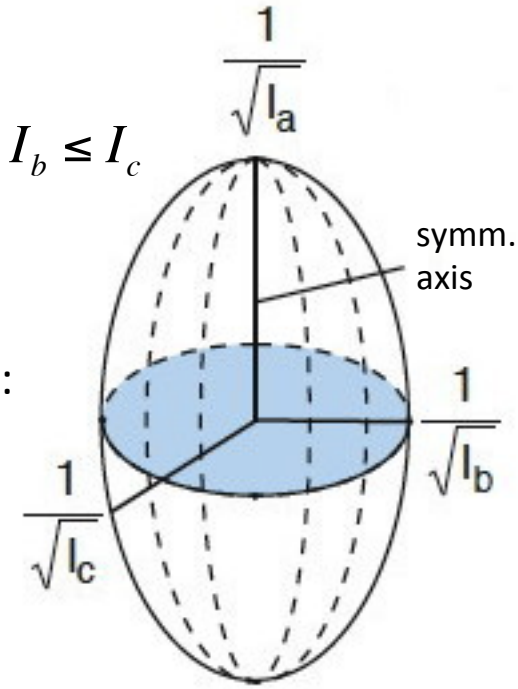

The 6 equations of motion for the individual point masses m_i are:

center of mass acceleration: $\ddot{\mathbf{R}} = \dfrac{\mathbf{F}}{m}$

and torque: $\vec{\tau} = \mathbf{r}\times\mathbf{F} = m_i\,\mathbf{r}\times\dfrac{d\mathbf{v}}{dt} = m_i\,\vec{r}\times\dfrac{d\left(\vec{\omega}\times\vec{r}\right)}{dt}$

$$\vec{\tau} = m_i\frac{d}{dt}\left(\vec{r}\times\vec{\omega}\times\vec{r}\right) = m_i\frac{d}{dt}\left(r^2\vec{\omega} - \left(\vec{r}\cdot\vec{\omega}\right)\vec{r}\right) = \frac{d\mathbf{L}}{dt} = \frac{d\left(\mathbf{I}\cdot\vec{\omega}\right)}{dt}$$

Kinetic energy of rotation:

$$E_{rot} = \frac{1}{2}\vec{\omega}\cdot\left(\mathbf{I}\cdot\vec{\omega}\right) = \frac{1}{2}\left(I_a\omega_a^2 + I_b\omega_b^2 + I_c\omega_c^2\right) = \frac{L_a^2}{2I_a} + \frac{L_b^2}{2I_b} + \frac{L_c^2}{2I_c}$$

Molecular spectroscopy: Rotation

The quantum analogy:

$$p_x \rightarrow -i\hbar \frac{\partial}{\partial x}$$

$$L \rightarrow \hbar\sqrt{J(J+1)}$$

(compare to the centrifugal term in the expression for the radial part of the hydrogen atom wavefunction)

The rotational energy:

$$E_{rot} = \frac{|J_a|^2}{2I_a} + \frac{|J_b|^2}{2I_b} + \frac{|J_c|^2}{2I_c} = \hbar^2 \left(\frac{J_a(J_a+1)}{2I_a} + \frac{J_b(J_b+1)}{2I_b} + \frac{J_c(J_c+1)}{2I_c} \right)$$

Molecular spectroscopy: Rotation

According to the relative sizes of the principal moments of inertia we discern:

Linear: $I_a = 0, I_b = I_c$

Spherical: $I_a = I_b = I_c$

Oblate symmetric: $I_a = I_b \leq I_c$

Prolate symmetric: $I_a \leq I_b = I_c$

Asymmetric: $I_a < I_b < I_c$

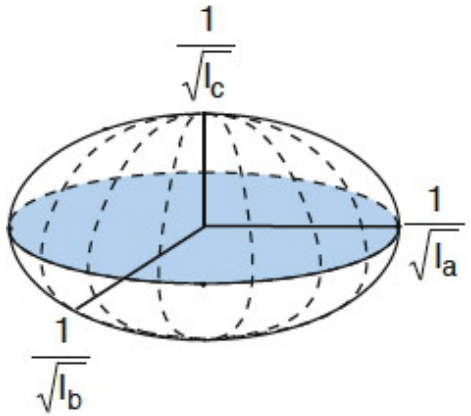

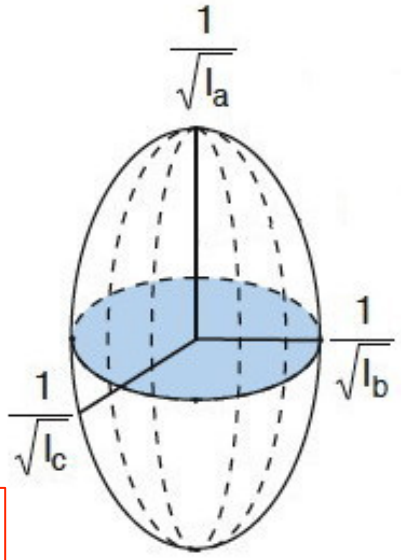

$$E_{rot} = \frac{|J_a|^2}{2I_a} + \frac{|J_b|^2}{2I_b} + \frac{|J_c|^2}{2I_c} = \hbar^2 \left(\frac{J_a(J_a+1)}{2I_a} + \frac{J_b(J_b+1)}{2I_b} + \frac{J_c(J_c+1)}{2I_c} \right)$$

Rotation: the linear rotor

Classicallv:

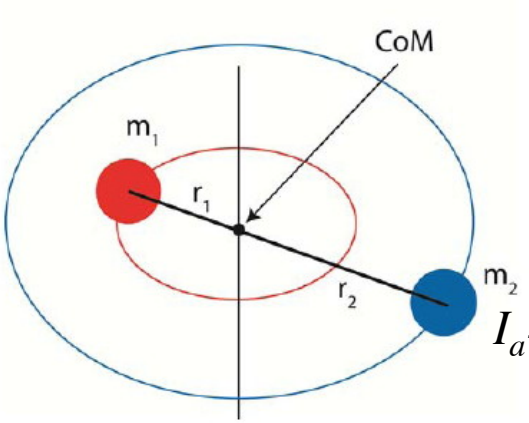

$I_a = 0$

$I_b = I_c$

$$\begin{cases} m_1 r_1 = m_2 r_2 \\ r_1 + r_2 = r \end{cases} \Rightarrow \begin{cases} r_1 = \dfrac{m_1}{m_1 + m_2} r \\ r_2 = \dfrac{m_2}{m_1 + m_2} r \end{cases}$$

$$\vec{v} = \vec{\omega} \times \vec{r}$$

$$\mu = \frac{m_1 m_2}{m_1 + m_2}$$

$$I = \mu r^2$$

$$L = I\omega$$

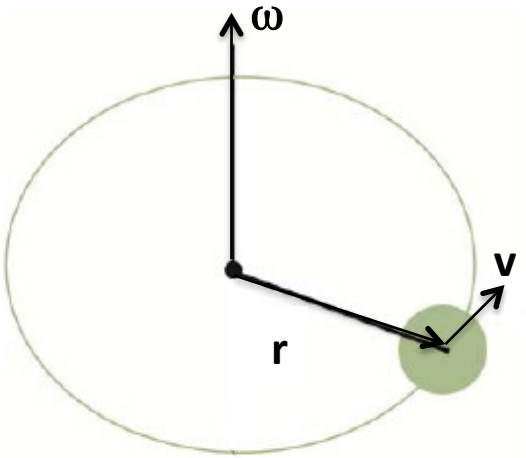

$$E_{rot} = \frac{1}{2}\mu v^2 = \frac{1}{2} I\omega^2 = \frac{L^2}{2I}$$

The QM linear rigid rotor: only one rotational constant *B* and one quantum number *J*=0,1,2,…

$$E_{rot} = \hbar^2 \frac{J(J+1)}{2I} = B\,J(J+1)$$
$$= hc\,\tilde{B}\,J(J+1)$$

with *B* in energy units [J]

with $\tilde{B}$ in wavenumbers [cm^{-1}]

Rotation: the QM linear rotor

We will show that the energy levels require only one rotational constant *B* and only one quantum number *J*=0,1,2,…

$$E_{rot} = \hbar^2 \frac{J(J+1)}{2I} = B\,J(J+1)$$
$$= hc\,\tilde{B}\,J(J+1)$$

with *B* in energy units [J]

with $\tilde{B}$ in wavenumbers [cm^{-1}]

The QM angular momentum operator is: $\mathbf{L} = \mathbf{r} \times \mathbf{p} = -i\hbar\left(\mathbf{r} \times \nabla\right)$

and: $$L^2 = -\hbar^2\left(\frac{1}{\sin\vartheta}\frac{\partial}{\partial\vartheta}\left(\sin\vartheta\frac{\partial}{\partial\vartheta}\right) + \frac{1}{\sin^2\vartheta}\frac{\partial^2}{\partial\phi^2}\right)$$

The Schrödinger equation, with $H = \frac{L^2}{2I}$, thus becomes:

$$-\frac{\hbar^2}{2I}\left(\frac{1}{\sin\vartheta}\frac{\partial}{\partial\vartheta}\left(\sin\vartheta\frac{\partial}{\partial\vartheta}\right) + \frac{1}{\sin^2\vartheta}\frac{\partial^2}{\partial\phi^2}\right)Y(\vartheta,\phi) = EY(\vartheta,\phi)$$

This is recognized as describing the angular dependence of the hydrogen atom wavefunction. Its derivation and solution ere therefore presumed familiar …

Rotation: the QM linear rotor

The Schrödinger equation is solved by a separation of variables: $Y(\theta,\phi) = \Theta(\theta)\Phi(\phi)$ which yields:

$$-\frac{1}{\Theta}\sin\theta\frac{d}{d\theta}\left(\sin\theta\frac{d\Theta}{d\theta}\right) - C_l\sin^2\theta = \frac{1}{\Phi}\frac{d^2\Phi}{d\phi^2} = C_m \qquad \frac{2I\,E}{\hbar^2} = C_l$$

The right-most side of the equation yields: $\Phi_m(\phi) = \frac{e^{im\phi}}{\sqrt{2\pi}}$ with $C_m \equiv -m^2$ and m an integer

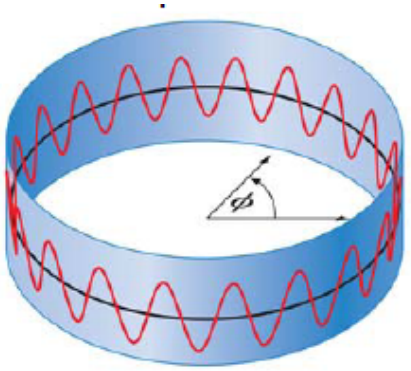

Whereas the left-most side of the equation is written as:

$$\frac{d}{d\xi}\left[\left(1-\xi^2\right)\frac{d\Theta}{d\xi}\right] + \left[C_l - \frac{m^2}{1-\xi^2}\right]\Theta = 0 \qquad \text{with } \xi \equiv \cos\theta$$

The solutions are given in terms of the Legendre polynomials $P_l(cos\theta)$, and with C_l=$l(l$+1) :

$$P_{l,m}(\xi) = (1-\xi^2)^{|m|/2}\frac{d^{|m|}P_l(\xi)}{d\xi^{|m|}}$$

Rotation: the QM linear rotor

The wavefunctions are known as the spherical harmonics:

$$Y_{l,m}(\theta,\phi) = \Theta_{l,m}(\theta)\Phi_m(\phi)$$

$$= \sqrt{\frac{(2l+1)}{4\pi}\frac{(l-m)!}{(l+m)!}} P_{l,m}(\cos\theta)e^{im\phi}$$

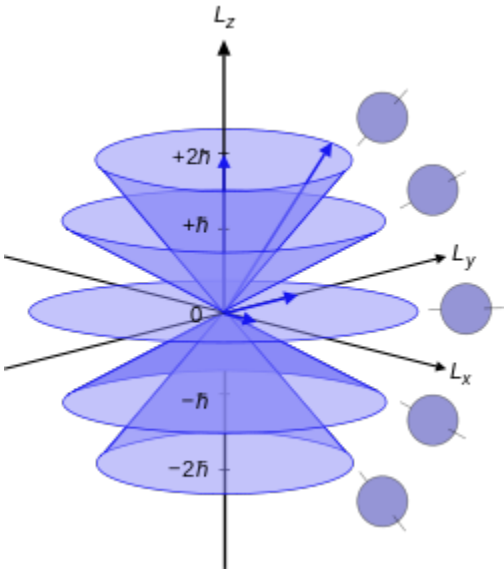

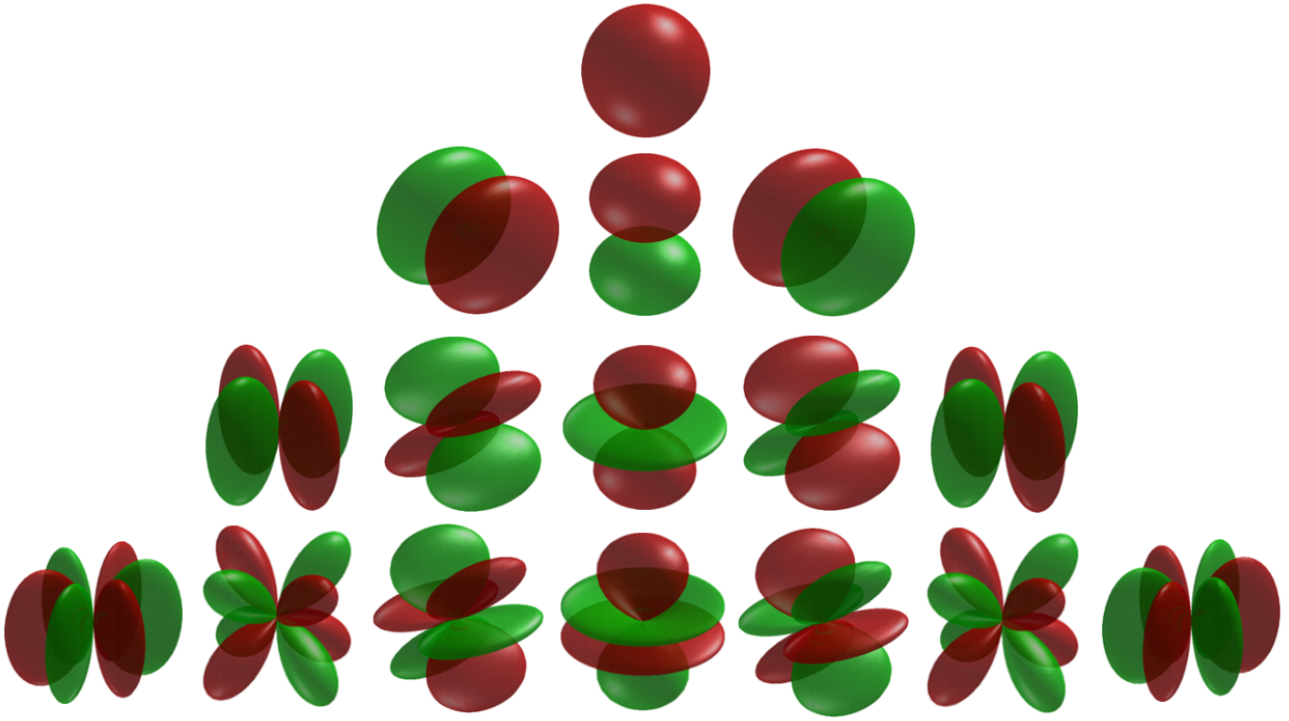

Rotation: the linear rotor

Here we are most interested in the energy levels of the rigid rotor, for which we find (after substitution of *J* for l, and m_J for m):

$$C_l = \frac{2IE}{\hbar^2} \quad \Rightarrow \quad E_J = \frac{\hbar^2}{2I} J(J+1)$$

$$J = 0, 1, 2, \ldots$$

$$m_J = -J, -J+1, \ldots, J-1, J$$

As we will see, transitions occur between neighboring levels, with a spacing that increases linearly with J:

$$\Delta E = E_{J+1} - E_J = 2B(J+1)$$

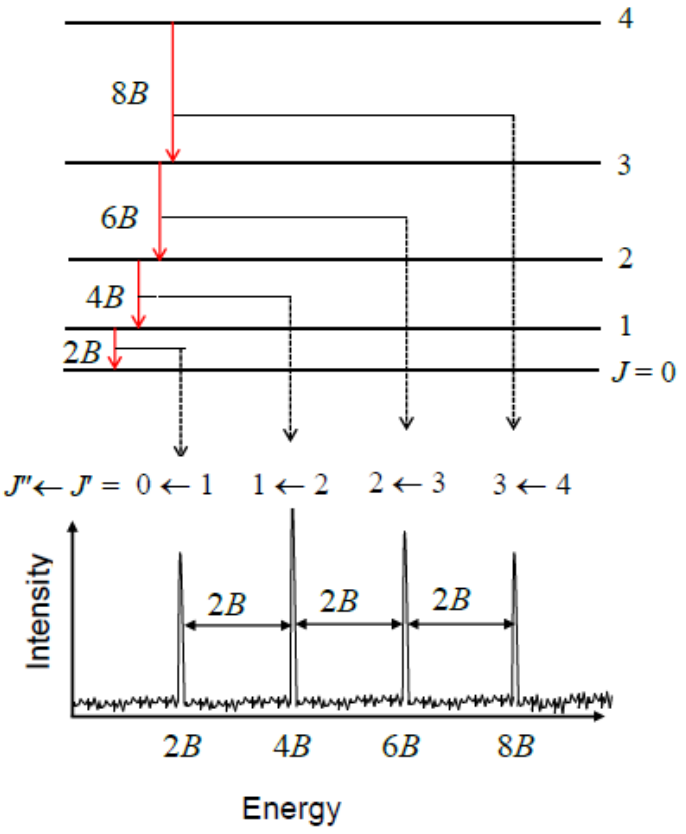

Consequently, the observed absorption lines are equidistant in frequency space.

Rotation: the linear rotor

In the case of a non-rigid molecule, the effect of centrifugal distortion can be described by higher order terms:

$$E_J = BJ(J+1) - DJ^2(J+1)^2 + \ldots$$

where the minus sign assures that the first distortion constant D has a positive value.

Since, in the absence of an external field, the energy is independent of m_J (i.e., the $(2J+1)$ m_J-levels have the same energy), each J-level is **$(2J+1)$-fold degenerate.**

Rotation: the symmetric rotor

Define the parallel and perpendicular moments of inertia with respect to the symmetry axis, the *z*-axis of the molecule:

$$I_\perp = I_x = I_y \neq I_z = I_{//}$$

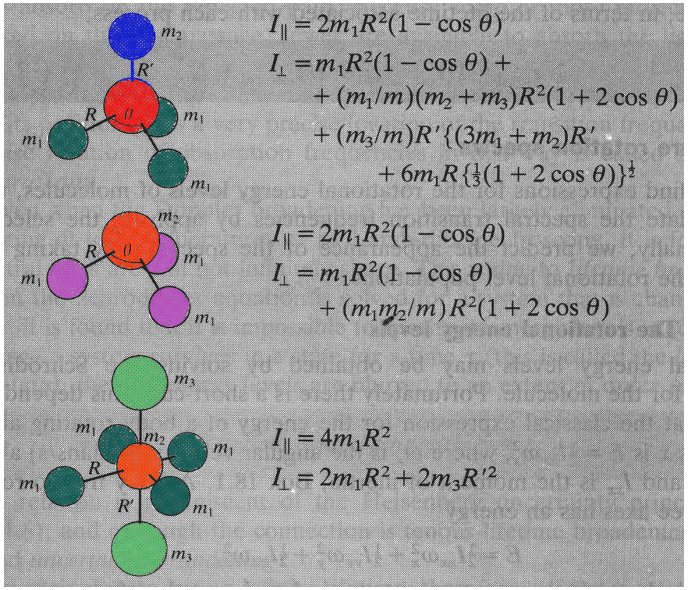

Then: $I_\perp < I_{//}$ for the oblate top (*z* = *c*-axis)

$I_\perp > I_{//}$ for the prolate top (*z* = *a*-axis)

$$E = \frac{J_x^2 + J_y^2}{2I_\perp} + \frac{J_z^2}{2I_{//}} = \frac{J}{2I_\perp} + \left(\frac{1}{2I_{//}} - \frac{1}{2I_\perp}\right)J_z^2$$

Prolate top: $E(J,K) = BJ(J+1) + (A-B)K_a^2$ (4.25)

Oblate top: $E(J,K) = BJ(J+1) + (C-B)K_c^2$ (4.26)

With the rotational constants: $A = \frac{\hbar^2}{2I_a}$, $B = \frac{\hbar^2}{2I_b}$, and $C = \frac{\hbar^2}{2I_c}$. (4.27)

The quantum numbers can take the values: *J*=0, 1, 2, … and *K*=0, ±1, ±2, …, ±*J*.

Rotation: the symmetric rotor

Prolate top: $$E(J,K) = BJ(J+1) + (A-B)K_a^2 \quad (4.25)$$

Oblate top: $$E(J,K) = BJ(J+1) + (C-B)K_c^2 \quad (4.26)$$

With the rotational constants: $A = \frac{\hbar^2}{2I_a}$, $B = \frac{\hbar^2}{2I_b}$, and $C = \frac{\hbar^2}{2I_c}$. (4.27)

Since *E(J, +K) = E(J, -K)*, each *(J,K)*- level except *J*=0 is doubly degenerate.
In addition, the space quantization of the J-vector with respect to an external reference frame gives a (2J+1) degeneracy in the absence of an external field.

Together, this gives a **2(2*J*+1) degeneracy** of each *(J,K)*-level with ***K* ≠ 0**, and a **(2J+1) degeneracy** for all levels with ***K* = 0**.

Rotation: the spherical rotor

For the spherical rotor $A = B = C$, such that the energy values are identical to those of a linear rotor, depending only on the quantum number J:

$$E_J = BJ(J+1) - DJ^2(J+1)^2 + \ldots$$

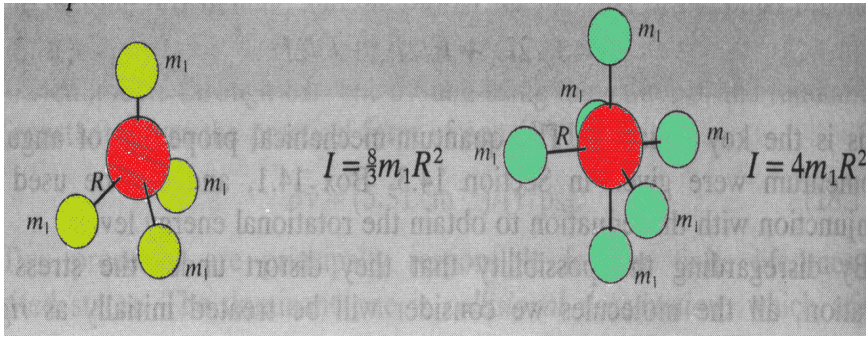

However, the angular momentum is still quantized relative to an arbitrary internal axis: the quantum number K may take any of its $(2J+1)$ values.
In addition, the space quantization of the J-vector with respect to an external reference frame gives a $(2J+1)$ degeneracy in the absence of an external field.

Together, this gives a **$(2J+1)^2$ degeneracy** of each level.

Rotation: K quantum number and internal space quantization

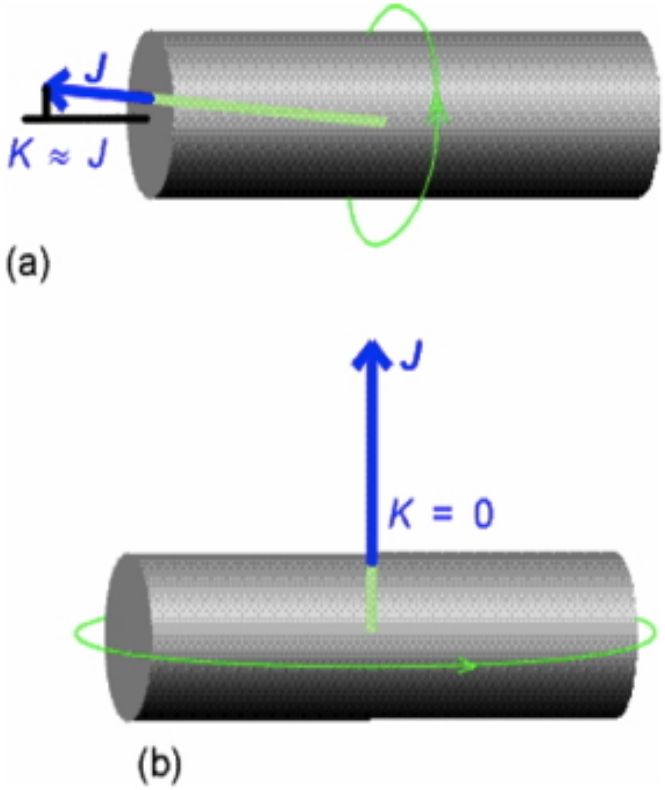

K≈J: rotation around the symmetry axis

K=0: end-over-end rotation

Rotation: m_J quantum number and external space quantization

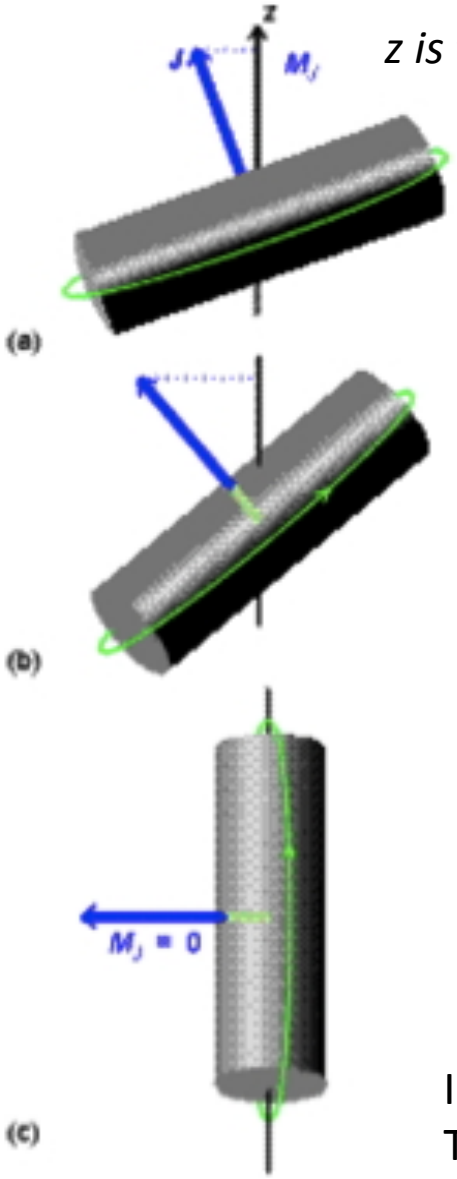

z is the laboratory, external axis

a) $m_J \approx J$: rotation around the laboratory axis

b) intermediate case

c) $m_J = 0$: rotation around an axis perpendicular to the laboratory axis

In all cases $K = 0$ and the molecule undergoes end-over-end rotation. The figures would need to be repeated for different values of K.

Selection rules in rotational spectroscopy

Absorption intensity of a transition in between two levels determined by:

1) the population of the lower level
2) transition matrix element

For an electric dipole transition $\mathbf{R}_{12} = \langle 1|\mathbf{p}|2\rangle$ the components are:

$$\begin{cases} R_x = \langle 1|\mu_x|2\rangle = \langle 1|\mu_0 \sin\vartheta\cos\varphi|2\rangle = \mu_0\langle 1|\sin\vartheta\cos\varphi|2\rangle \\ R_y = \langle 1|\mu_y|2\rangle = \langle 1|\mu_0 \sin\vartheta\sin\varphi|2\rangle = \mu_0\langle 1|\sin\vartheta\sin\varphi|2\rangle \\ R_z = \langle 1|\mu_z|2\rangle = \langle 1|\mu_0 \cos\vartheta|2\rangle = \mu_0\langle 1|\cos\vartheta|2\rangle \end{cases}$$

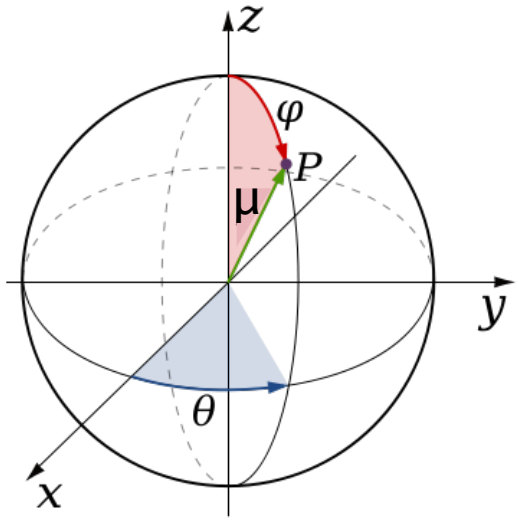

⇒ zero transition probability if $\mu_0 = 0$: pure rotational spectroscopy requires that the molecule possesses **a permanent dipole moment.**

⇒ if $\mu_0 \neq 0$, we use the angular part of the wavefunctions 1 and 2 to derive special requirements that need to be fulfilled in order for $\mathbf{R}_{12}$ to be **not** identical zero: the rotational **selection rules**.

Selection rules in rotational spectroscopy

The angular parts of the wavefunctions of a linear rotor are spherical harmonic functions (as we have seen 9 slides ago):

$$Y_{J,M}(\theta,\phi) = \Theta_{J,M}(\theta)\Phi_M(\phi) = P_{J,M}(\cos\theta)\Phi_M(\phi)$$

Substitution yields:

$$\begin{aligned} R_z &= \mu_0 \langle \psi_1 | \cos\vartheta | \psi_2 \rangle \\ &= \mu_0 \int \psi^*_{J",M"} \psi_{J',M'} \cos\vartheta \sin\vartheta d\vartheta d\varphi \\ &= \mu_0 C_{J",M"} C_{J',M'} \int_0^{\pi} P_{J",M"}(\cos\vartheta) P_{J',M'}(\cos\vartheta) \cos\vartheta \sin\vartheta d\vartheta \int_0^{2\pi} e^{iM"\varphi} e^{iM'\varphi} d\varphi \end{aligned}$$

The first integral is identical zero, unless $J'=J"\pm1$ (use recursive identities for $P_{J,M}$)
The second integral is equal to 2π if $M'=M"$ and otherwise identical zero

➔ $\Delta J = \pm1$ and $\Delta M=0$ for an electric field along the z-axis, and:

$$R_z(J',M',J",M') = R_z(J+1,M,J,M)$$

$$= \mu_0 \sqrt{\frac{(J+1)^2 - M^2}{(2J+1)(2J+3)}}$$

Selection rules in rotational spectroscopy

Similarly, one can show that:

$$R_x(J',M',J'',M') = R_x(J+1,M+1,J,M)$$

$$= -\frac{\mu_0}{2}\sqrt{\frac{(J+M+2)(J+M+1)}{(2J+1)(2J+3)}}$$

$$R_y(J',M',J'',M') = R_z(J+1,M-1,J,M)$$

$$= \frac{\mu_0}{2}\sqrt{\frac{(J-M+1)(J-M+2)}{(2J+1)(2J+3)}}$$

And $\Delta J = \pm 1$ and, since an electric field along the *x*- or *y*-axis is able to apply a torque about the *z*-axis (i.e., the symmetry axis), $\Delta M = \pm 1$.

For unpolarized light, there is no preferential alignment of the molecules in an external field and summation over all *M* values yields a matrix element squared that is independent of *M*:

$$|\mathbf{R}|^2 = \sum_{M'}\left(|\mathbf{R}_x|^2 + |\mathbf{R}_y|^2 + |\mathbf{R}_z|^2\right)$$

Selection rules in rotational spectroscopy

For $\Delta J = +1$:

$$\left|R(J';J'',M'')\right|^2 = \left|R(J+1 \leftarrow J, M)\right|^2 = \mu_0^2 \frac{J+1}{2J+1}$$

And for $\Delta J = -1$:

$$\left|R(J',M';J'')\right|^2 = \left|R(J \leftarrow J+1, M)\right|^2 = \mu_0^2 \frac{J+1}{2J+3}$$

ratio reflects degeneracy of the levels involved: $g_J = 2J+1$, $g_{J+1} = 2J+3$

Taking the degeneracy of the initial level into account, we find the same expression in absorption as in emission:

$$\left|R(J',J'')\right|^2 = \mu_0^2 (J+1)$$

Note that in pure rotational spectroscopy, the transition with $\Delta J = -1$ can be interpreted as a transition from a higher to a lower energy level, i.e., emission instead of absorption.
The distinction between $\Delta J = +1$ and $\Delta J = -1$ becomes more meaningful when we consider ro-vibrational transitions.

Intensities in rotational spectroscopy

The intensity of a transition is proportional to the absorbance:

$$a(\nu) = \alpha(\nu) \cdot l = \left[n_1 - \frac{g_1}{g_2} n_2 \right] \cdot S \cdot f(\nu) \cdot l$$

The populations are given by the Boltzmann distribution:

$$n_i = n \frac{g_i e^{-E_i/kT}}{Q}$$ with the partition function: $$Q \approx Q_R = \sum_{j=0}^{\infty} (2j+1) e^{-Bj(j+1)/kT} = \frac{kT}{B} +$$

The line strength can be expressed in terms of the transition matrix element:

$$S = \frac{h\nu}{c} B_{12} = \frac{h\nu}{c} \frac{g_2}{g_1} B_{21} = \frac{h\nu}{c} \frac{g_2}{g_1} \frac{c^3}{8\pi h\nu^3} A_{21} = \frac{h\nu}{c} \frac{g_2}{g_1} \frac{c^3}{8\pi h\nu^3} \frac{16\pi^3\nu^3}{3\varepsilon_0 hc^3} \left| \mathbf{R}^{21} \right|^2$$

Intensities in rotational spectroscopy

Inserting the previously derived equation for the ΔJ=+1 matrix element squared:

$$a(J) \propto \frac{B(J+1)}{kT}(2J+3)\cdot\left[1-e^{-\Delta E/kT}\right]e^{-BJ(J+1)/kT}\cdot\Delta E$$

$$\propto (J+1)^3(2J+3)\cdot e^{-BJ(J+1)/kT}$$

where we have used: $\left[1-e^{-\Delta E/kT}\right]\approx\frac{\Delta E}{kT}$

since $\Delta E = 2B(J+1) << kT$

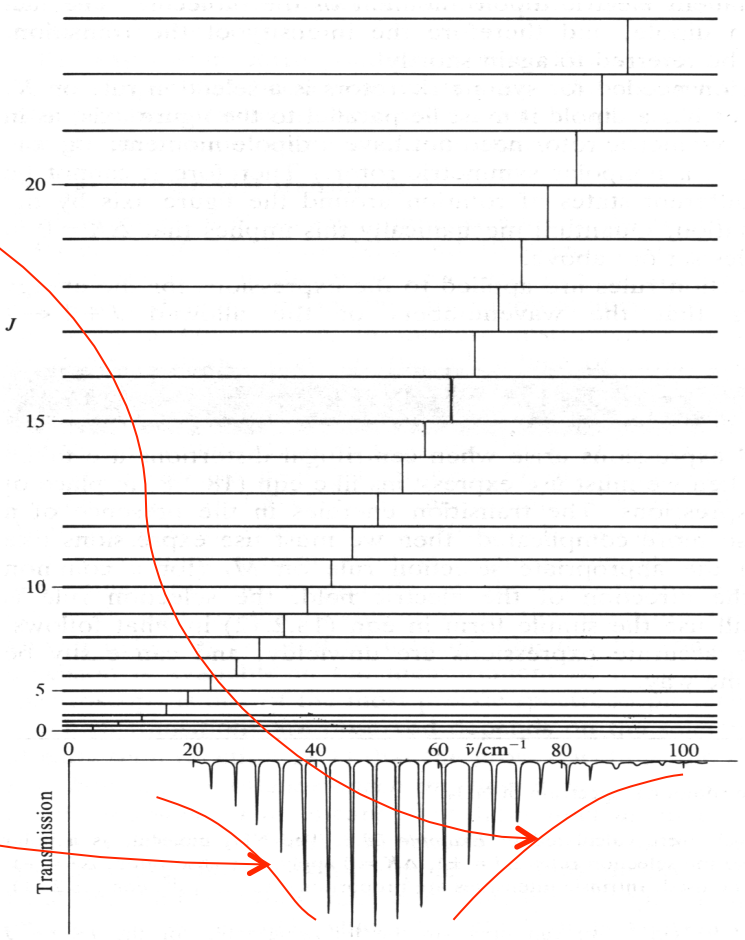

Intensities in rotational spectroscopy

Inserting the previously derived equation for the ΔJ=+1 matrix element squared:

$$a(J) \propto \frac{B(J+1)}{kT}(2J+3)\cdot\left[1-e^{-\Delta E/kT}\right]e^{-BJ(J+1)/kT}\cdot\Delta E$$

$$\propto (J+1)^3(2J+3)\cdot e^{-BJ(J+1)/kT}$$

Line intensities depend on temperature!

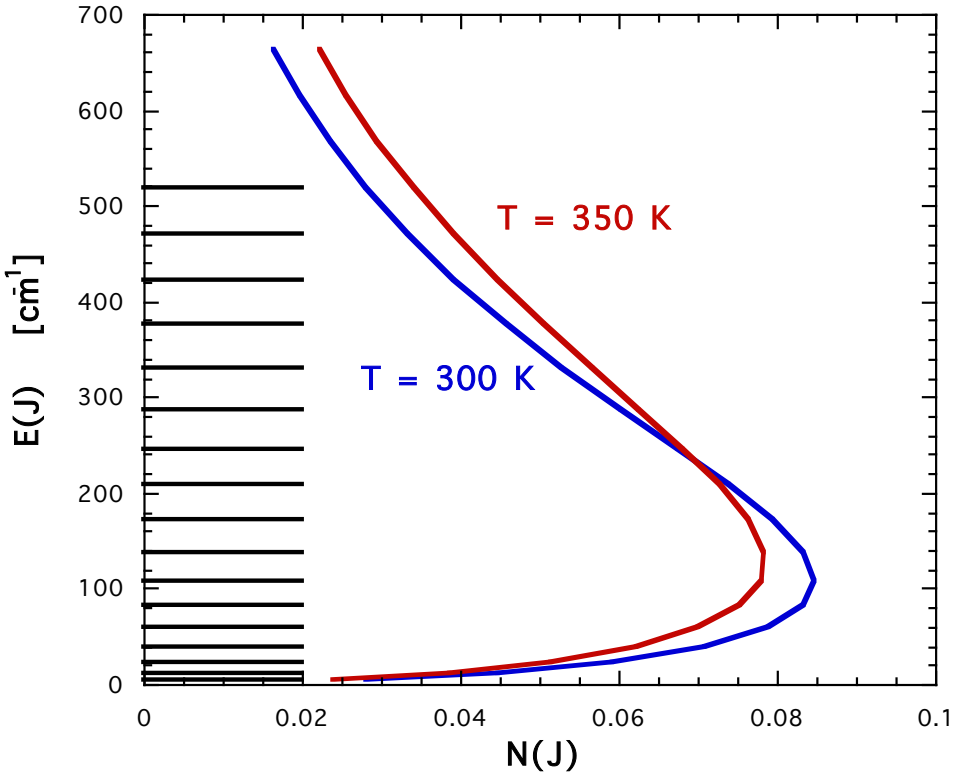

Vibrational spectroscopy: the harmonic oscillator

$F = -k \cdot x$

Potential energy surface for a diatomic approximated by a parabola:

$$V(R) = \tfrac{1}{2} k (R - R_e)^2$$

The Schrödinger equation for the internal motion of the molecule becomes:

$$-\frac{\hbar^2}{2\mu}\frac{\partial^2 \psi}{\partial x^2} + V(x)\psi = E\psi$$

$$\frac{1}{\mu} = \frac{1}{M_1} + \frac{1}{M_2}$$

(dominated by the lightest atom)

$$\left(-\frac{\hbar^2}{2\mu}\frac{d^2}{dx^2} + \frac{\mu\omega^2 x^2}{2}\right)\psi = E\psi$$

$$\omega = \sqrt{k/\mu}$$

Dimensionless:

$$\left(\frac{d^2}{dy^2} + \left(\varepsilon - y^2\right)\right)\psi(y) = 0$$

with $y \equiv \sqrt{\frac{\mu\omega}{\hbar}}\, x$, and $\varepsilon \equiv \frac{2E}{\hbar\omega}$

Vibrational spectroscopy: the harmonic oscillator

The solution is given in terms of Hermite polynomials for ψ:

$$\psi_v(y) = \frac{1}{\sqrt{2^v v! \sqrt{\pi}}} H_v(y) e^{-\frac{y^2}{2}}$$

whereas the energy eigenvalues are given by:

$$\varepsilon_v = 2v + 1$$

$$E_v = \hbar\omega\left(v + \tfrac{1}{2}\right)$$

$$\text{with } \omega = \sqrt{\frac{k}{\mu}};\ v = 0, 1, 2, \ldots$$

⇒ equidistant energy levels!

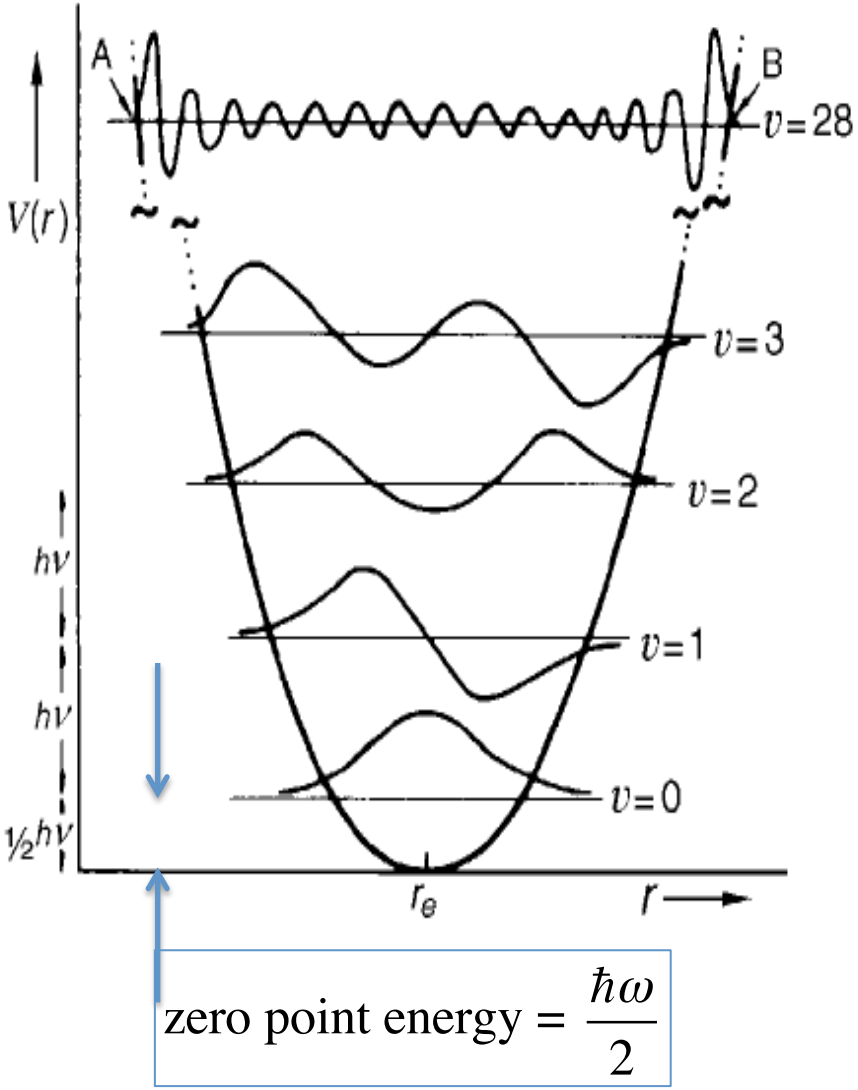

Vibrational spectroscopy: anharmonicity

Morse potential:

$$V(r) = D_e\left(1 - e^{-a(r-r_e)}\right)^2$$

$$\omega = \sqrt{\frac{2a^2 D_e}{\mu}} = \sqrt{\frac{\tilde{k}}{\mu}}$$

With the exact solution:

$$E_v = \hbar\omega\left(v + \tfrac{1}{2}\right) - \chi_e\hbar\omega\left(v + \tfrac{1}{2}\right)^2$$

$$\chi_e = \frac{a\hbar}{2\sqrt{2\mu D_e}}$$

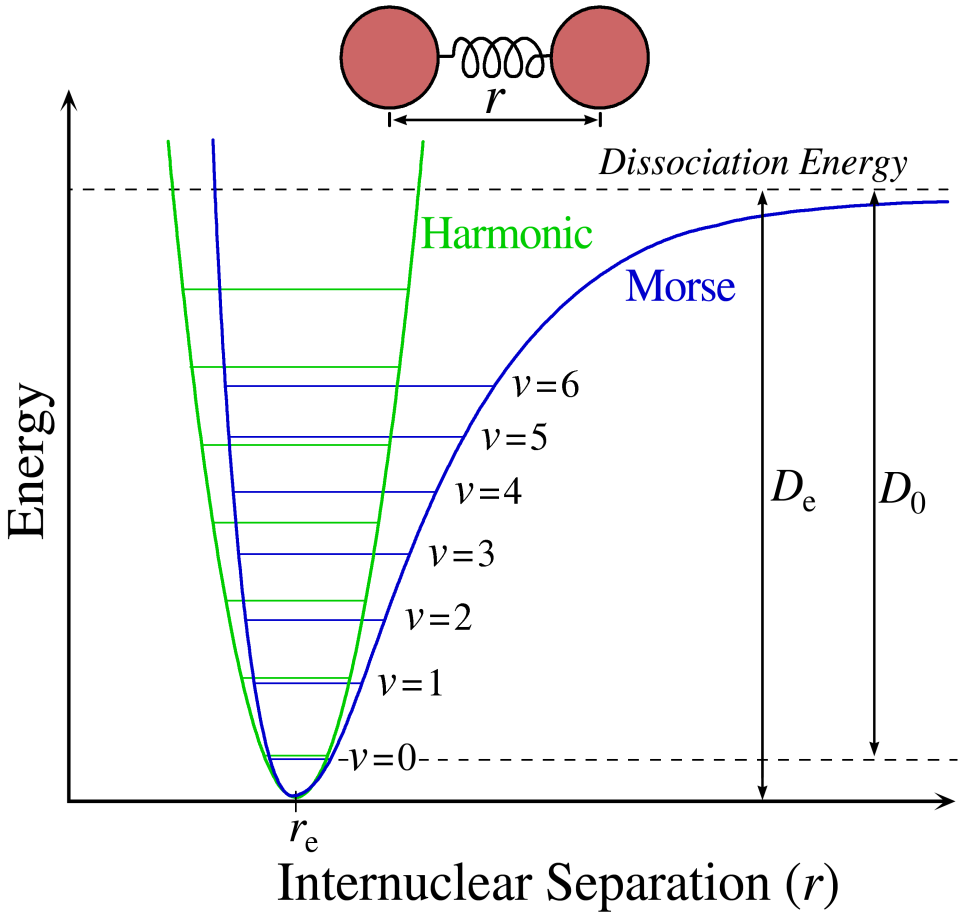

Gerneral: $E_v = \hbar\omega\left(v + \tfrac{1}{2}\right) - \chi_e\hbar\omega\left(v + \tfrac{1}{2}\right)^2 + y_e\hbar\omega\left(v + \tfrac{1}{2}\right)^3 + \ldots$

Vibrational spectroscopy: the harmonic oscillator transitions

Transitions: $\Delta v = \pm 1$

based on the orthogonality of the harmonic oscillator eigenfunctions

To see this, expand μ as a Taylor series:

$$\mu = \mu_0 + \dot{\mu}_0 x + \tfrac{1}{2!}\ddot{\mu}_0 x^2 + \ldots$$

and evaluate $R^{v'v''} = \langle \psi_{v'} | \mu | \psi_{v''} \rangle$:

$$R(v',v'') = \mu_0 \langle \psi_{v'} | \psi_{v''} \rangle + \dot{\mu}_0 \langle \psi_{v'} | x | \psi_{v''} \rangle + \tfrac{1}{2}\ddot{\mu}_0 \langle \psi_{v'} | x^2 | \psi_{v''} \rangle + \ldots$$

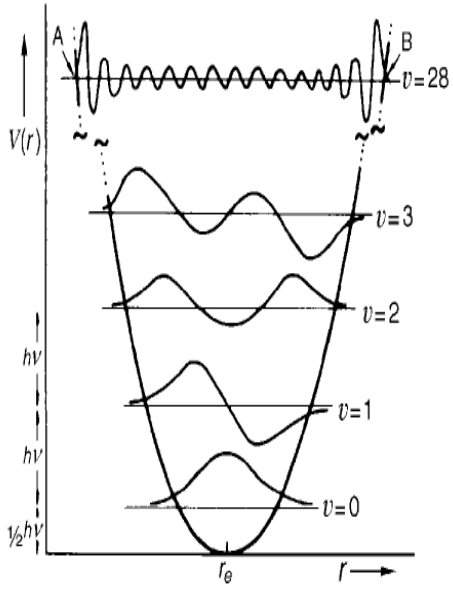

- orthoganality means $\langle \psi_{v'} | \psi_{v''} \rangle = 0$ when $v' \neq v''$
- the second term is non-zero only if $v' = v'' \pm 1$
- the derivatives of μ are zero for homo-nuclear diatomics
- the higher order terms result in weakly allowed $v' = v'' \pm 2$, $v' = v'' \pm 3$, ...
  - electrical anharmonicity: 2nd and higher derivatives of $\mu \neq 0$
  - mechanical anharmonicity: higher order matrix elements ≠ 0 (i.e., anharmonic potential)

Rotational-vibrational spectroscopy

Born-Oppenheimer approximation:

$$\begin{cases} E = E_{vib} + E_{rot} \\ \psi = \psi_{vib}\psi_{rot} \end{cases}$$

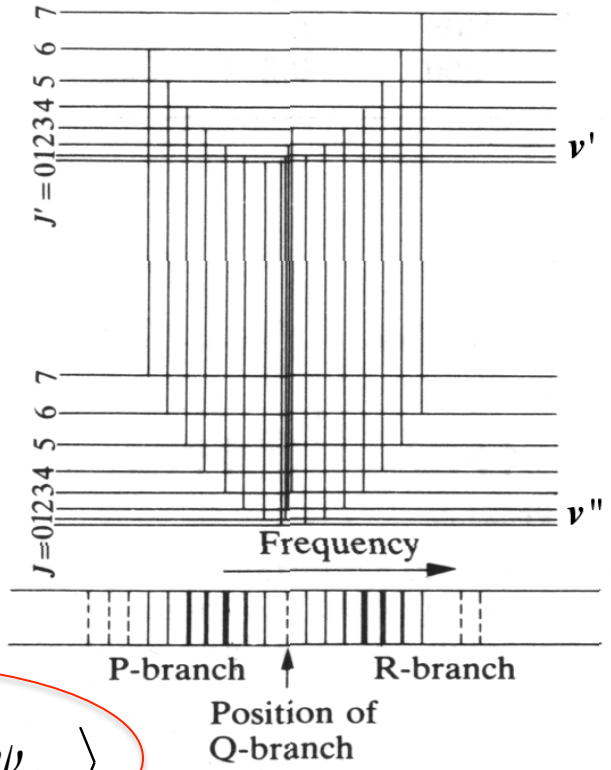

Herewith the (components of) the transition dipole moment become:

$$R_x = \left\langle \psi_{v'}\psi_{J'K'} \middle| \mu_x \middle| \psi_{v''}\psi_{J''K''} \right\rangle = \left\langle \psi_{v'} \middle| \mu \middle| \psi_{v''} \right\rangle \left\langle \psi_{J'K'} \middle| \sin\vartheta\cos\varphi \middle| \psi_{J''K''} \right\rangle$$

Such that the previously derived selection rules apply, with the understanding the dipole moment is not the permanent dipole moment, but rather the vibrational ***transition*** dipole moment.

For a linear molecule: $\Delta v = \pm 1 \quad \text{and} \quad \Delta J = \pm 1$

Rotational-vibrational spectra

Linear or spherical top molecule (one moment of inertia):

$$\begin{aligned}\Delta E &= E(v',J') - E(v'',J'') \\ &= \left[E_{v'} - E_{v''}\right] + \left[B_{v'}J'(J'+1) - B_{v''}J''(J''+1) + \ldots\right] \\ &= \nu_0 \; + \; B'J'(J'+1) - B''J''(J''+1) + \ldots\end{aligned}$$

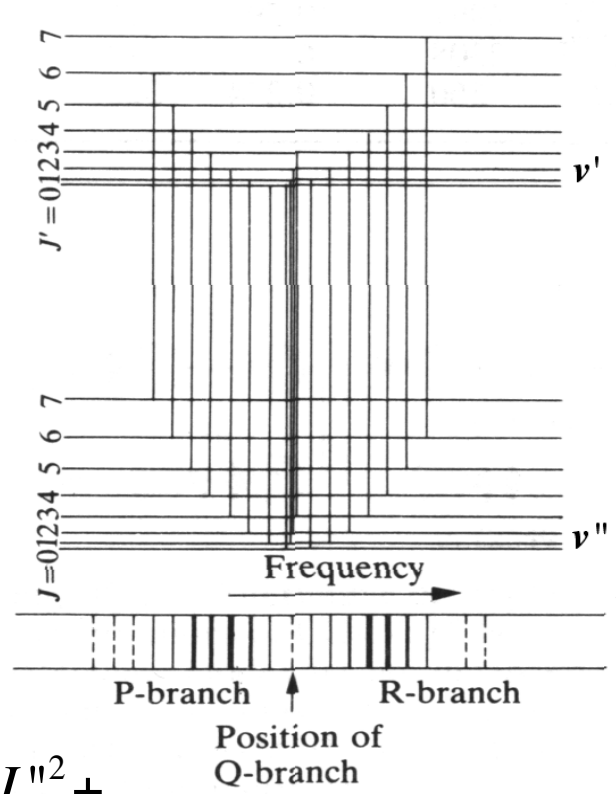

P-branch $\quad \Delta E = \nu_0 \; -(B'+B'')J'' + (B'-B'')J''^2 + \ldots$

Q-branch $\quad \Delta E = \nu_0 \; +(B'-B'')J''(J''+1) + \ldots$

R-branch $\quad \Delta E = \nu_0 \; +(B'+B'')(J''+1) + (B'-B'')(J''+1)^2 + \ldots$

parallel band: $\dot{\mu}$ aligned with molecular symmetry axis, and $\Delta J = \pm 1$, i.e. no Q-branch

perpendicular band: $\dot{\mu}$ perpendicular to molecular symmetry axis, and $\Delta J = 0, \pm 1$

Rotational-vibrational spectra

P-branch $\Delta E = \nu_0 - (B' + B'')J'' + (B' - B'')J''^2 + \ldots$

Q-branch $\Delta E = \nu_0 + (B' - B'')J''(J''+1) + \ldots$

R-branch $\Delta E = \nu_0 + (B' + B'')(J''+1) + (B' - B'')(J''+1)^2 + \ldots$

parallel band: $\dot{\mu}$ aligned with molecular symmetry axis, and $\Delta J = \pm 1$, i.e. no Q-branch

perpendicular band: $\dot{\mu}$ perpendicular to molecular symmetry axis, and $\Delta J = 0, \pm 1$

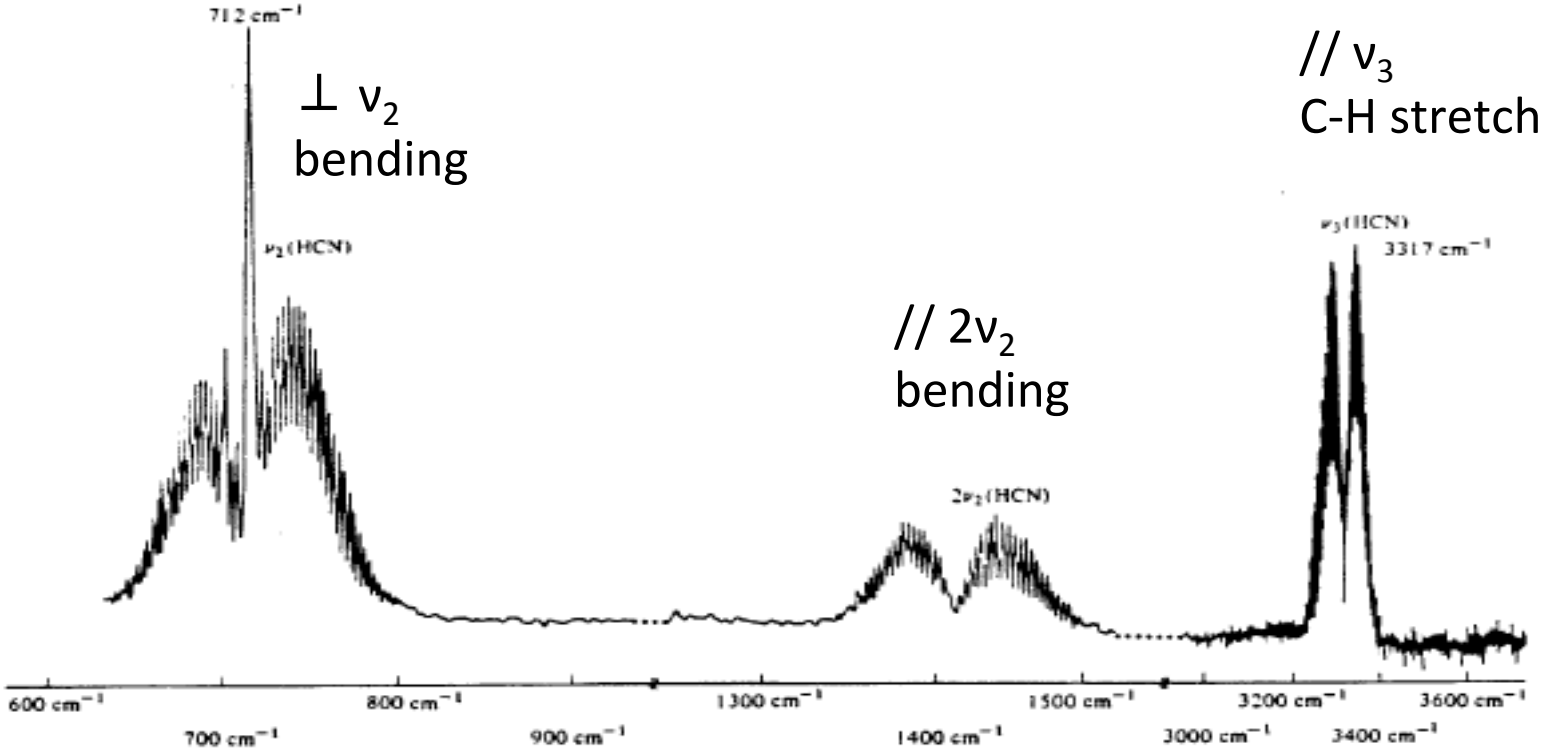

Rotational-vibrational spectra

P-branch $$\Delta E = \nu_0 - (B' + B'')J'' + (B' - B'')J''^2 + \ldots$$

R-branch $$\Delta E = \nu_0 + (B' + B'')(J''+1) + (B' - B'')(J''+1)^2 + \ldots$$

parallel band: $\dot{\mu}$ aligned with molecular symmetry axis, and $\Delta J = \pm 1$, i.e. no Q-branch

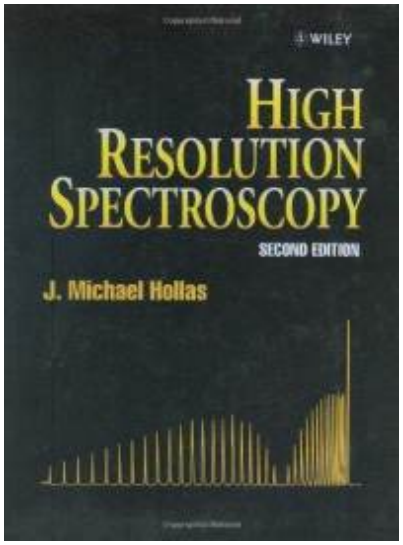

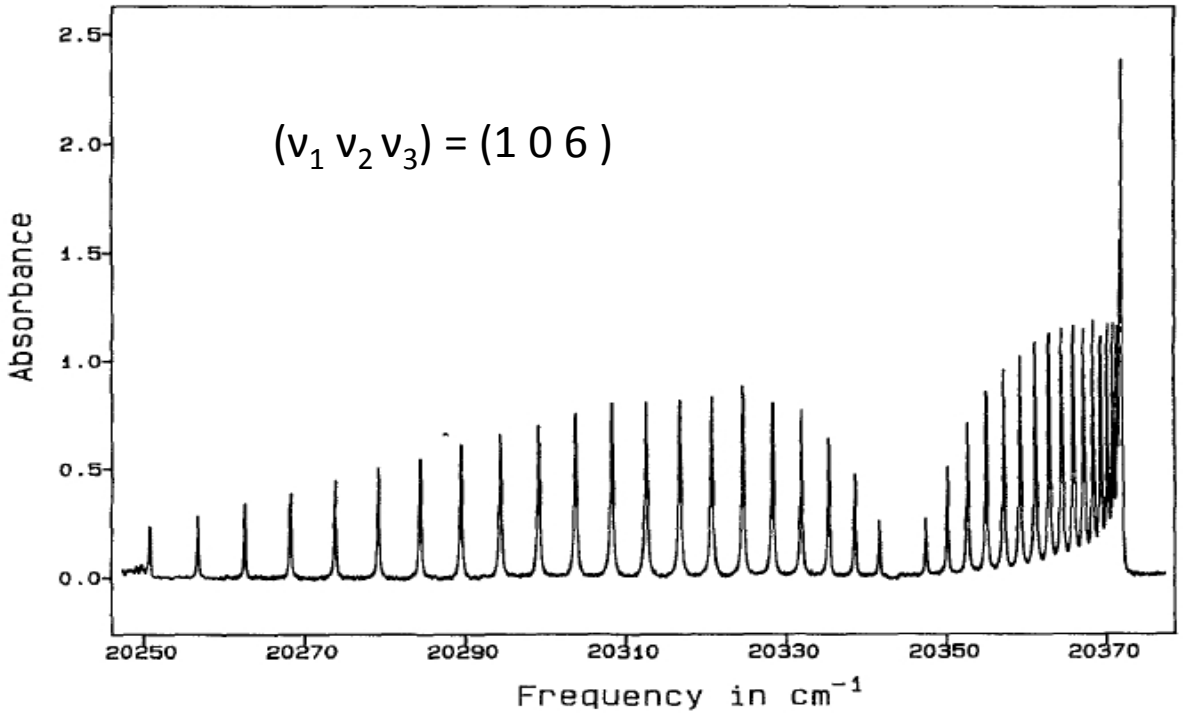

FIG. 6. The spectrum of the 106 overtone of HCN (100 Torr, $\Delta t = 80\ \mu$s, and $L = 24$ km). Near the last displayed line of the P branch is the beginning of the hot band, which is shown in Fig. 8.

. J. Chem. Phys. 1993, 99 (9), 6287-6301

Symmetric top spectra

We recall the rotational structure of a symmetric top:

$$E(J,K) = BJ(J+1) + (A-B)K_a^2$$
$$E(J,K) = BJ(J+1) + (C-B)K_c^2$$

The selection rules for a parallel band are:

$$\begin{cases} \Delta J = 0, \pm 1, \ \Delta K = 0 & \text{if } K \neq 0 \\ \Delta J = \pm 1, \ \Delta K = 0 & \text{if } K = 0 \end{cases}$$

⇒ only vertical transitions in the figure!

For a perpendicular band:

$$\Delta J = 0, \pm 1, \qquad \Delta K = \pm 1$$

⇒ crossed transitions in the figure!

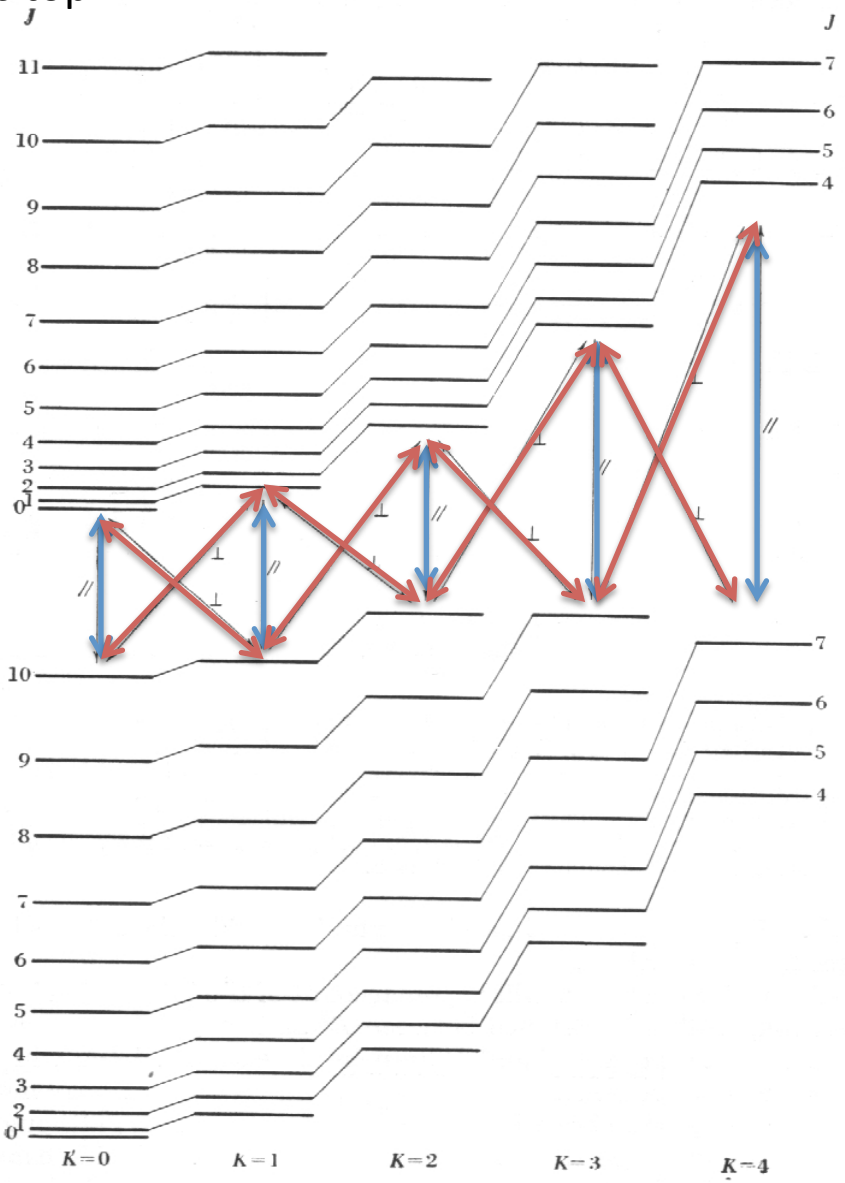

FIG. 121. Combination of two non-degenerate vibrational levels of a symmetric top

Symmetric top spectra

Consider the a parallel band of a prolate symmetric top:

$$E(J,K) = BJ(J+1) + (A-B)K_a^2$$

$$\begin{cases} \Delta J = 0, \pm 1, \ \Delta K = 0 & \text{if } K \neq 0 \\ \Delta J = \pm 1, \ \Delta K = 0 & \text{if } K = 0 \end{cases}$$

⇒ *K* sub-bands are displaced because of a small difference between (*A”-B”*) and (*A’-B’*)

small $[(A'-B')-(A''-B'')] \cdot K_a^2$

large $[(A'-B')-(A''-B'')] \cdot K_a^2$

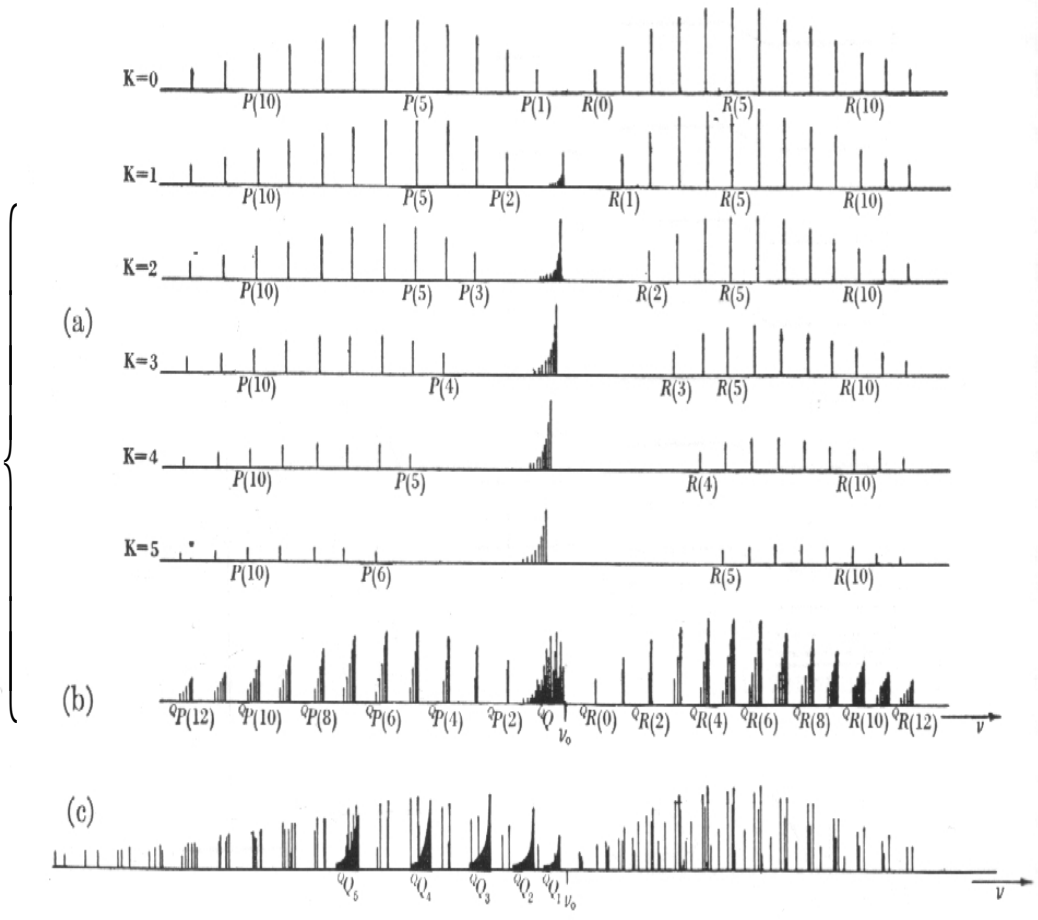

FIG. 122. **Sub-bands of a || band and complete || band of a symmetric top.**—The sub-bands

Symmetric top spectra

Consider the a perpendicular band of a prolate symmetric top:

$$E(J,K) = BJ(J+1) + (A-B)K_a^2 \qquad \Delta J = 0,\pm 1, \qquad \Delta K = \pm 1$$

⇒ *(K, ΔK)* sub-bands are displaced, even if *B'=B"* and *A'=A"*

(0,0)

(1,-1)

(1,+1)

(2,-1)

(2,+1)

(3,-1)

(3,+1)

total:

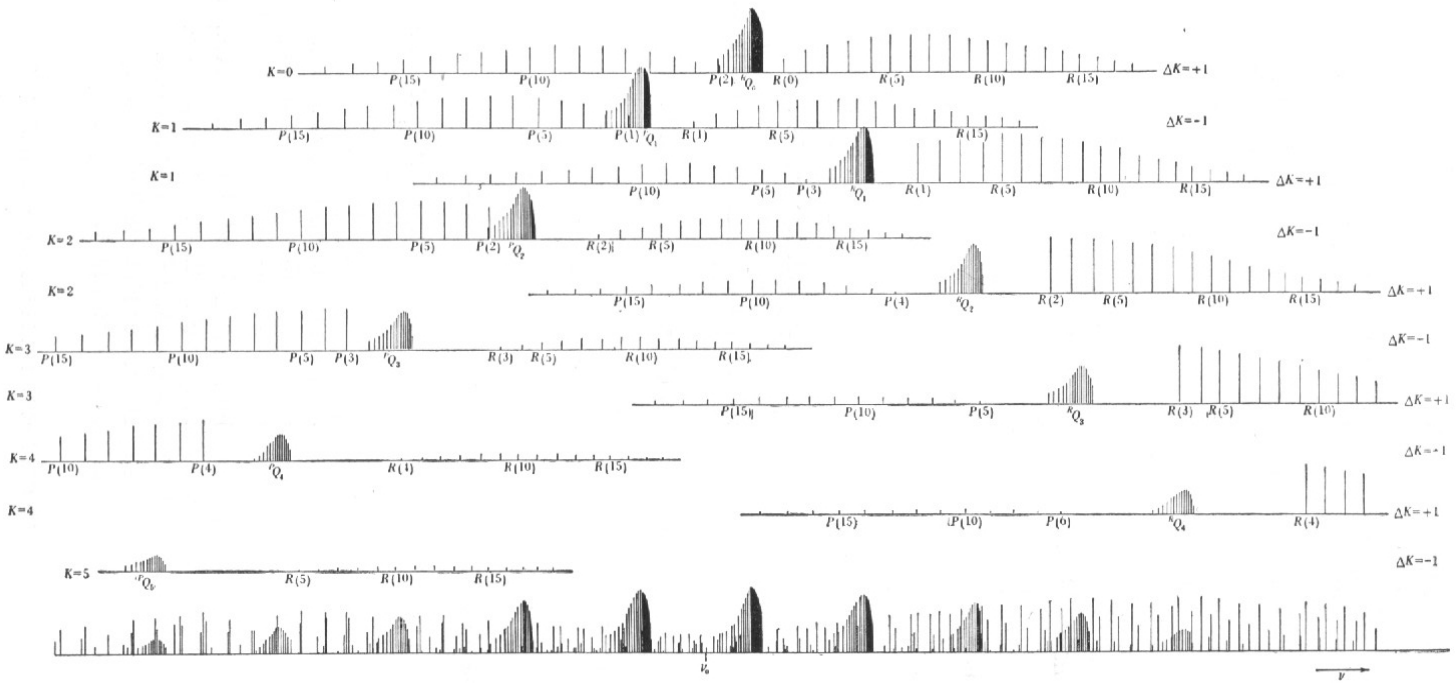

FIG. 128. **Sub-bands of a ⊥ band and complete ⊥ band of a symmetric top.**—The complete band is shown in the bottom strip. The spectrum is drawn under the assumption that $A' = 5.18$, $A'' = 5.25$, $B' = 0.84$, $B'' = 0.85$ cm^{-1} and $\zeta_i = 0$. The intensities were calculated for a temperature of 144° K. It should be realized that if the lines of an individual Q branch are not resolved the resulting "line" would stand out much more prominently than might appear from the spectrum given.

Intensities in rotational spectroscopy

The intensity of a transition is proportional to the absorbance:

$$a(\nu) = \alpha(\nu) \cdot l = \left[n_1 - \frac{g_1}{g_2} n_2 \right] \cdot S \cdot f(\nu) \cdot l$$

The populations are given by the Boltzmann distribution:

$$n_i = n \frac{g_i e^{-E_i/kT}}{Q}$$

with the partition function:

$$Q \approx Q_R = \sum_{j=0}^{\infty} (2j+1) e^{-Bj(j+1)/kT} = \frac{kT}{B} + \frac{1}{3} + \frac{1}{15}\frac{B}{kT} + \ldots \approx \frac{kT}{B} \qquad (B << kT)$$

The line strength can be expressed in terms of the transition matrix element:

$$S = \frac{h\nu}{c} B_{12} = \frac{h\nu}{c}\frac{g_2}{g_1} B_{21} = \frac{h\nu}{c}\frac{g_2}{g_1}\frac{c^3}{8\pi h\nu^3} A_{21} = \frac{h\nu}{c}\frac{g_2}{g_1}\frac{c^3}{8\pi h\nu^3}\frac{16\pi^3\nu^3}{3\varepsilon_0 hc^3}\left|\mathbf{R}^{21}\right|^2$$

Intensities in rotational-vibrational spectroscopy

Inserting the previously derived equation for the ΔJ=+1 matrix element squared:

$$a(J) \propto \frac{B(J+1)}{kT}(2J+3)\cdot\left[1-e^{-\Delta E/kT}\right]e^{-BJ(J+1)/kT}\cdot\Delta E$$

$$\propto \frac{B(J+1)}{kT}(2J+3)\cdot e^{-BJ(J+1)/kT}$$

where we have used that

$$\left[1-e^{-\Delta E/kT}\right]\approx 1$$

since now

ΔE ≈ constant and >> kT.

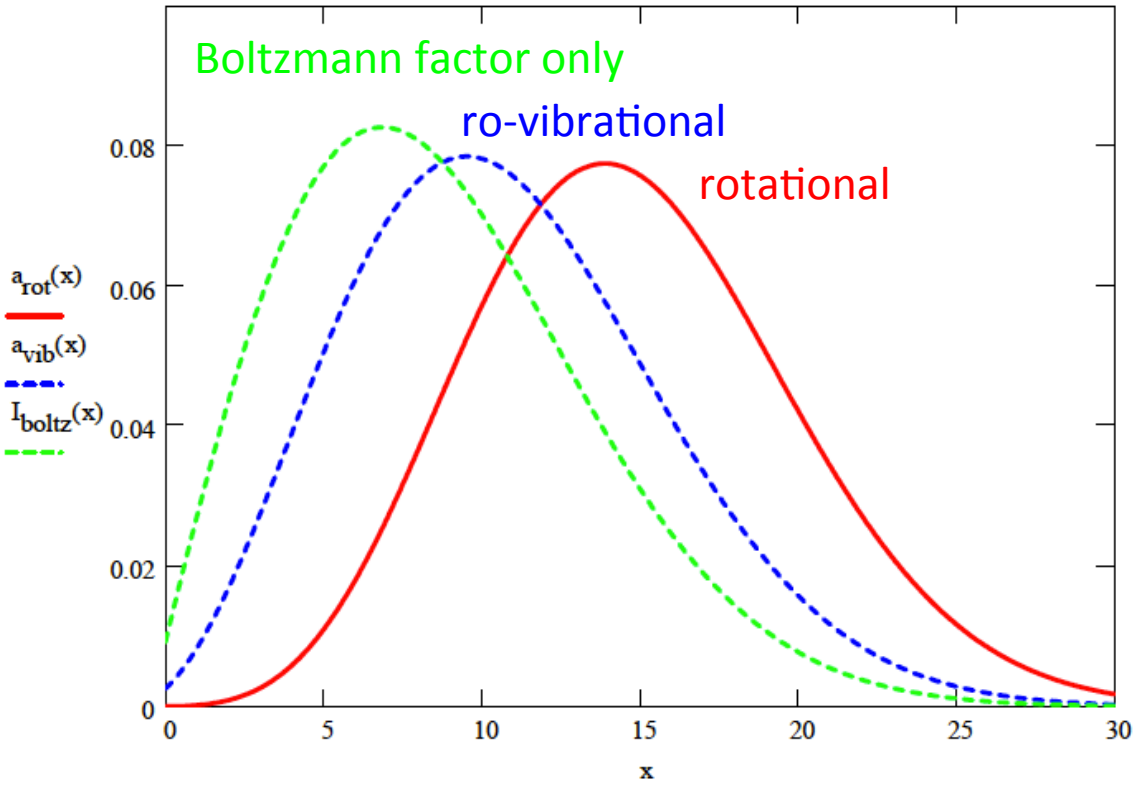

Electronic transitions: selection rules

The transition intensity is proportional to the ground state population and the square of the transition dipole moment. Consider the latter, applying the B-O approximation:

$$\mathbf{R} = \left\langle \psi_e' \psi_v' \middle| \mathbf{p} \middle| \psi_e'' \psi_v'' \right\rangle = -e \left\langle \psi_e' \psi_v' \middle| \mathbf{r} \middle| \psi_e'' \psi_v'' \right\rangle$$
$$= -e \iint \psi_e'^{*} \psi_v'^{*} \mathbf{r} \psi_e'' \psi_v'' d\tau_n d\tau_e$$
$$= -e \int \psi_v'^{*} \left(\int \psi_e'^{*} \mathbf{r} \psi_e'' d\tau_e \right) \psi_v'' d\tau_n$$

The quantity in brackets is the purely electronic transition moment $\mathbf{R}_e$:

$$\mathbf{R}_e = -e \int \psi_e'^{*} \mathbf{r} \psi_e'' d\tau_e$$

Further application of the B-O approximation then leads to:

$$\mathbf{R} = \mathbf{R}_e \int \psi_v'^{*} \psi_v'' d\tau_n$$

Electronic transitions: selection rules

$$\mathbf{R} = \mathbf{R}_e \int \psi_v'^{*} \psi_v'' \, d\tau_n$$

(1) $\Delta\Lambda = 0, \pm 1$

(2) $\Delta S = 0$

This selection rule is no longer strictly obeyed when a large nuclear charge gives rise to strong spin-orbit coupling (Hund's case (c)). For example, the violet color of gas phase I_2 is caused by relatively strong absorption of the transition, (the name iodine is derived the Greek *iodes* for purple).

(3) $\Delta\Sigma = 0 \text{ and } \Delta\Omega = 0, \pm 1$

This selection rule describes the transitions between multiplet components.

(4) $+ \leftrightarrow + \text{ and } - \leftrightarrow - \text{ are allowed, whereas } + \leftrightarrow - \text{ is forbidden}$

Selection rule number 4 is only relevant for $\Sigma - \Sigma$ transitions. For centrosymmetric molecules, it is replaced by:

(5) $g \leftrightarrow u \text{ is allowed, whereas } g \leftrightarrow g \text{ and } u \leftrightarrow u \text{ are forbidden}$

This selection rule is also known as Laporte's rule. It is easily rationalized by realizing that the components of the dipole moment operator transform like x, y, and z, and are all of odd parity, or *u*. Since $u \times u \times u = u$ and $g \times u \times g = u$, the integral in Eq. vanishes if ψ' and ψ" are of the same parity. Similarly, for $\Sigma - \Sigma$ transitions, we need to consider only the z-component of the dipole moment, which has + symmetry. Since $(+) \times (+) \times (-) = (-)$, transitions with $+ \longleftrightarrow -$ are forbidden.

Franck-Condon Principle

$$\mathbf{R} = \mathbf{R}_e \int \psi_v'^{*} \psi_v'' \, d\tau_n$$

The square of the vibrational overlap integral is known as the Franck-Condon factor

The most probable transitions are those that maximize the overlap of the wavefunctions for a “vertical” transition.

That is, the electronic transition is so much faster than the vibrational transition that the nuclear coordinates do not change during the electronic transition.
The nuclei have therefore essentially the same positions and velocities before and after the transition.

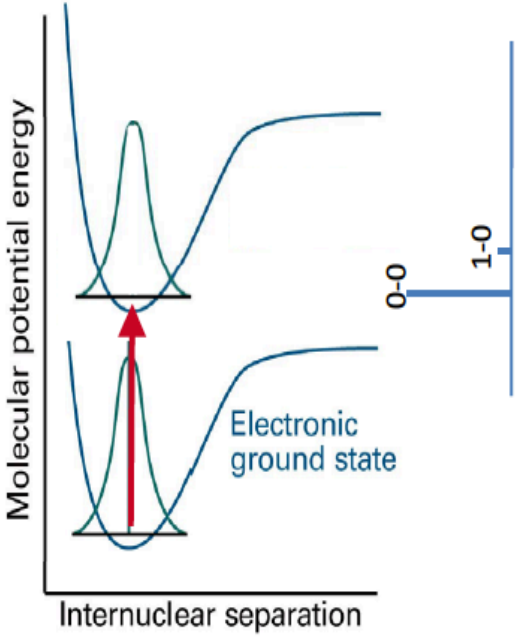

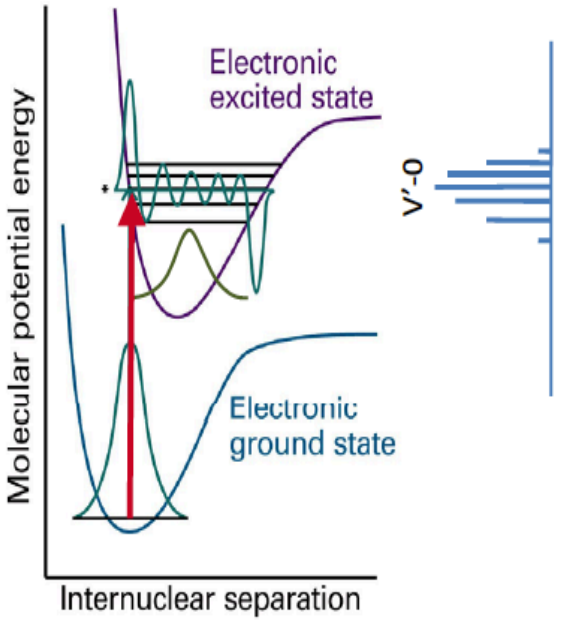

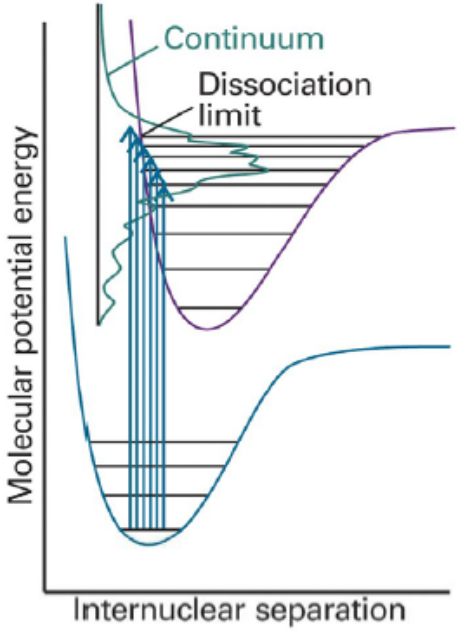

Dissociation Energy and the Birge-Sponer plot

D_0 can be determined by extrapolation of the vibrational progression, e.g., if:

$$E_v = \hbar\omega\left(v+\tfrac{1}{2}\right) - \chi_e\hbar\omega\left(v+\tfrac{1}{2}\right)^2$$

with $v = 0, 1, \ldots, v_{diss}$, where v_{diss} is determined by the condition that $(dE_v/dv)v_{diss} = 0$

$$\Rightarrow \begin{cases} (v_{diss}+\tfrac{1}{2}) = \dfrac{1}{2\chi_e} \\ D_e = \dfrac{\hbar\omega}{2} + D_0 = \dfrac{\hbar\omega}{2} + \left(E_v\right)_{diss} = \dfrac{\hbar\omega}{4\chi_e} \end{cases}$$

Or graphically, using:

$$D_0 \equiv \left(E_v\right)_{diss} = \sum_{v=1}^{v_{diss}} \left(E_v - E_{v-1}\right) = \sum_{v=1}^{v_{diss}} \Delta E_v$$

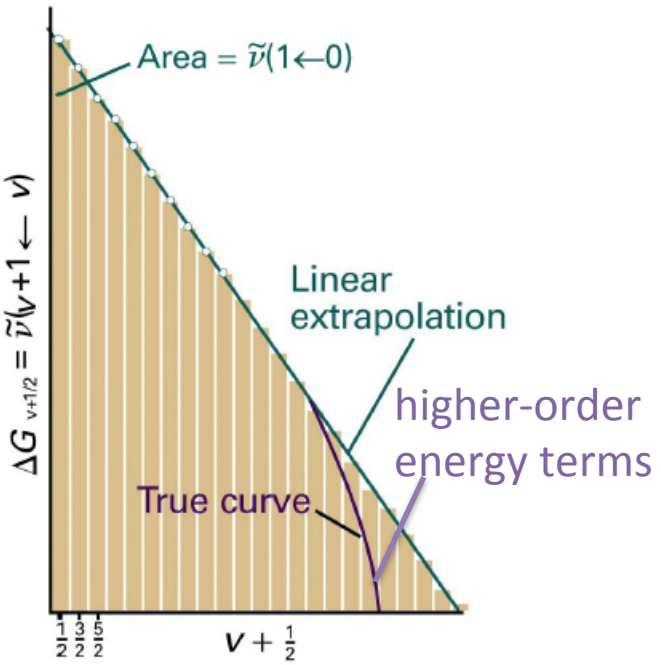

Dissociation Energy and the Birge-Sponer plot

D_0 can be determined by extrapolation of the vibrational progression, e.g., if:

$$E_v = \hbar\omega\left(v+\tfrac{1}{2}\right) - \chi_e\hbar\omega\left(v+\tfrac{1}{2}\right)^2$$

with $v = 0, 1, \ldots, v_{diss}$, where v_{diss} is determined by the condition that $(dE_v/dv)v_{diss} = 0$

$$\Rightarrow \begin{cases} \left(v_{diss}+\tfrac{1}{2}\right) = \dfrac{1}{2\chi_e} \\ D_e = \dfrac{\hbar\omega}{2} + D_0 = \dfrac{\hbar\omega}{2} + \left(E_v\right)_{diss} = \dfrac{\hbar\omega}{4\chi_e} \end{cases}$$

Or graphically, using:

$$D_0 \equiv \left(E_v\right)_{diss} = \sum_{v=1}^{v_{diss}} \left(E_v - E_{v-1}\right) = \sum_{v=1}^{v_{diss}} \Delta E_v$$

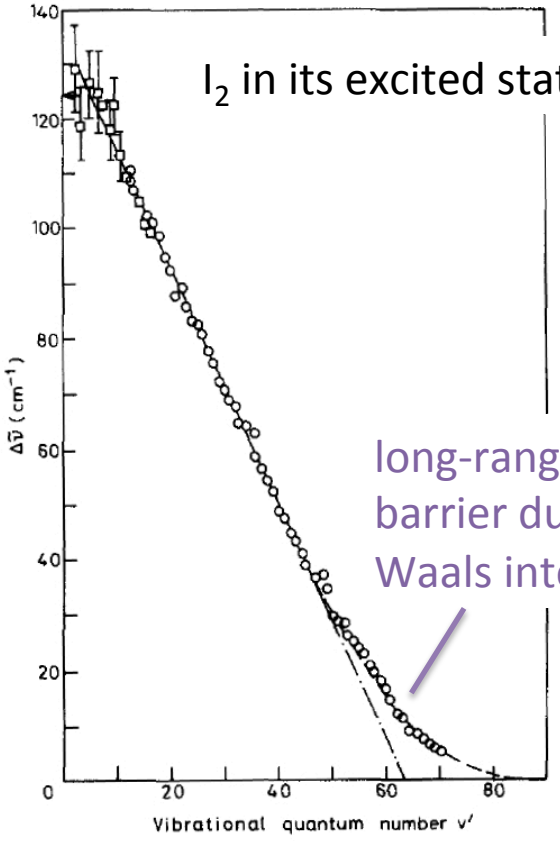

Applications of Frequency Combs

Two examples:

1) Using the broad-band nature of a frequency comb for the detection of atmospheric radicals in Antarctica.

2) Ultra-precise and accurate frequency measurements for a spectroscopic determination of the unit of temperature.

Frequency Comb – Cavity Enhanced Spectroscopy: A multiplexed detection scheme for field measurements in Antarctica

Laboratoire interdisciplinaire de Physique

Grilli et al. (2012). Frequency comb based spectrometer for in situ and real time measurements of IO, BrO, NO_2, and H_2CO at pptv and ppqv levels. *Environm. Science & Technology*, *46*(19), 10704

Grilli et al. (2012). Cavity-enhanced multiplexed comb spectroscopy down to the photon shot noise. *Physical Review A*, *85*(5), 1

Grilli et al. (2013). First investigations of IO, BrO, and NO2 summer atmospheric levels at a coastal East Antarctic site using mode-locked cavity enhanced absorption spectroscopy. *Geophys. Res. Lett.*, *40*(4), 791

© Thomas Paris, TA62

FC-CEAS time and spectrally multiplexed spectrometer

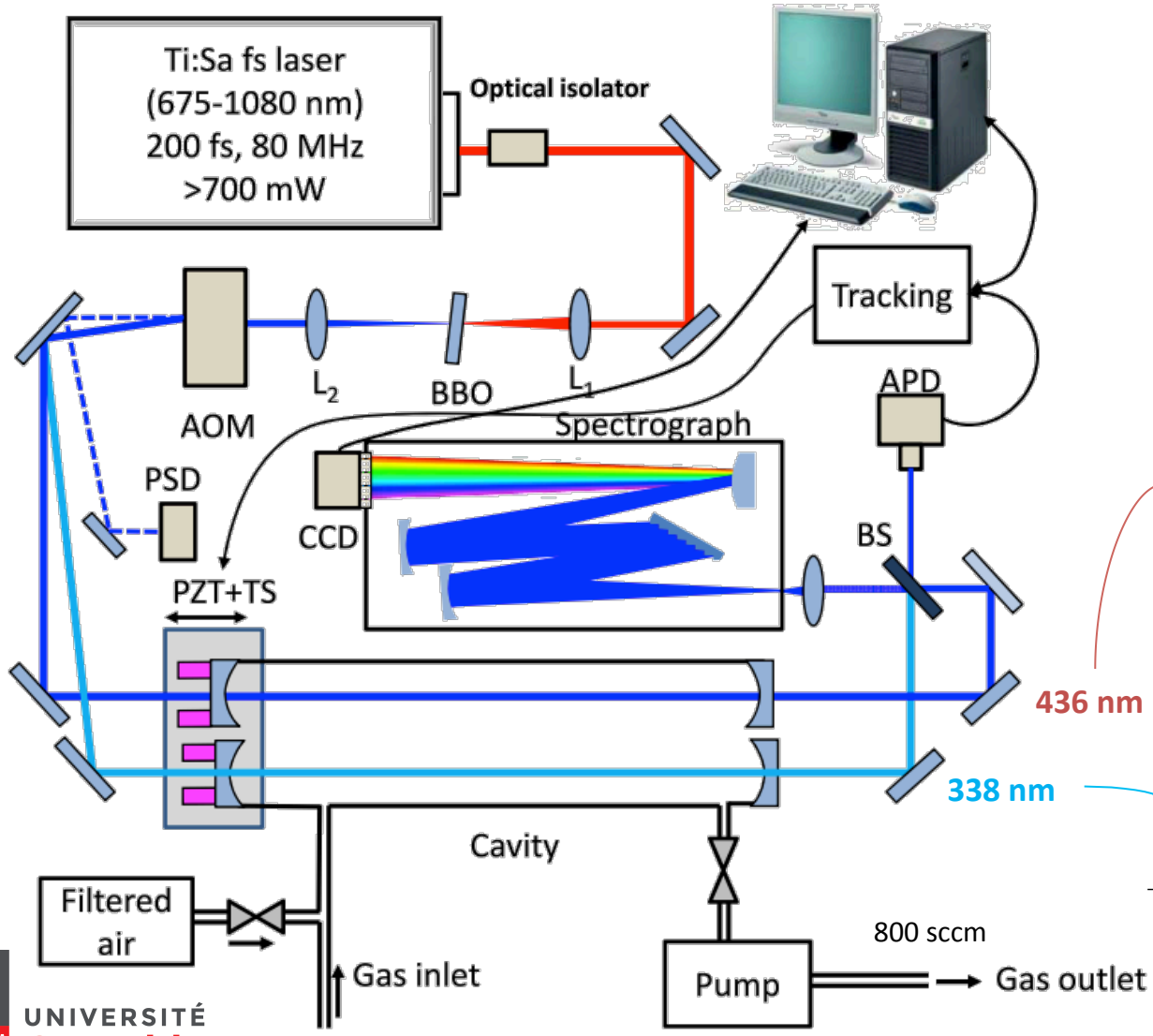

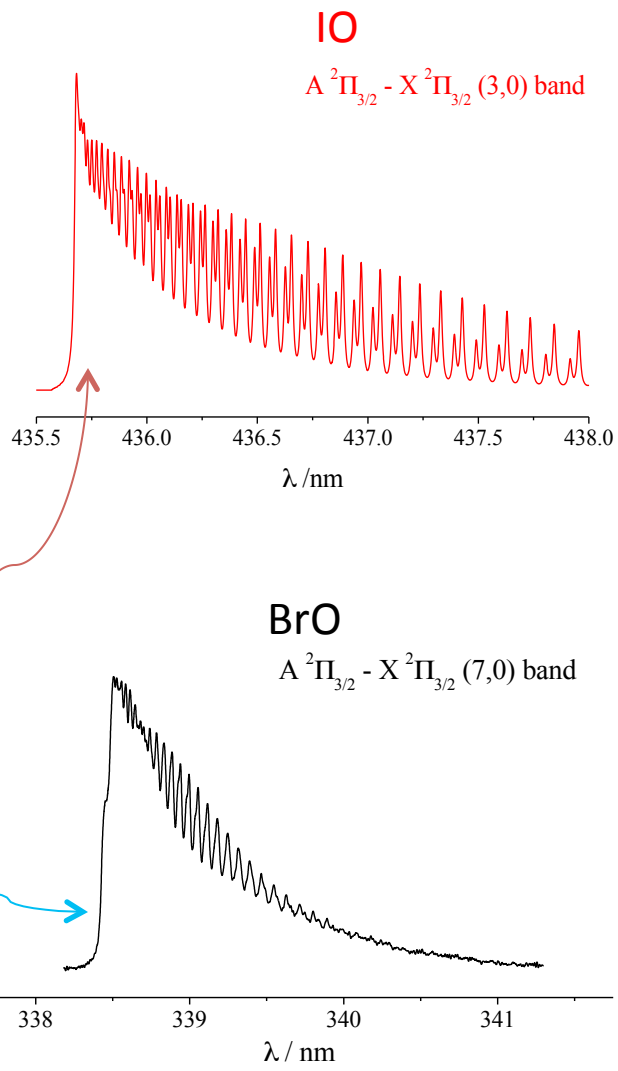

Stability test: Allan variance plot BrO and IO

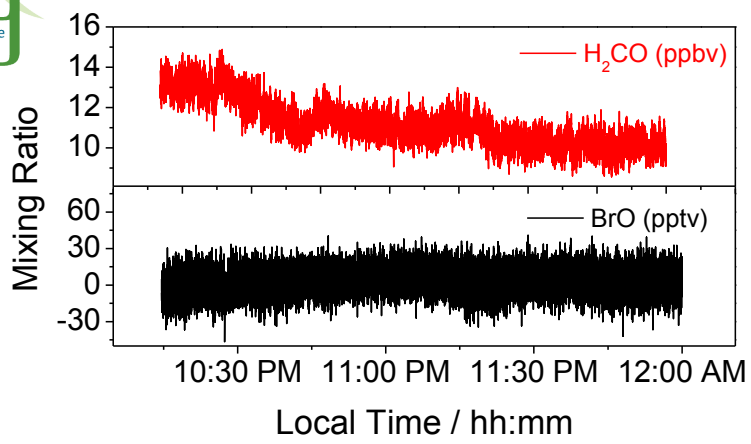

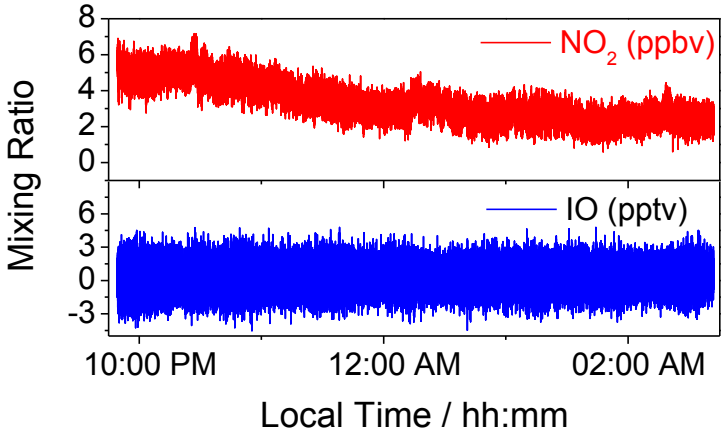

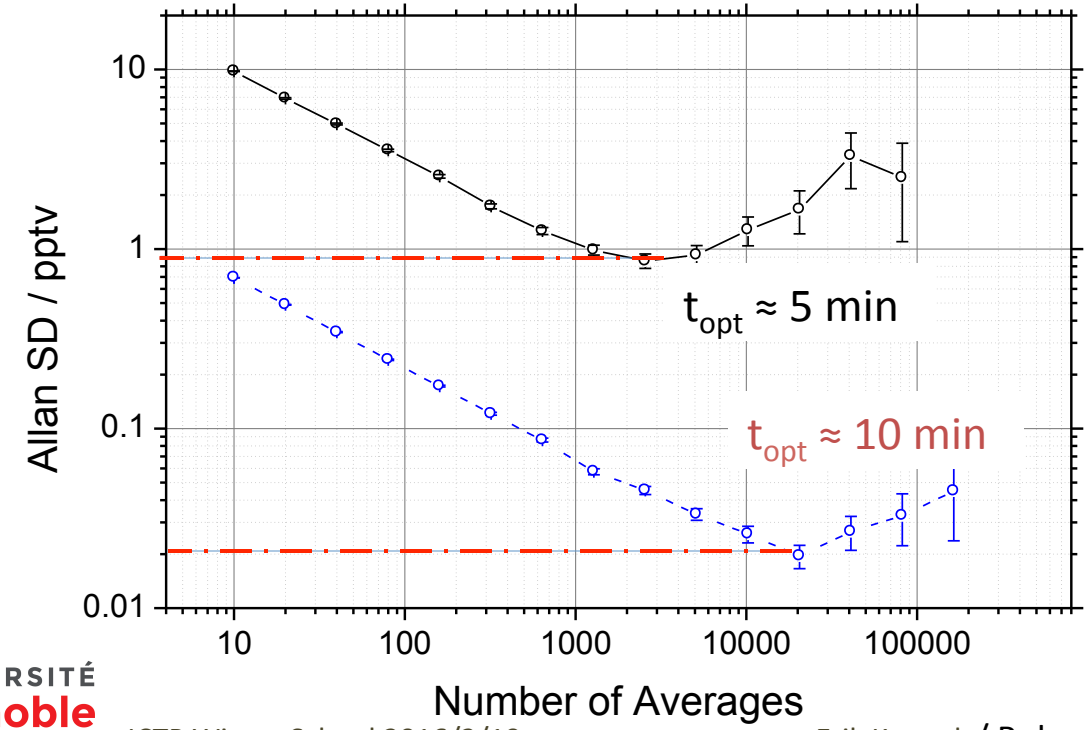

AV Plot at 338.5 nm

$[BrO]_{min}$ = 1 ppt

AV Plot at 436 nm

$[IO]_{min}$ = 0.02 ppt

The long trip to Antarctica...

The installation at DDU…

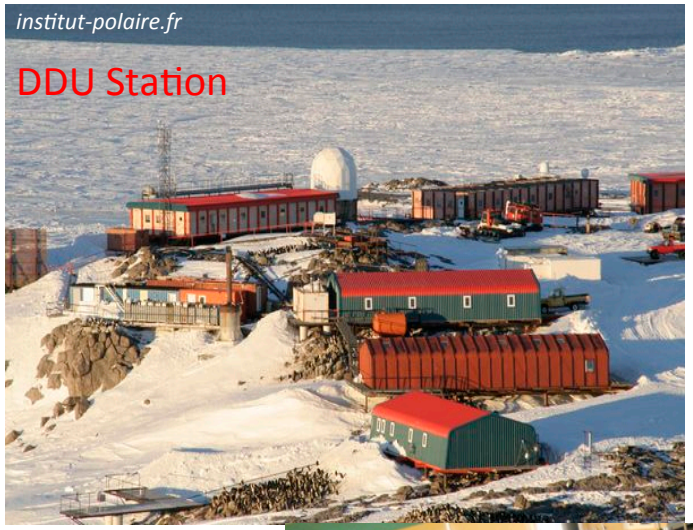

The unit kelvin

Present format for the definition of the kelvin:

The kelvin, unit of thermodynamic temperature, is the fraction 1/273.16 of the thrmodynamic temperature of the triple point of water.

It follows that the thermodynamic temperature of the triple point of water is exactly 273.16 kelvin, T_{tpw} = 273.16 K.

Metrologia **4, 43, 1968.**

The new explicit-constant definition:

The kelvin, unit of thermodynamic temperature, is such that the Boltzmann constant is exactly 1.380 65X X × 10^{-23} joule per kelvin.

It is essential that the value of k_B to be adopted for the new definition of the kelvin is as consistent as possible with the current definition.

A refined value of the Boltzmann constant proposed for the new kelvin should be ideally determined by at least three fundamentally different methods!!!

DBT basic principles

$$\Delta\nu_D = \sqrt{\ln 2}\,\frac{\nu_0}{c}\sqrt{2\frac{k_B T}{M}}$$

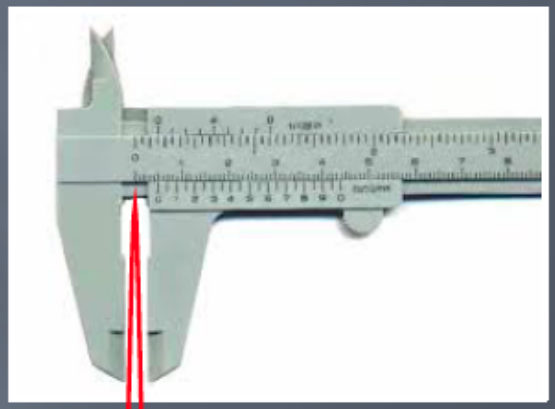

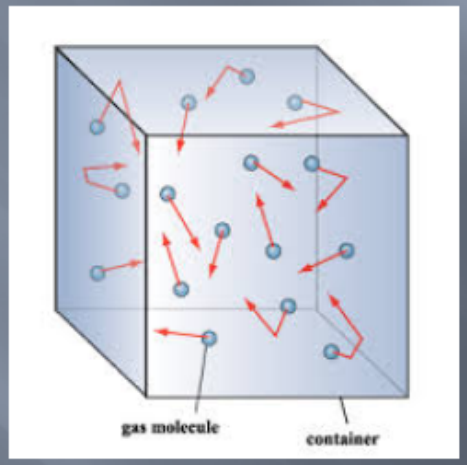

$$N(v)dv = 4\pi N\left(\frac{m}{2\pi kT}\right)^{3/2} v^2 \exp\left[-\frac{mv^2}{2kT}\right]dv$$

- Measure T
- Measure k_B

Accurate determination of line profiles: The story of X and Y

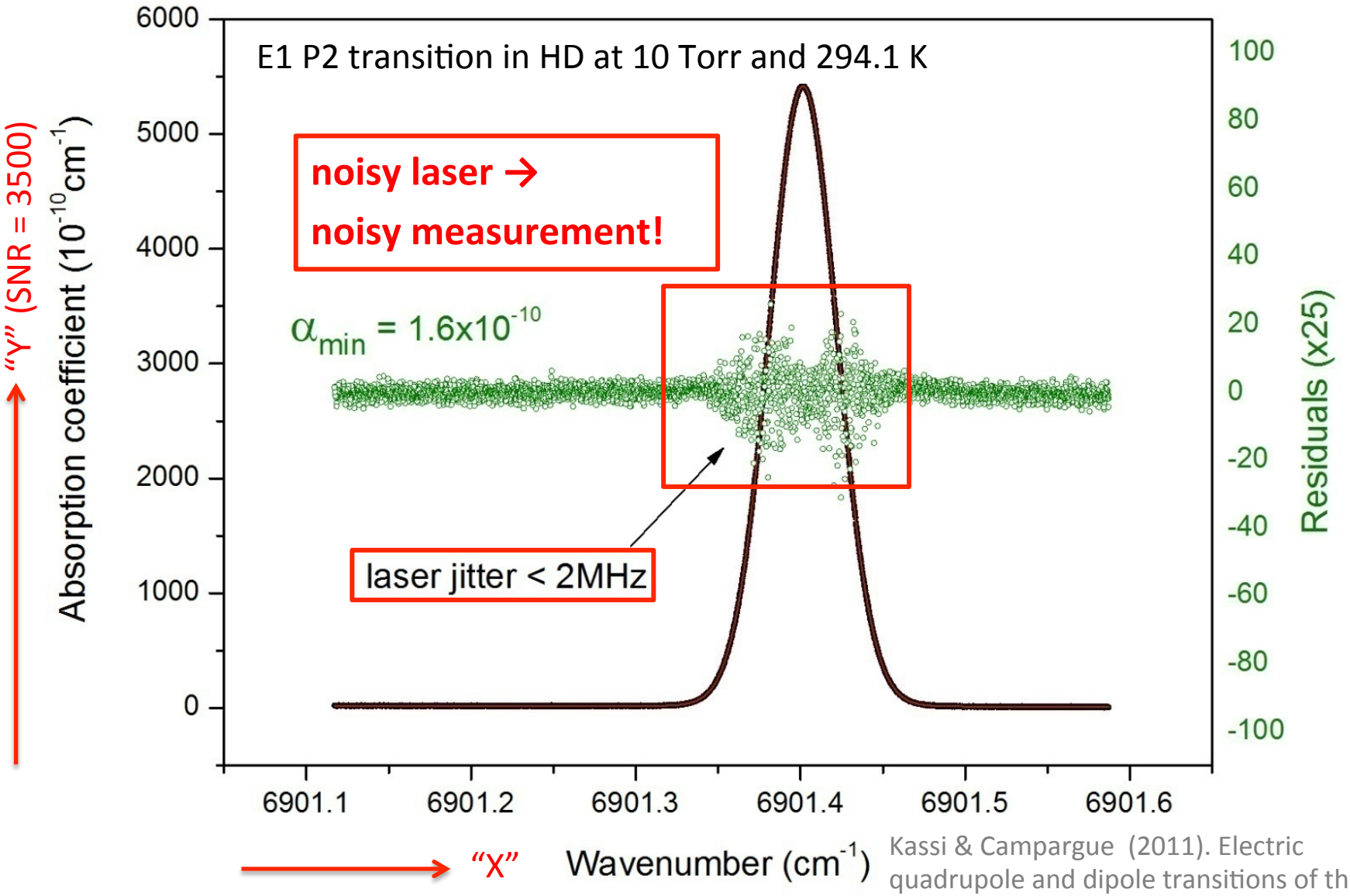

Kassi & Campargue (2011). Electric quadrupole and dipole transitions of the first overtone band of HD by CRDS between 1.45 and 1.33 µm. *J. of Mol. Spectrosc.*, *267*, 36.

Frequency Stabilized vs. Optical Feedback FS-CRDS

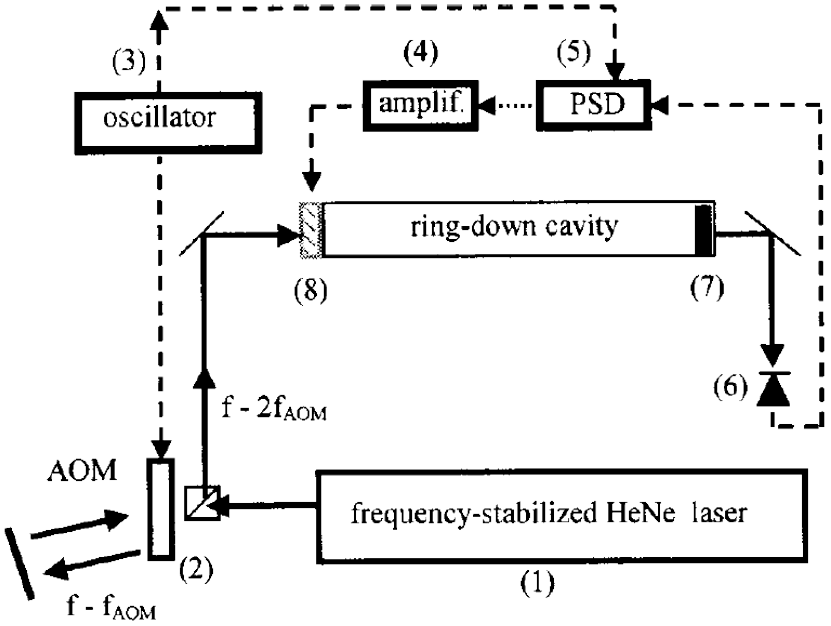

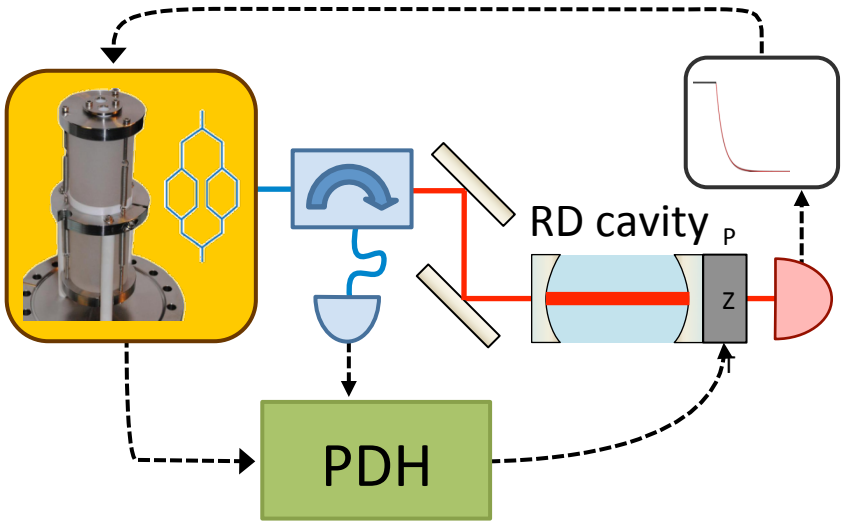

- RD cavity length locked to I_2-stabilized HeNe laser
- Tuning by AOM shifting
- ECDL probe laser scanned

  or PDH-locked to RD cavity

- Sub-kHz probe laser locked to ultrastable V-shaped cavity (< 20 Hz/s)
- Single-sideband tuning
- RD cavity length PDH-locked onto stable probe laser

Hodges et al., *Rev. Sci. Instrum. 75*, 849–863 *(2004)*
Cygan et al., *Rev. Sci. Instrum. 82*, 063107 *(2011)*

Burkart et al., *Opt. Lett. 38, 2062-2064 (2013)*
Burkart et al., *Opt. Lett. 39, 4695-4698 (2014)*

Frequency Stabilized Optical Feedback FS-CRDS

Experimental CO_2 spectrum at 10 Pa and 296 K

- SNR = 80,000
- $\alpha_{min} = 4\ 10^{-12}\ cm^{-1}$

HITRAN 2012 simulation

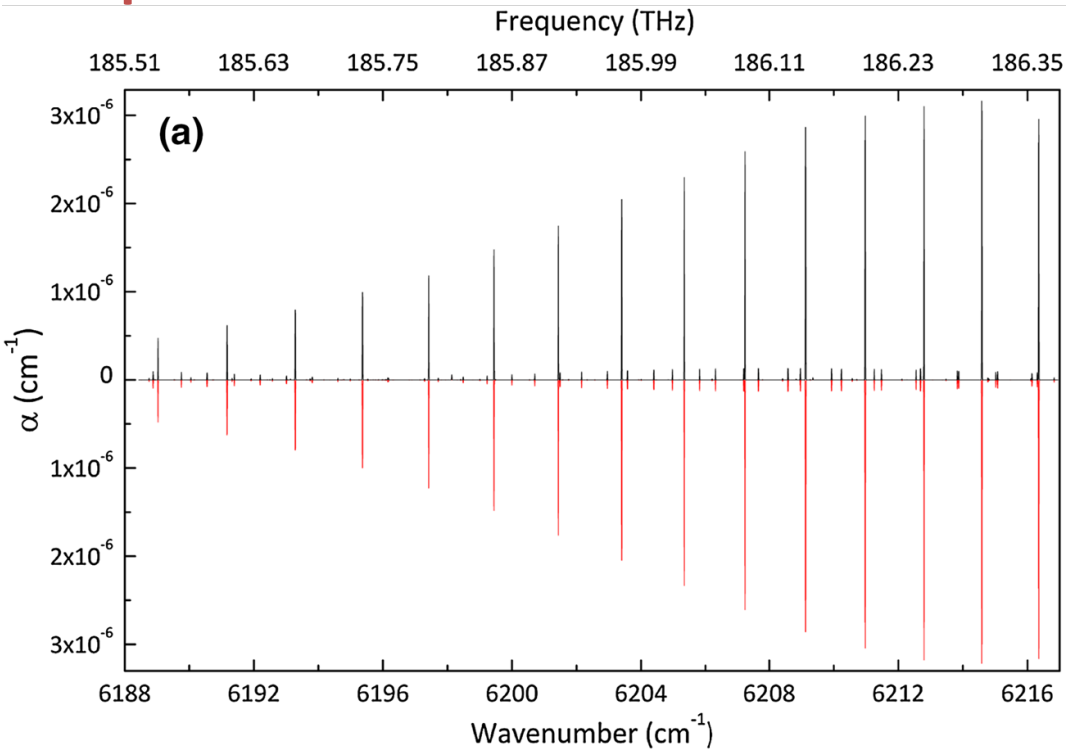

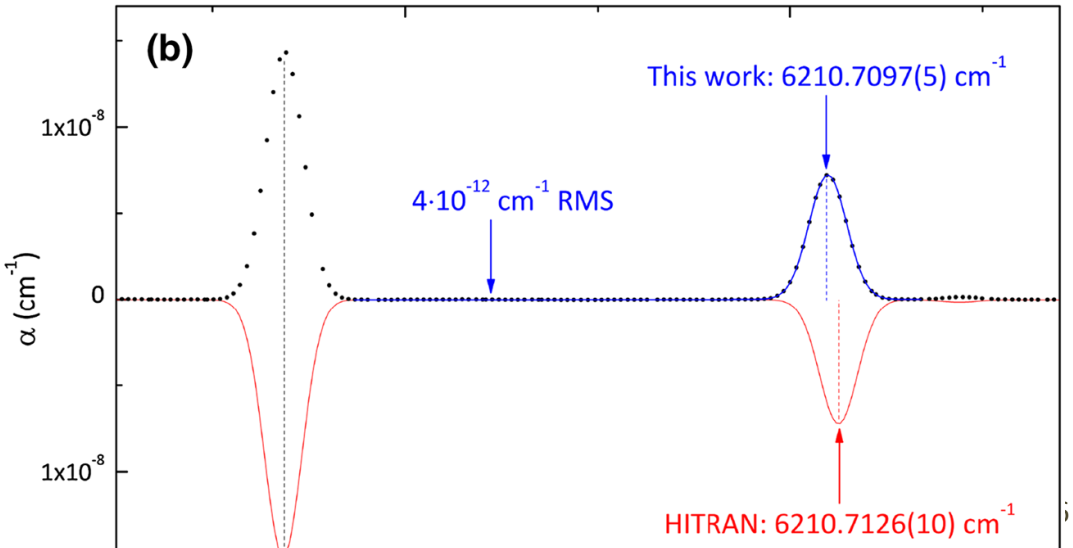

Burkart, PhD thesis, Grenoble (2015)

Frequency Stabilized Optical Feedback FS-CRDS

Isolated 30013 ← 00001 P16 line of CO_2 at 6,214.588 cm^{-1} broadened by N_2 at a total pressure of 150 Pa and a CO_2 concentration of 5.04 10^{-3}, with first-order polynomial baseline correction. **T=295.8 ± 0.1 K.**

Table 1 Comparison of the models used for fitting the line profile in Fig. 7.

Profile	QF	T_D (K)	$10^4\Gamma$ (cm^{-1})	$10^9 A$ (cm^{-2})
Voigt	16001	293.37	1.335	3.0590
NG	44043	294.56	1.353	3.0575
Galatry	62158	296.40	1.249	3.0564
qSD Voigt	62104	296.41	1.248	3.0564
qSDNG	79322	295.90	1.275	3.0567
pCqSDNG	79711	295.91	1.338	3.0567

QF fit quality figure, T_D Doppler temperature, Γ Lorentzian width, *A* integrated absorption, *NG* Nelkin-Ghatak, *qSD* quadratic speed-dependent, *pC* partially correlated

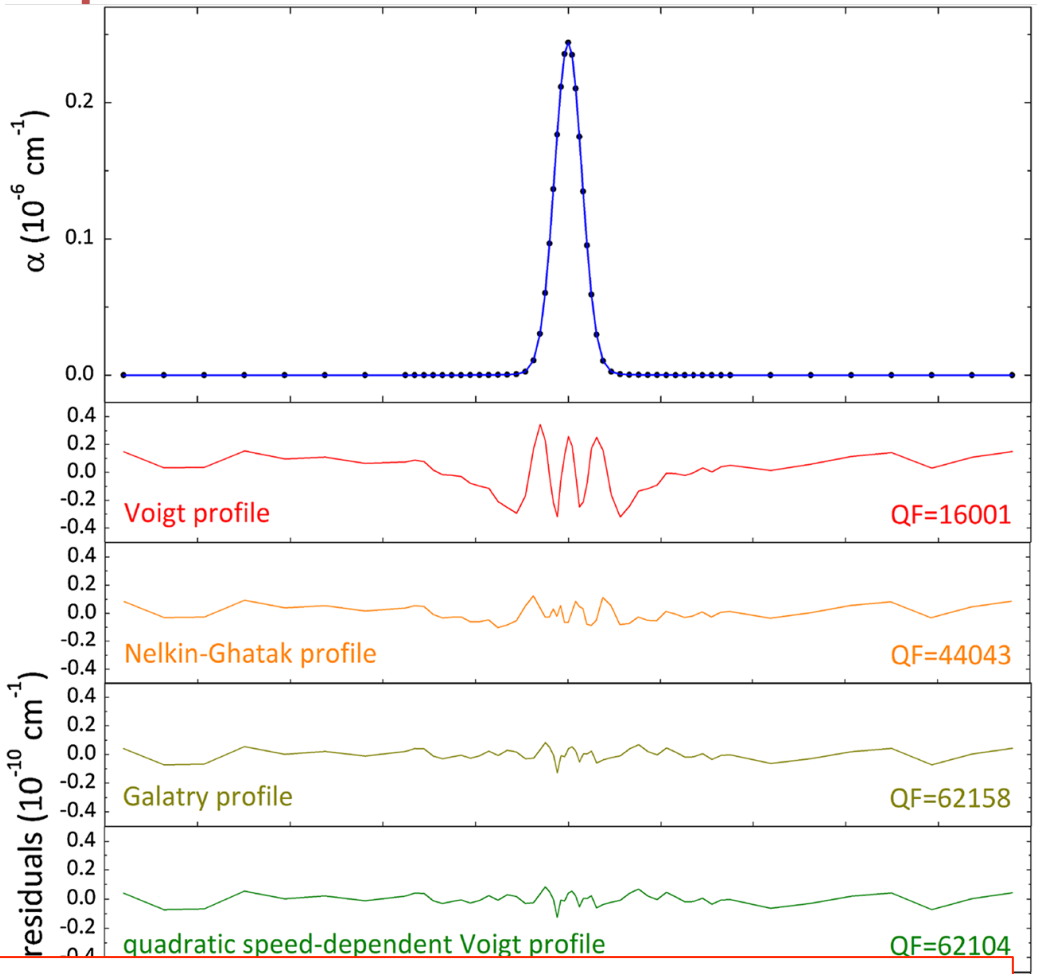

Doppler Broadening Thermometry, as proposed by Ch. Bordé in 2000:

How far can and should we go in reducing the number of base units of the SI: A challenge in the application of modern physics, in: Conference Given at the Symposium on the Occasion of the 125th Anniversary of the Metric Convention, Paris, 2000.

The history of k_B

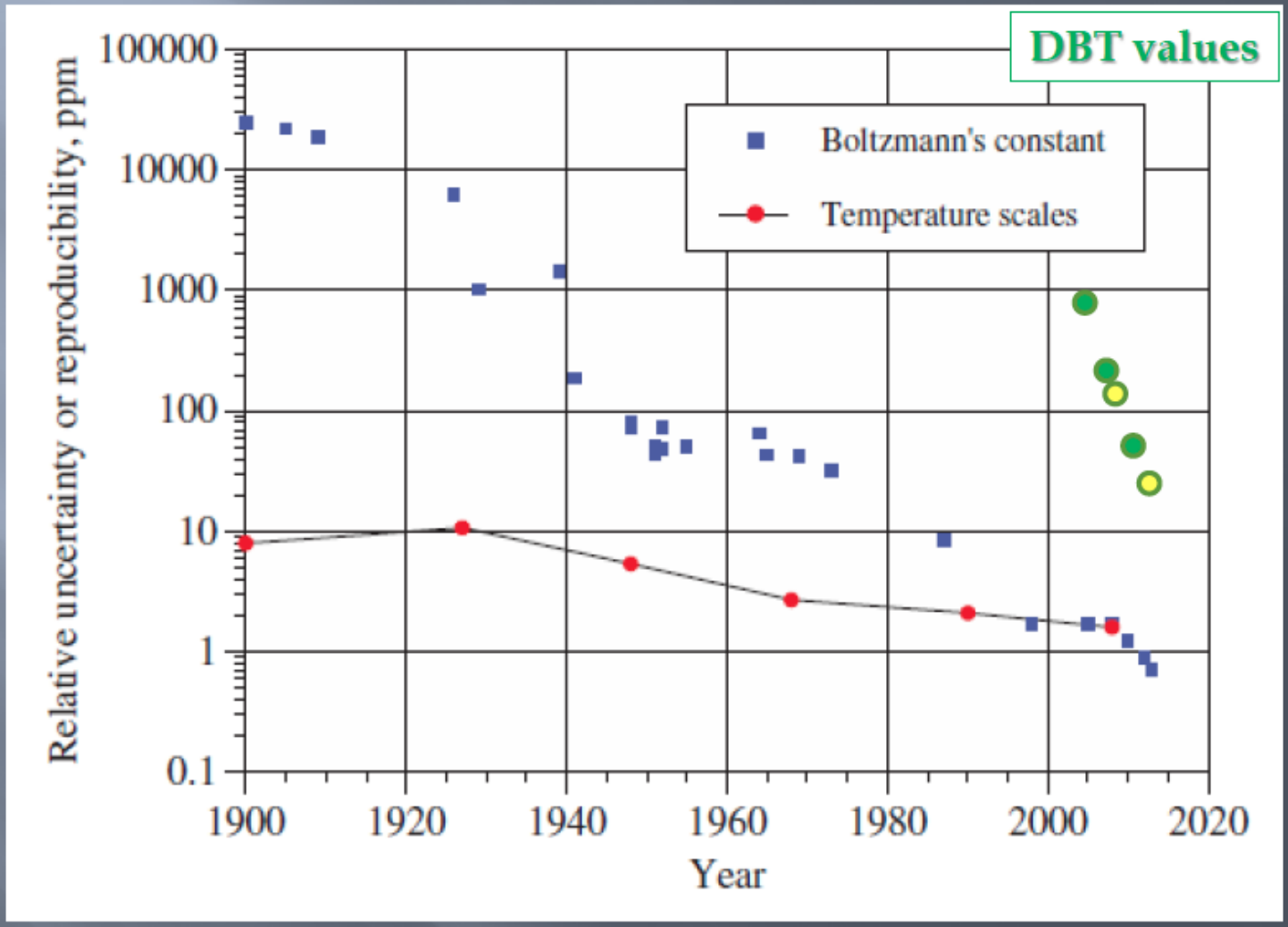

Current k_B value at UniNA2

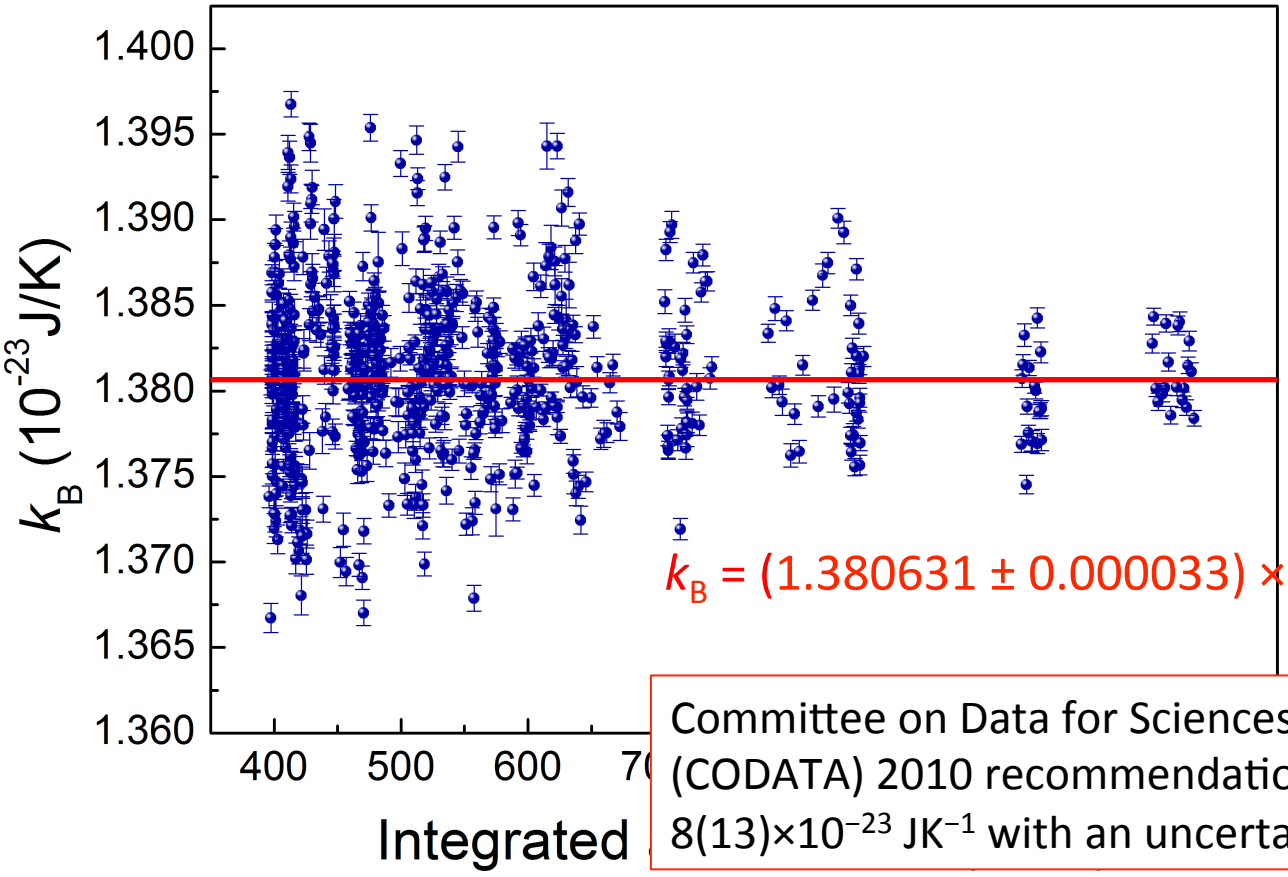

$k_B = (1.380631 \pm 0.000033) \times 10^{-23}$ J/K (24 ppm)

Committee on Data for Sciences and Technology (CODATA) 2010 recommendation = 1.380 648 8(13)×10^{-23} JK^{-1} with an uncertainty of 0.9ppm

Moretti, Castrillo, Fasci, De Vizia, Casa, Galzerano, Merlone, Laporta, Gianfrani, Phys. Rev. Lett. 111, 060803 (2013)

Uncertainty budget

Components from [24]	Type A	Type B
Reproducibility of Doppler width measurements	15.7×10^{-6}	
Frequency scale		$< 2 \times 10^{-6}$
Line-centre frequency		0.278×10^{-6}
Line-emission width and FM broadening		10×10^{-6}
Optical saturation effects		$< 1.8 \times 10^{-8}$
Detector non-linearity		$< 2 \times 10^{-6}$
AM modulation effects		$< 1.2 \times 10^{-6}$
Cell's temperature	3.7×10^{-8}	1.1×10^{-6}
Hyperfine structure effects		$< 10^{-6}$
Line-shape model		14.9×10^{-6}
New components		
Finite detection bandwidth		4×10^{-11}
Relativistic effects		Negligible
Optical zero		$< 2 \times 10^{-7}$
Combined relative uncertainty = 24×10^{-6}		

Castrillo, Moretti, Fasci, De Vizia, Casa, Gianfrani, J. Mol. Spectrosc. 300, 131-138 (2014).
Fasci, De Vizia, Merlone, Moretti, Castrillo, Gianfrani, Metrologia 52, S233-S241 (2015).

How to reach the requires 1 ppm?

The “French proposal”:

Determine collisional parameters at elevated pressure (2-25 Pa) with Doppler fixed, determine k_B at low pressure (0.1 to 2.5 Pa) that should lead to an error budget totaling 2.3 ppm.

> Lemarchand et al. (2013). A revised uncertainty budget for measuring the Boltzmann constant using the Doppler broadening technique on ammonia. *Metrologia*, *50*(6), 623–630.

The “Italian proposal”:

Global fitting procedure over a range of pressures. Detailed simulations (10 – 467 Pa) show that < 1 ppm should be possible.

> Amodio et al. (2015). Investigating the ultimate accuracy of Doppler-broadening thermometry by means of a global fitting procedure. *Phys. Rev. A*, *92*(3), 1–8.

How to reach the requires 1 ppm?

Global fitting procedure over a range of pressures

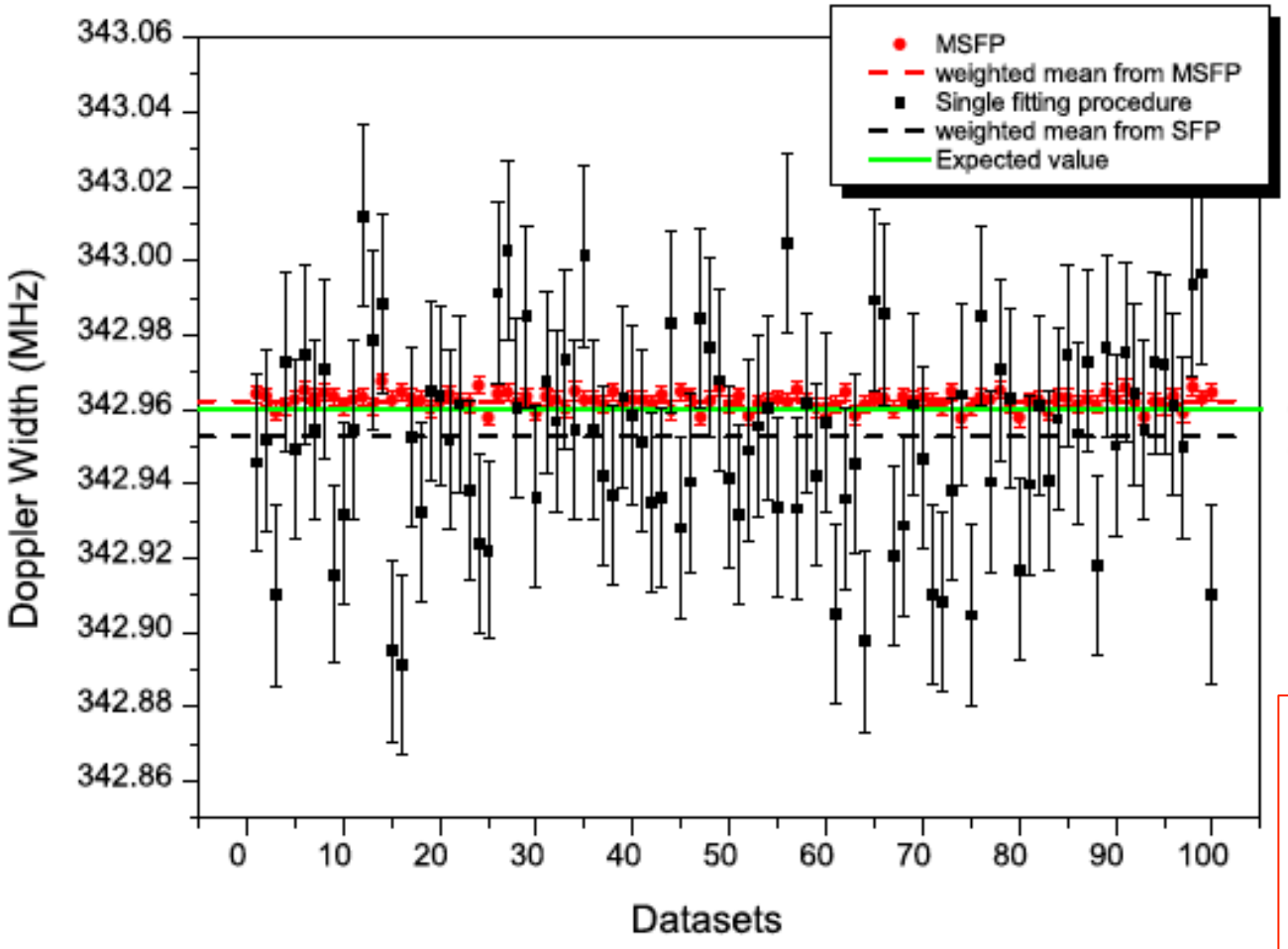

Retrieved from multispectra fits

Expected value

Retrieved from single fits

Multispectrum fit procedure is both more precise and more accurate: Recall IUPAC Task Group recommendation!

THE END!

Many thanks to my colleagues at the Laboratory of Interdisciplinary Physics,

and in particular **Alain Campargue**, **Roberto Grilli**, **Daniele Romanini**, and **Samir Kassi**

and

Livio Gianfrani for his slides on Doppler Broadening Thermometry

and

Ha Tran for sharing her SPEC-ATMOS (Fréjus, June 2015) presentation